

**PACLITAXEL-LOADED MICROSPHERES INCORPORATED INTO  
CHITOSAN AND HYALURONIC ACID FILMS FOR PREVENTION OF POST-  
SURGICAL ADHESIONS**

by

**JIN FANG WANG**

B. Sc. (Medical Science), Hebei Medical University, 1993

M.Eng. (Bioprocess Technology), Asian Institute of Technology, 1997

A THESIS SUBMITTED IN PARTIAL FULFILLMENT OF THE  
REQUIREMENTS FOR THE DEGREE OF MASTER OF SCIENCE

in

THE FACULTY OF GRADUATE STUDIES

Faculty of Pharmaceutical Sciences  
Division of Pharmaceutics and Biopharmaceutics

We accept this thesis as confirming to the required standard

THE UNIVERSITY OF BRITISH COLUMBIA  
September 2001

© JinFang Wang, 2001

In presenting this thesis in partial fulfilment of the requirements for an advanced degree at the University of British Columbia, I agree that the Library shall make it freely available for reference and study. I further agree that permission for extensive copying of this thesis for scholarly purposes may be granted by the head of my department or by his or her representatives. It is understood that copying or publication of this thesis for financial gain shall not be allowed without my written permission.

Department of Pharmaceutical Sciences

The University of British Columbia  
Vancouver, Canada

Date Jan 14, 2001

## ABSTRACT

Post-surgical adhesions are abnormal attachments between tissues or organs, which frequently occur following surgical trauma. They are currently treated using either barriers or drugs. In this work, drug-loaded barriers were developed using paclitaxel as a drug and chitosan and hyaluronic acid (HA) as film matrices. Our novel approach was to disperse paclitaxel-loaded poly (L-lactic acid) (PLLA) microspheres in chitosan and crosslinked HA film matrices (hydrogel systems) to avoid the precipitation of hydrophobic paclitaxel in hydrophilic hydrogel matrices.

Microspheres were prepared using low molecular weight (2k g/mol) PLLA and employing the solvent evaporation method. Paclitaxel-loaded microspheres possessed higher than theoretical drug content due to the water-soluble component of PLLA diffusing into the aqueous phase during microsphere preparation. Differential scanning calorimetry (DSC) scans showed that compared to control microspheres, the glass transition temperature increased by 7 °C for 10% paclitaxel-loaded microspheres. The melting temperature of PLLA microspheres decreased as paclitaxel loading increased, with a decrease of 7 °C for 25% paclitaxel-loaded microspheres. This is evidence that the paclitaxel was miscible with PLLA in the microspheres.

Microsphere-loaded films were prepared by dispersing the microspheres in chitosan and HA solutions using 0.01% polysorbate 80. The HA was crosslinked using 1-ethyl-3-(3-dimethyl amino-propyl) carbodiimide hydrochloride (EDAC) and the cast films were dried at room temperature. SEM micrographs revealed uniform dispersion and no aggregates of the microspheres in the film matrices.

Degradation studies were carried out in phosphate buffered saline with albumin (PBS-A), pH 7.4 at 37 °C. The increased retention time of PLLA in microspheres with incubation in PBS-A on gel permeation chromatography (GPC) indicated the decrease in MW and shortening of polymer chains due to hydrolysis. The erosion of both PLLA microspheres alone and microsphere-loaded film matrices started after 2-4 hours incubation in PBS-A as shown by SEM data.

In vitro release of paclitaxel from PLLA microspheres was biphasic. An initial rapid phase of release was likely due to the diffusional release of paclitaxel from the superficial surface region of the microspheres. The slower phase of release may be due to the increased crystallinity of the matrix, with slower water uptake, decreased paclitaxel diffusivity and decreased degradation rate. The release of paclitaxel from the film matrices involved the release of paclitaxel from PLLA microspheres and then diffusion through film matrices to the external medium. For both microspheres and film matrices containing microspheres, increased drug loading led to a faster release rate and an increased extent of release.

This work demonstrated that by dispersing paclitaxel-loaded microspheres in chitosan and HA films, elegant formulations could be achieved in which there was a uniform dispersion of paclitaxel through the film matrices. The hydrogel films exerted a small controlling effect on the release of paclitaxel from microsphere-loaded film matrices.

## TABLE OF CONTENTS

<b>ABSTRACT.....</b>	<b>ii</b>
<b>TABLE OF CONTENTS.....</b>	<b>iv</b>
<b>LIST OF TABLES.....</b>	<b>x</b>
<b>LIST OF FIGURES.....</b>	<b>xii</b>
<b>LIST OF ABBREVIATIONS.....</b>	<b>xvi</b>
<b>ACKNOWLEDGMENTS.....</b>	<b>xix</b>
<b>1. INTRODUCTION.....</b>	<b>1</b>
<b>2. BACKGROUND.....</b>	<b>3</b>
<b>2.1. Post-surgical adhesions.....</b>	<b>3</b>
2.1.1. Formation of post-surgical adhesions.....	3
2.1.2. Approaches to adhesion prevention and reduction.....	5
2.1.2.1. Use of barriers to prevent adhesions.....	5
2.1.2.2. Use of drugs to prevent adhesions.....	6
<b>2.2. Paclitaxel.....</b>	<b>6</b>
2.2.1. Source and structure of paclitaxel.....	6
2.2.2. Chemistry of paclitaxel.....	8
2.2.2.1. Stability of paclitaxel.....	8
2.2.2.2. Solubility of paclitaxel.....	8
2.2.3. Mechanism of action, clinical use and toxicity of paclitaxel.....	9
2.2.4. Preclinical effectiveness of paclitaxel in post-surgical adhesions.....	9
<b>2.3. Polymer chemistry.....</b>	<b>10</b>
2.3.1. Structure of polymers.....	10
2.3.2. Molar mass of polymers.....	11
2.3.2.1. Molar mass averages of polymers.....	11
2.3.2.2. Molar mass distribution.....	11
2.3.3. Polymer crystallinity.....	12
2.3.3.1. Models of polymer crystallinity.....	13
2.3.3.2. Degree of crystallinity.....	13

2.3.4.	Thermal properties of semi-crystalline polymers.....	14
2.3.4.1.	Glass transition.....	14
2.3.4.2.	Melting transition.....	14
<b>2.4.</b>	<b>Biodegradable polymers as biomaterials .....</b>	<b>17</b>
2.4.1.	Biodegradation of biodegradable polymers.....	17
2.4.1.1.	Solubilization .....	18
2.4.1.2.	Ionization followed by dissolution.....	18
2.4.1.3.	Chemical hydrolysis.....	18
2.4.2.	Poly (L-lactic acid) (PLLA) .....	19
2.4.2.1.	Structure, thermal properties and applications of PLLA .....	19
2.4.2.2.	Biocompatibility of PLLA .....	20
2.4.2.3.	Biodegradation of PLLA.....	20
2.4.3.	Chitosan.....	21
2.4.3.1.	Physicochemical and biological properties of chitosan .....	21
2.4.3.2.	Pharmaceutical applications of chitosan .....	22
2.4.3.3.	Biodegradation of chitosan .....	23
2.4.3.4.	Adhesion prevention effect of chitosan .....	23
2.4.4.	Hyaluronic acid (HA).....	24
2.4.4.1.	Physicochemical properties of HA .....	24
2.4.4.2.	Biodegradation and crosslinking of HA .....	24
2.4.4.3.	Clinical and pharmaceutical applications of HA .....	25
2.4.4.4.	Adhesion prevention effect of HA .....	26
<b>2.5.</b>	<b>Development of controlled release paclitaxel-loaded polymer films.....</b>	<b>26</b>
2.5.1.	PLLA microspheres.....	26
2.5.1.1.	Preparation of poly (lactic acid) microspheres .....	26
2.5.1.2.	Drug release from polymeric microspheres .....	27
2.5.1.3.	Selection of 2 k g/mol PLLA for microspheres .....	28
2.5.2.	Drug release from microsphere-loaded films .....	28
<b>2.6.</b>	<b>Objectives.....</b>	<b>30</b>
<b>3.</b>	<b>EXPERIMENTAL .....</b>	<b>31</b>
<b>3.1.</b>	<b>Materials and supplies.....</b>	<b>31</b>
3.1.1.	Paclitaxel .....	31
3.1.2.	Chemicals and solvents .....	31
3.1.3.	Glassware .....	32

3.1.4. Phosphate-buffered saline with albumin (PBS-A), HPLC mobile phase and poly (vinyl alcohol) (PVA) solution.....	32
<b>3.2. Equipment .....</b>	<b>33</b>
3.2.1. Apparatus for microsphere preparation .....	33
3.2.2. HPLC.....	33
3.2.3. Scanning electron microscope.....	33
3.2.4. Particle size analyzer .....	33
3.2.5. Differential scanning calorimeter (DSC) .....	34
3.2.6. X-ray powder diffractometer.....	34
3.2.7. Gel permeation chromatography .....	34
3.2.8. Centrifuge, incubator and oven .....	34
3.2.9. Other equipment .....	35
<b>3.3. Preparation of PLLA microspheres .....</b>	<b>35</b>
<b>3.4. Physicochemical characterization of microspheres .....</b>	<b>38</b>
3.4.1. Particle size analysis.....	38
3.4.2. Surface morphology of microspheres.....	38
3.4.3. Evaluation of the water-soluble fraction of PLLA .....	39
3.4.4. Recovery assays for total content of paclitaxel in microspheres.....	39
3.4.5. Determination of the total content of paclitaxel in microspheres.....	39
3.4.6. X-ray powder diffraction.....	40
3.4.7. Thermal analysis.....	40
3.4.8. Paclitaxel analysis .....	40
3.4.8.1. Extraction of paclitaxel from PBS-A release medium.....	40
3.4.8.2. Reconstitution of paclitaxel .....	40
3.4.8.3. Quantitative analysis of paclitaxel using HPLC .....	41
3.4.9. Validation of the paclitaxel standard curves used for HPLC analysis .....	41
<b>3.5. Casting of chitosan and HA films .....</b>	<b>42</b>
3.5.1. Casting of chitosan films .....	42
3.5.1.1.1. Preparation of chitosan solutions.....	42
3.5.1.1.2. Casting chitosan films without microspheres .....	42
3.5.1.1.3. Casting chitosan films containing microspheres.....	42
3.5.2. Casting crosslinked hyaluronic acid films without and with microspheres ...	43
<b>3.6. Characterization of chitosan and HA films .....</b>	<b>44</b>
3.6.1. Measurement of the thickness of the films.....	44
3.6.2. Surface morphology and cross-sectional view of chitosan films with control and 25% paclitaxel-loaded microspheres .....	44

<b>3.7. In vitro degradation studies .....</b>	<b>44</b>
3.7.1. Degradation of PLLA microspheres.....	44
3.7.1.1. Molecular weight .....	45
3.7.1.1.1. Calibration of the GPC column.....	45
3.7.1.1.2. Molecular weight of microspheres.....	45
3.7.1.2. Thermal properties .....	45
3.7.1.3. Surface morphology .....	46
3.7.1.4. Mass loss of degraded microspheres.....	46
3.7.2. Degradation of chitosan and hyaluronic acid films.....	46
3.7.2.1. Mass loss of films .....	46
3.7.2.2. Surface morphology .....	47
<b>3.8. In vitro release studies .....</b>	<b>47</b>
3.8.1. In vitro release of paclitaxel from microspheres .....	47
3.8.2. In vitro release of paclitaxel from microsphere-loaded films .....	47
3.8.2.1. In vitro release of paclitaxel from microsphere-loaded chitosan films.....	47
3.8.2.2. In vitro release of paclitaxel from microsphere-loaded HA films .....	48
<b>3.9. Statistical treatment of data .....</b>	<b>48</b>
<b>4. RESULTS.....</b>	<b>50</b>
<b>4.1. Characterization of PLLA microspheres.....</b>	<b>50</b>
4.1.1. Effect of PLLA concentrations on yields of control microspheres .....	50
4.1.2. Surface morphology of microspheres.....	51
4.1.3. Particle size distributions of microspheres .....	51
4.1.4. Determination of paclitaxel content in PLLA microspheres .....	54
4.1.5. X-ray powder diffraction patterns (XRPD) of microspheres .....	57
4.1.6. Thermal properties of paclitaxel, PLLA and microspheres.....	59
<b>4.2. Characterization of chitosan and HA films .....</b>	<b>64</b>
4.2.1. Thickness of films .....	64
4.2.2. Surface morphology and cross-sectional views of chitosan films without and with microspheres.....	65
<b>4.3. Degradation of PLLA microspheres and microsphere-loaded films .....</b>	<b>69</b>
4.3.1. Degradation of PLLA (2k g/mol) microspheres.....	69
4.3.1.1. GPC analysis.....	69
4.3.1.1.1. Validation of GPC column.....	69
4.3.1.1.2. GPC analysis of degradation of microspheres .....	69

4.3.1.1.3. PLLA stability during storage.....	70
4.3.1.2. Thermal properties.....	75
4.3.1.3. Surface morphology.....	79
4.3.1.4. Mass loss.....	79
4.3.2. Degradation of films without and with microspheres.....	85
4.3.2.1. Surface morphology of films.....	85
4.3.2.2. Mass loss of films.....	90
4.3.2.2.1. Mass loss of chitosan films.....	90
4.3.2.2.2. Mass loss of HA films.....	90
<b>4.4. Validation of paclitaxel standard curves in acetonitrile: water 60: 40.....</b>	<b>92</b>
<b>4.5. In vitro release studies.....</b>	<b>92</b>
4.5.1. Paclitaxel release profiles from PLLA (2k g/mol) microspheres.....	92
4.5.2. Release study of paclitaxel from microsphere-loaded films.....	93
4.5.2.1. Release study of paclitaxel from chitosan films incorporated with microspheres of different size ranges.....	93
4.5.2.2. Release study of paclitaxel from chitosan films and HA films loaded with microspheres of different drug loadings.....	94
<b>5. DISCUSSION.....</b>	<b>104</b>
<b>5.1. Preparation and characterization of microspheres.....</b>	<b>104</b>
5.1.1. Effect of stir speed and emulsifier concentration on microsphere size.....	104
5.1.2. Effect of PLLA concentration on particle size distribution.....	104
5.1.3. Surface morphology and cross-sectional views of microspheres.....	105
5.1.4. Paclitaxel content in PLLA microspheres.....	106
5.1.5. X-ray powder diffraction patterns of PLLA microspheres.....	107
5.1.6. Thermal properties of PLLA and PLLA microspheres.....	107
<b>5.2. PLLA microspheres in chitosan films.....</b>	<b>109</b>
<b>5.3. In vitro degradation of PLLA microspheres and chitosan and HA films ....</b>	<b>109</b>
5.3.1. In vitro degradation of PLLA microspheres.....	109
5.3.1.1. Molecular weight.....	110
5.3.1.2. Thermal properties.....	111
5.3.1.3. Surface morphology.....	112
5.3.1.4. Mass loss.....	113
5.3.2. In vitro degradation of chitosan films.....	114
5.3.3. In vitro degradation of crosslinked HA films.....	114

5.3.4. In vitro degradation of PLLA microspheres in film matrices .....	115
<b>5.4. In vitro release study of paclitaxel from microspheres and microsphere-loaded films .....</b>	<b>116</b>
5.4.1. In vitro release of drug from PLLA microspheres (to external medium).....	117
5.4.2. In vitro release of paclitaxel from film matrices loaded with microspheres	117
5.4.2.1. In vitro release of paclitaxel from chitosan films loaded with microspheres of different size ranges .....	117
5.4.2.2. In vitro release of paclitaxel from chitosan and HA films loaded with 50-90 $\mu$ m microspheres .....	118
<b>6. SUMMARY AND CONCLUSIONS.....</b>	<b>122</b>
<b>7. REFERENCES.....</b>	<b>123</b>

## LIST OF TABLES

<b>Table 1.</b> Proposed mechanisms of adhesion prevention by class of drugs (from Wiseman, 1997). .....	6
<b>Table 2.</b> Conditions for preparation of PLLA (2k g/mol) microspheres in different size ranges. Polymer concentration was 5% w/v. ....	38
<b>Table 3.</b> Theoretical loadings of paclitaxel in MW 150k g/mol chitosan films loaded with 50-90 $\mu\text{m}$ PLLA (2k g/mol) microspheres of different drug loadings. ....	43
<b>Table 4.</b> Theoretical loadings of paclitaxel in HA films incorporated with 50-90 $\mu\text{m}$ PLLA (2k g/mol) microspheres of different drug loadings. ....	44
<b>Table 5.</b> Percent yields of control microspheres in different size ranges prepared using between 5 and 20% w/v PLLA (2k g/mol). Data are mean values based on measurements of four batches at each PLLA concentration $\pm$ standard deviation. ...	51
<b>Table 6.</b> Particle size distributions of paclitaxel-loaded microspheres prepared using 5% and 10% w/v PLLA (2k g/mol). For microspheres prepared using 5% w/v PLLA, values are the mean $\pm$ standard deviation of three measurements from single batches. For microspheres prepared using 10% w/v PLLA, data are mean $\pm$ standard deviation of three measurements from three batches.....	54
<b>Table 7.</b> Precision and efficiency of extraction of paclitaxel from spiked solutions and precision of organic-aqueous phase separation in the total content assay. Values of mean $\pm$ standard deviation are determined based on four measurements.....	56
<b>Table 8.</b> Total content of paclitaxel in PLLA (2k g/mol) microspheres prepared using a) 5% w/v PLLA and b) 10% w/v PLLA. Analyses of microspheres prepared using 5% w/v PLLA were determined in single batches for each size range. For microspheres prepared using 10% w/v PLLA, values were measured based on 3 batches for each drug loading. ....	56
<b>Table 9.</b> Thermal properties of 50-90 $\mu\text{m}$ microspheres prepared using 10% w/v PLLA (2k g/mol). Values are means of measurements from each of three batches $\pm$ standard deviation. Thermal properties were obtained from heat-cool-reheat-recool cycles at a scan rate of 20 $^{\circ}\text{C}/\text{min}$ . The first cycle was to heat from $-20$ to 170 $^{\circ}\text{C}$ and hold for 5 min, then cool back to $-20$ $^{\circ}\text{C}$ . The second cycle was to reheat from $-20$ $^{\circ}\text{C}$ to 170 $^{\circ}\text{C}$ and hold for 5 min, then recool back to $-20$ $^{\circ}\text{C}$ . ....	61
<b>Table 10.</b> Thickness of PLLA (2k g/mol) microsphere loaded A) chitosan and B) HA films containing between 0 and 5% paclitaxel. Measurements were conducted on four locations for each film. For each drug loading, four films were measured. Values are means of four film samples $\pm$ standard deviation. ....	64

**Table 11.** GPC retention times of degraded PLLA (2k g/mol) microspheres with 0 to 25% paclitaxel loadings incubated in PBS-A at 37 °C. Values are one set of data from single samples running at one time. .... 70

**Table 12.** Thermal properties of non-degraded and degraded PLLA (2k g/mol) control microspheres and paclitaxel-loaded microspheres. Samples were scanned at 20 °C/min over a temperature range of -20 to 170 °C. For control microspheres and 25% paclitaxel-loaded microspheres, values are means of measurements from each of three batches ± standard deviation. For 5% and 10% paclitaxel-loaded microspheres, values are from each single batch..... 76

**Table 13.** Inter- and intra-day precision of standard curves of paclitaxel in acetonitrile: water 60: 40..... 96

**Table 14.** Accuracy of standard curves of paclitaxel in acetonitrile: water 60: 40..... 97

## LIST OF FIGURES

- Figure 1.** Schematic representation of paclitaxel-loaded PLLA microspheres within chitosan film..... 2
- Figure 2.** Adhesion formation following surgical trauma (peritoneal trauma) (from DiZerega, 1993). ..... 4
- Figure 3.** The chemical structure of paclitaxel. Numbers are assigned to carbons in the structure in IUPAC nomenclature..... 7
- Figure 4.** Schematic drawings of A) the fringed micelle model and B) the chain folded model of crystallinity. .... 16
- Figure 5.** The chemical structure of poly (L-lactic acid). The asterisk (\*) denotes a chiral carbon in the polymer backbone. .... 20
- Figure 6.** The chemical structure of (1) chitin and (2) chitosan..... 22
- Figure 7.** The chemical structure of hyaluronic acid. .... 24
- Figure 8.** Flowchart of preparation of paclitaxel loaded microspheres (adapted from Deluca et al., 1992). ..... 37
- Figure 9.** SEM micrographs of 50-90  $\mu\text{m}$  PLLA (2k g/mol) microspheres with paclitaxel loading of A) 0, B) 5, C) 10 and D) 25%. (Magnification of all micrographs is 1000x.) ..... 53
- Figure 10.** Particle size distributions of A) 20% paclitaxel-loaded microspheres prepared using 5% w/v PLLA (2k g/mol) in different size ranges and B) 5-25% paclitaxel-loaded microspheres prepared using 10% w/v PLLA (2k g/mol) (50-90  $\mu\text{m}$ ). ..... 55
- Figure 11.** XRPD patterns of paclitaxel, PLLA (2k g/mol) and PLLA (2k g/mol) microspheres with paclitaxel loadings of 0, 5, 10 and 25%..... 58
- Figure 12.** DSC scan of paclitaxel over a temperature range of 0 to 300  $^{\circ}\text{C}$  at a scan rate of 20  $^{\circ}\text{C}/\text{min}$ . ..... 62
- Figure 13.** DSC heating/reheating scans of PLLA (2k g/mol) following two cycles of heat-cool-reheat-recool at a scan rate of 20  $^{\circ}\text{C}/\text{min}$ . A) The first cycle: heating from  $-20$  to 170  $^{\circ}\text{C}$  and holding for 5 min, then cooling to  $-20$   $^{\circ}\text{C}$ ; B) the second cycle: reheating from  $-20$  to 170  $^{\circ}\text{C}$  and holding for 5 min, then cooling to  $-20$   $^{\circ}\text{C}$ . ..... 62
- Figure 14.** DSC heating/reheating scans of PLLA (2k g/mol) microspheres with paclitaxel loadings between 0 and 25% following two cycles of heat-cool-reheat-recool at a scan rate of 20  $^{\circ}\text{C}/\text{min}$ . A) The first cycle: heating from  $-20$  to 170  $^{\circ}\text{C}$

and holding for 5 min, then cooling to $-20^{\circ}\text{C}$ ; B) the second cycle: reheating from $-20$ to $170^{\circ}\text{C}$ and holding for 5 min, then recooling to $-20^{\circ}\text{C}$ .	63
<b>Figure 15.</b> SEM micrograph of surface feature of chitosan film without microspheres. (Magnification is 1000x.)	66
<b>Figure 16.</b> SEM micrographs of chitosan films loaded with control PLLA (2k g/mol) microspheres. A) The surface features. (Magnification of micrographs is 1000x and 200x.) B) The cross-sectional view. (Magnification of the micrograph is 1000x.)	67
<b>Figure 17.</b> SEM micrographs of chitosan films loaded with 25% paclitaxel-loaded PLLA (2k g/mol) microspheres. A) The surface features. (Magnification of micrographs is 1000x and 200x.) B) The cross-sectional view. (Magnification of the micrograph is 1000x.)	68
<b>Figure 18.</b> GPC elution profiles of polystyrene standards with molecular weights ranging from 600 to 4000 g/mol at $40^{\circ}\text{C}$ : (Solvent: THF. Solvent flow rate: 1.0 ml/min. Injection volume: 50 $\mu\text{l}$ ).	72
<b>Figure 19.</b> GPC standard curve for polystyrene standards with molecular weights from 600 to 4000 g/mol on a column with a nominal pore size of $10^3 \text{ \AA}$ at $40^{\circ}\text{C}$ . (Solvent: THF. Solvent flow rate: 1.0 ml/min. Injection volume: 50 $\mu\text{l}$ ).	73
<b>Figure 20.</b> GPC elution profile of degrading PLLA (2k g/mol) control microspheres after 4 weeks incubation in PBS-A at $37^{\circ}\text{C}$ . (Solvent: THF. Solvent flow rate: 1.0 ml/min. Injection volume: 50 $\mu\text{l}$ ).	74
<b>Figure 21.</b> DSC scans of A) degrading control PLLA (2k g/mol) microspheres and B) degrading 25% paclitaxel-loaded PLLA (2k g/mol) microspheres incubated in PBS-A at $37^{\circ}\text{C}$ after 0, 2 and 4 weeks.	77
<b>Figure 22.</b> DSC scans of PLLA (2k g/mol) microspheres with paclitaxel loadings between 0 and 25% incubated in PBS-A at $37^{\circ}\text{C}$ after 2 weeks.	78
<b>Figure 23.</b> SEM micrographs of control PLLA (2k g/mol) microspheres incubated in PBS-A at $37^{\circ}\text{C}$ after A) 2 hours, B) 1, C) 2, D) 3, E) 4 and F) 5 weeks. Magnification of micrographs is 200x (top right hand pictures) and 1000x (all others).	80
<b>Figure 24.</b> SEM micrographs of 25% paclitaxel-loaded PLLA (2k g/mol) microspheres incubated in PBS-A at $37^{\circ}\text{C}$ after A) 2 hours, B) 1, C) 2, D) 3, E) 4 and F) 5 weeks. Magnification of micrographs is 1000x (left hand pictures) and 500x (right hand pictures).	82
<b>Figure 25.</b> Mass loss (%) of control PLLA (2k g/mol) microspheres incubated in PBS-A at $37^{\circ}\text{C}$ over 5 weeks.	84

- Figure 26.** SEM micrographs of chitosan films incubated in PBS-A at 37 °C A) after 1 week and B) 6 weeks. (Magnification of micrographs is 600x and 500x.) ..... 86
- Figure 27.** SEM micrographs of chitosan films loaded with control PLLA (2k g/mol) microspheres incubated in PBS-A at 37 °C after A) 2 hours, B) 2, C) 3, and D) 6 weeks. Magnification of micrographs is 1000x (left hand pictures) and 200x (right hand pictures)..... 87
- Figure 28.** SEM of chitosan films loaded with 25% paclitaxel-loaded PLLA (2k g/mol) microspheres incubated in PBS-A at 37 °C after A) 2 hours, B) 1, C) 2, and D) 6 weeks. Magnification of micrographs is 1000x (left hand pictures) and 200x (right hand pictures)..... 88
- Figure 29.** SEM micrographs of HA films loaded with control PLLA (2k g/mol) microspheres incubated in PBS-A at 37 °C after A) 4, B) 12 and C) 20 hrs. Magnification of micrographs is 1000x (left hand pictures) and 200x (right hand pictures)..... 89
- Figure 30.** Mass loss (%) of chitosan films without and with control PLLA (2k g/mol) microspheres incubated in PBS-A at 37 °C over 6 weeks. .... 91
- Figure 31.** Mass loss (%) of HA films without and with control PLLA (2k g/mol) microspheres incubated in PBS-A at 37 °C over 20 hours. .... 91
- Figure 32.** HPLC chromatogram of paclitaxel and 7-epitaxol. (Column: Novo-Pak C18 column. Mobile phase: acetonitrile: water: methanol 58: 37: 5. Mobile phase flow rate: 1 ml/min.)..... 98
- Figure 33.** In vitro release profiles of paclitaxel from 50-90 µm PLLA (2k g/mol) microspheres with 5, 10 and 25% paclitaxel loadings. (A: Cumulative release of paclitaxel vs. time; B: Cumulative percent release of paclitaxel vs. time)..... 99
- Figure 34.** In vitro release profiles of paclitaxel from chitosan films containing 20% paclitaxel-loaded PLLA (2k g/mol) microspheres. Microspheres were in different size ranges: < 10, 10-50 and 50-90 µm and paclitaxel loading was 1% in all chitosan films. (A: Cumulative release of paclitaxel vs. time; B: Cumulative percent release vs. time.)..... 100
- Figure 35.** In vitro release of paclitaxel from chitosan films containing 50-90 µm PLLA (2k g/mol) microspheres with different drug loadings. Chitosan films possessed 1, 2 and 5% loadings by loading 5, 10 and 25% paclitaxel-loaded microspheres. (A: Cumulative amount released vs. time; B: Cumulative percent released vs. time).. 101
- Figure 36.** In vitro release of paclitaxel from HA films containing 50-90 µm PLLA (2k g/mol) microspheres with different drug loadings. HA films possessed 1, 2 and 5%

loadings by loading 5, 10 and 25% paclitaxel-loaded microspheres. (A: Cumulative amount released vs. time; B: Cumulative percent released vs. time). ..... 102

**Figure 37.** Comparison of the in vitro release of paclitaxel from 50-90  $\mu\text{m}$ , 5% paclitaxel-loaded PLLA (2k g/mol) microspheres and chitosan and HA films containing the same microspheres. Both chitosan and HA films possessed a total paclitaxel content of 1%, obtained by loading 5% paclitaxel-loaded PLLA microspheres. .... 103

**Figure 38.** Schematic representation of paclitaxel release from films containing paclitaxel-loaded microspheres..... 120

## LIST OF ABBREVIATIONS

% w/v	percent weight in volume
% w/w	percent by weight
$2\theta$	X-ray diffraction angle
$^{\circ}\text{C}$	degrees Celsius
$\mu\text{g}$	microgram
$\mu\text{l}$	microlitre
$\mu\text{m}$	micrometer
$\mu\text{mol}$	micromole
$\text{C}_{18}$	octadecylsilane
DCM	dichloromethan or methylene chloride
DSC	differential scanning calorimetry
g	gram
GPC	gel permeation chromatography
HPLC	high performance liquid chromatography
J	joule
K	kilo
kV	kilovolts
L	liter
M	mass
m	meter
mg	milligrams
min	minute

ml	milliliter
Mn	number average molecular weight
mol	mole
Mt	amount of drug released at time t
Mw	weight average molecular weight
MW	molecular weight
o/w	oil in water
PBS-A	phosphate buffered saline with albumin
PDLLA	poly (D,L-lactic acid)
PLGA	poly (lactic-co-glycolic acid)
PLLA	poly (L-lactic acid)
PVA	poly (vinyl alcohol)
rpm	revolutions per minute
RSD	relative standard deviation
SEM	scanning electron microscope
t	time
T	temperature
Tg	glass transition temperature
Tm	melting transition temperature
THF	tetrahydrofuran
W	watt
Xc	degree of crystallinity
XRPD	X-ray powder diffraction

$\Delta H_f$       enthalpy of fusion

## ACKNOWLEDGMENTS

I would like to thank my supervisor, Dr. Helen Burt for her guidance, encouragement and patience over the course of my study. I would also like to thank my committee members for their direction of my research project: Drs. Stelvio Bandiera, Robert Miller, Kishor Wasan, and Keith McErlane. I also thank Dr. Gail Bellward for helping holding my committee meeting.

Thanks to Ms. Mary Mager for her assistance in using the scanning electron microscope and to John Jackson for his helpful discussion and technical support. I would also like to give my appreciation to my colleagues in the laboratory: Chuck Winternitz, Richard Liggins, Chris Tudan, Christine Allen, Chris Springate, Ruiwen Shi, Jason Zastre, and Linda Liang for their help.

Thanks to Angiotech Pharmaceuticals Inc. for providing funding for this project.

Special thanks to Xikun Liang for his understanding and supporting.

## 1. INTRODUCTION

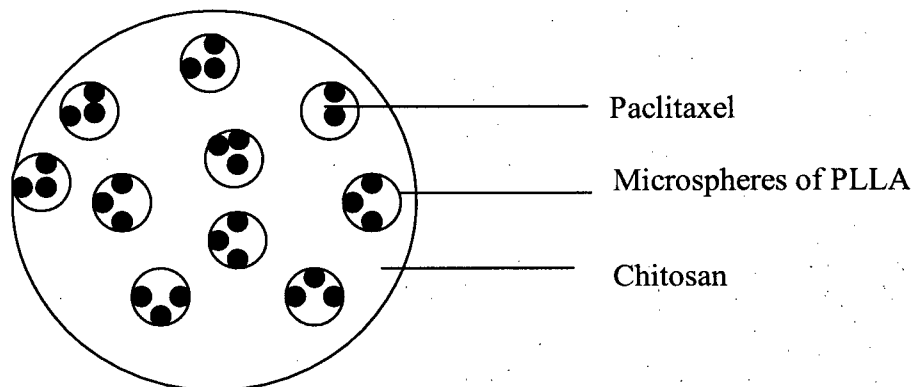
Post-surgical adhesions are abnormal attachments between tissues or organs following surgical trauma. Fibroblast proliferation is involved in the formation of adhesions. Post-surgical adhesions are currently treated using either physical barriers, or films placed between two tissue surfaces to prevent adherence, or drugs alone. The purpose of this study was to combine these methods and design a biocompatible and biodegradable system, which might act as both a barrier and a drug delivery device.

Paclitaxel is an anti-proliferative agent and has been shown to be effective in the prevention of post-surgical adhesions in animal models (Hopkins et al., 1997). Chitosan and hyaluronic acid are biocompatible and biodegradable polysaccharides. They have been formulated as barriers in the form of either films or gels for the prevention of post-surgical adhesions.

Due to the hydrophobicity of paclitaxel and the hydrophilicity of chitosan and hyaluronic acid, the loading of paclitaxel in the film results in precipitation and aggregation of paclitaxel crystals. Therefore, to create a more uniform dispersion of the drug throughout the film matrix, paclitaxel was initially encapsulated in a biocompatible and biodegradable polymer, poly (L-lactic acid) (PLLA) to make microspheres that were then dispersed in the films (Figure 1). To our knowledge, there are no studies to date, in which this novel approach of dispersing drug-loaded microspheres within a film matrix has been utilized.

In this work, low molecular weight, 2k g/mol, PLLA was used to encapsulate paclitaxel in microspheres to allow for a rapid biodegradation of the polymer and release of paclitaxel.

**Figure 1.** Schematic representation of paclitaxel-loaded PLLA microspheres within chitosan film.



In this project, it was hypothesized that suitable controlled release delivery systems for paclitaxel in chitosan and hyaluronic acid film matrices may be achieved by dispersing paclitaxel loaded PLLA microspheres in chitosan and hyaluronic acid film matrices.

## **2. BACKGROUND**

### **2.1. Post-surgical adhesions**

#### **2.1.1. Formation of post-surgical adhesions**

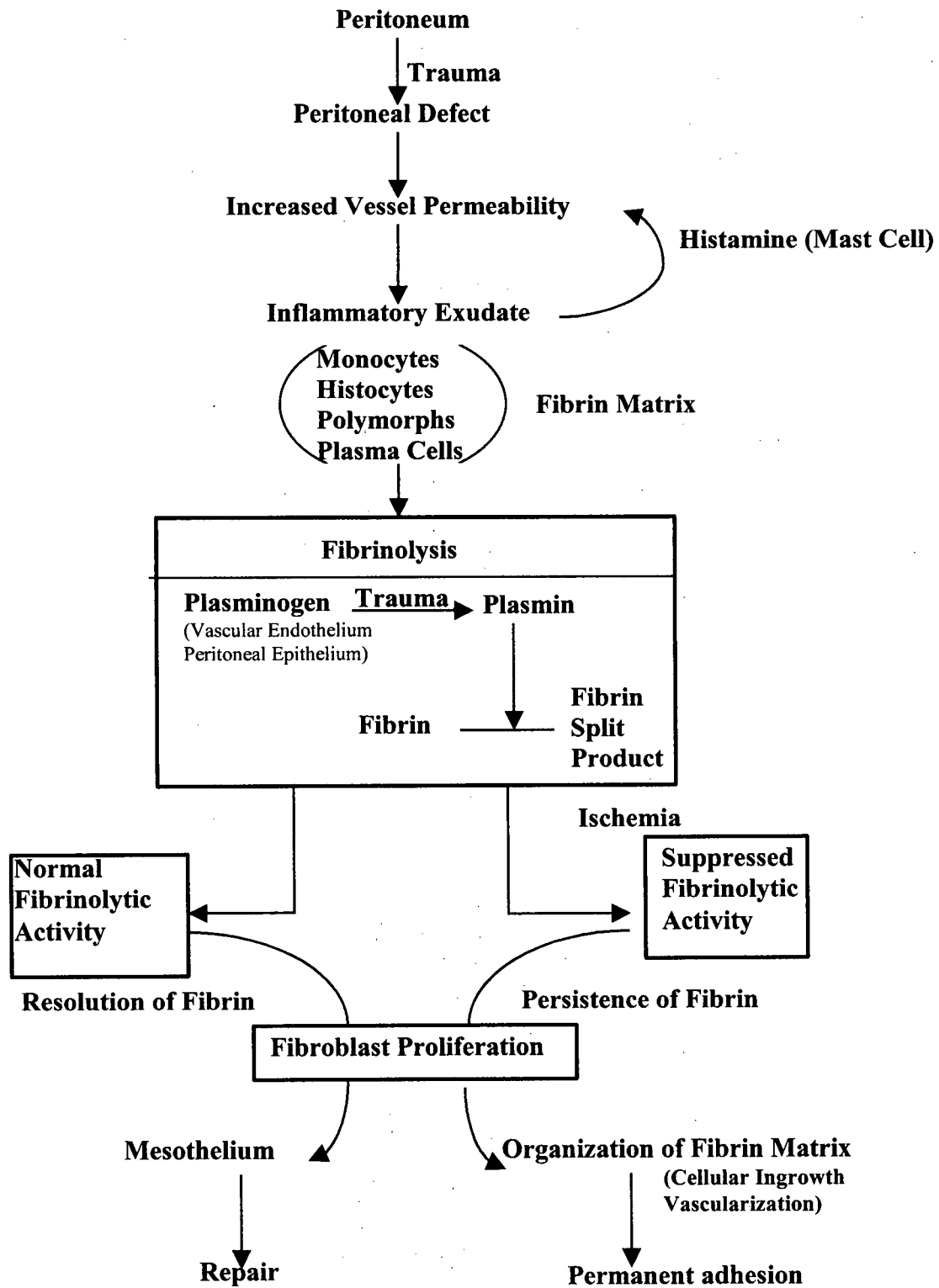
Adhesions are abnormal attachments between tissues or organs that form after an inflammatory stimulus, most commonly surgery (Wiseman, 1994). Three events must occur for permanent adhesions to form (Figure 2):

1. Injury and inflammation: adhesions occur as a result of the inflammation, granulation, and scar formation that follow trauma. A variety of stimuli can induce damage and adhesions: surgical trauma, granulomatous reactions (surgical starch, talc, or cotton lint), infection, ischemia, or radiation. In the traumatized tissues, increased permeability of blood vessels produces a serosanguinous exudate rich in inflammatory cells (Holtz, 1984).

2. Fibrin deposition and reversal of normal fibrinolytic mechanisms: inflammatory exudation or bleeding provide a source of fibrin, which forms a glue by which two adjacent, otherwise unattached, structures may adhere. The ischemic or injured tissue loses its ability to lyse fibrin. Additionally, the ischemic tissue inhibits fibrinolysis by normal adjacent tissue (Wiseman, 1994).

3. Granulation and fibrous ingrowth: if fibrin is not removed, the temporary fibrinous adhesions will develop into permanent fibrous adhesions, by a process of granulation. Macrophages, blood vessels, and fibroblasts invade the fibrin meshwork under the influence of growth factors, cytokines, and inflammatory mediators. Collagen and other connective tissue elements are laid down to form the more permanent band-like adhesion (Wiseman, 1994).

**Figure 2.** Adhesion formation following surgical trauma (peritoneal trauma) (from DiZerega, 1993).



### **2.1.2. Approaches to adhesion prevention and reduction**

There are two major approaches to the prevention or reduction of post-surgical adhesions besides minimizing surgical trauma: use of barriers and use of drugs (Wiseman, 1994).

#### **2.1.2.1. Use of barriers to prevent adhesions**

A physical barrier is interposed between two surfaces, preventing their adherence (Wiseman, 1994). An ideal barrier agent should be non-reactive, stay in place for several days, persist during critical phases of serosal reepithelization and undergo resorption following healing (Gomel, 1996; Harris et al., 1995). The barriers can be classified as: nonabsorbable adhesion barriers, e.g. polytetrafluoroethylene (Gore-Tex<sup>®</sup> surgical membrane) (Boyers and DeCherney, 1988; Haney et al., 1995, 1996); absorbable adhesion barriers, e.g. oxidized regenerated cellulose (Interceed<sup>®</sup>), carboxymethyl cellulose, poloxamer 407, fibrin sealant (Linsky et al., 1987; Saravelos and Li, 1996; Arnold et al., 2000; Haney et al. 1996). Gore-Tex<sup>®</sup> surgical membrane and Interceed<sup>®</sup> have been approved for use in humans (Saravelos and Li, 1996). In addition, a protective coating over healing tissue during the initial postoperative interval is an alternative to a barrier. Dextran and sodium hyaluronate coating solution (Urman et al., 1991) have been shown to be effective in preventing adhesions. Because of multiple animal models and diverse clinical uses, each involving a different level of trauma and blood exposure, efficacy data have been contradictory.

### 2.1.2.2. Use of drugs to prevent adhesions

Based on the mechanisms of adhesion, different classes of drugs have been evaluated by Wiseman (1997) (Table 1).

**Table 1.** Proposed mechanisms of adhesion prevention by class of drugs (from Wiseman, 1997).

Class of drug	Example(s)	Proposed mechanism
Anti-inflammatory	Antihistamines, indomethacin,	Reduce vascular permeability, reduce histamine release and stabilize lysosomes
Fibrinolytic agents	Hyaluronidase, plasminogen activator,	Fibrinolysis, stimulation of plasminogen activator
Anticoagulants	Heparin,	Decrease fibrin deposition
Antibiotics	Tetracycline, cephalosporins,	Prevention of infection thereby decreasing the inflammatory response that would predispose to adhesion formation

To date, none of these drugs has been shown to be uniformly effective.

## 2.2. Paclitaxel

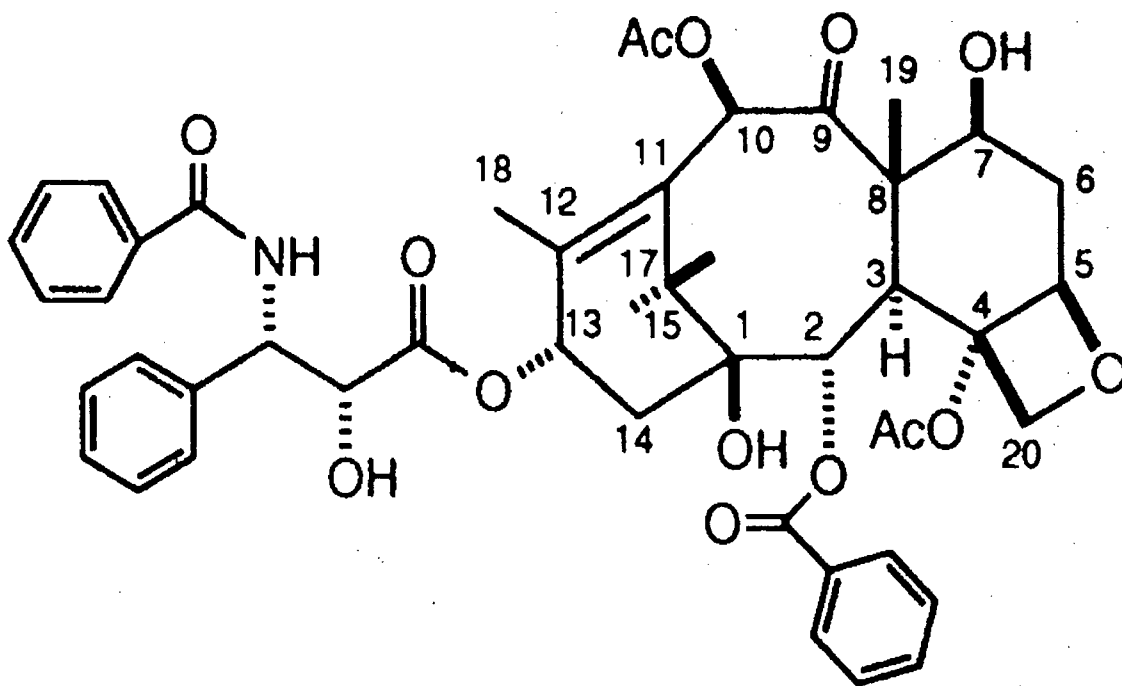
### 2.2.1. Source and structure of paclitaxel

Paclitaxel was initially obtained from *Taxus brevifolia* bark with a 0.02% yield. Subsequently, paclitaxel has been detected or isolated from various other *Taxus* species.

The taxanes baccatin III and 10-deacetyl baccatin III can both be converted into paclitaxel in high yield (Kingston, 1991).

The structure of paclitaxel (Figure 3) consists of a complex taxane ring system linked to a rare four-member oxetan ring at positions C-4 and C-5, and to an ester side chain at C-13. This side chain is necessary for paclitaxel's unique microtubule effects (Rowinsky, 1992). Deletion of the side chain gives baccatin III, which shows a 1700-fold decrease in anti-mitotic activity (Lataste et al., 1984; Miller et al., 1981). Modification of the side chain substituents resulted in a 10 to 300-fold reduction in activity (Wani et al., 1971; Lataste et al., 1984).

**Figure 3.** The chemical structure of paclitaxel. Numbers are assigned to carbons in the structure in IUPAC nomenclature.



## **2.2.2. Chemistry of paclitaxel**

### **2.2.2.1. Stability of paclitaxel**

Due to a number of functional groups in the structure, paclitaxel can undergo hydrolysis, epimerization, acylation, oxidation and reduction reactions. The C-7 hydroxyl group of paclitaxel is part of a  $\beta$ -hydroxycarbonyl system encompassing C-7, C-8 and C-9, and as such is subject to epimerization. The driving force for the epimerization may be in part due to the formation of a hydrogen bond between the 7-epi-hydroxyl group and the C-4 acetate carbonyl group (Kingston, 1991). The epimerization of C-7 hydroxyl group was responsible for only a slight decrease in activity (Lataste et al., 1984).

The stability of paclitaxel in organic solvent systems, such as methanol, chloroform, and isobutyl alcohol was studied by MacEachern-Keith et al. (1997). The results suggested that the degradation of paclitaxel followed first-order kinetics, the principal degradation product being 7-epi-taxol. The chemical degradation of paclitaxel in aqueous buffers (Dordunoo and Burt, 1996) was found to be pH dependent with the greatest stability in the pH range of 3 to 5. Hydrolytic degradation followed pseudo-first order kinetics and the major products were baccatin III, 10-deacetylbaccatin III and baccatin V.

### **2.2.2.2. Solubility of paclitaxel**

Due to its hydrophobicity, paclitaxel has a low aqueous solubility. The values reported vary from 0.7 to 30  $\mu\text{g/ml}$  at 37  $^{\circ}\text{C}$  (Mathew et al., 1992; Liggins, 1998; Lundberg, 1997; Swindell and Krauss, 1991). The difference in solubility is believed to be due to the presence of different hydrate forms or different crystallinities of paclitaxel

(Adams, 1993; Perrone et al., 1996; Liggins et al., 1997). The solubility in hydrocarbon is very high, i.e. 75 mg/ml in triacetin (Meerum Terwogt, 1997).

### **2.2.3. Mechanism of action, clinical use and toxicity of paclitaxel**

The target of paclitaxel is microtubules, which are primary constituents of the mitotic spindle and cytoplasm of interphase cells. They have a role in controlling movement of chromosomes during metaphase and anaphase. The microtubules formed in the presence of paclitaxel are extraordinarily stable and dysfunctional, thereby causing the death of the cell by disrupting the normal microtubule dynamics required for cell division and vital interphase processes (Alastair and Wood, 1995).

Paclitaxel has been used to treat a variety of cancers, such as ovarian cancer, breast cancer and lung cancer (Spenser et al., 1994). The major dose-limiting toxicity associated with paclitaxel administration is neutropenia. Other toxicities including mucositis, hypersensitivity reactions and anemia, have been noted (Finely et al., 1994).

### **2.2.4. Preclinical effectiveness of paclitaxel in post-surgical adhesions**

During adhesion formation, fibrin provides the initial bridge between two tissue surfaces; when the bridge is made of fibrin only, it is amenable to lysis by fibrinolytic mechanisms. However, when fibroblasts proliferate and invade the fibrin meshwork, the temporary adhesion will likely undergo organization into a permanent adhesion (DiZerega, 1993). As an antiproliferative agent, paclitaxel reduces post-surgical adhesions mainly by inhibition of fibroblast proliferation.

The adhesion prevention effect of paclitaxel has been shown in animal models. Hopkins et al. (1997) infused paclitaxel (Taxol<sup>®</sup>) intraperitoneally to rats after they underwent laparotomy. Different groups of rats received Taxol<sup>®</sup> at 2.5 mg/kg, 3.0 mg/kg,

or 3.5 mg/kg daily over a period of 7 days via an intraperitoneal catheter. The data showed that the highest dose of Taxol<sup>®</sup> inhibited surgical adhesions significantly.

In our lab, the anti-adhesion effect of paclitaxel has been studied using the cecal side wall abrasion model in rats (Jackson et al., 2000). Paclitaxel was administered by either intraperitoneal (i.p.) injection of Taxol<sup>®</sup>, or by application of paclitaxel loaded hyaluronic acid (HA) films to the site of the surgical trauma. A control group received no treatment. Taxol<sup>®</sup> treatment groups received Taxol<sup>®</sup> on the day of operation and daily doses of Taxol<sup>®</sup> 4 mg/kg i.p. for 3 days (Group 2), 4 days (Group 3) and 5 days (Group 4). Paclitaxel-HA treatment groups received 1% paclitaxel loaded HA films and 5% paclitaxel loaded films right after the abrasion procedure. Seven days postoperatively, the animals were euthanised and evaluated. For controls (no treatment, n = 10), all animals showed some degree of adhesion formation. For the groups receiving Taxol<sup>®</sup>, 4 out of 10 (Group 2), 7 out of 9 (Group 3), and 5 out of 8 (Group 4) animals showed no evidence of adhesion formation. For the groups receiving paclitaxel loaded HA films, 5 out of 10 (1% paclitaxel) and 8 out of 9 (5% paclitaxel) showed no evidence of adhesion formation.

## **2.3. Polymer chemistry**

### **2.3.1. Structure of polymers**

A polymer is a large molecule constructed from many smaller structural units called monomers covalently bonded together. When only one species of monomer is used to build a macromolecule the product is called a homopolymer. If the chains are composed of two types of monomer unit the material is known as a copolymer (Cowie, 1973).

## 2.3.2. Molar mass of polymers

### 2.3.2.1. Molar mass averages of polymers

Normally a polymeric product contains molecules having many different chain lengths (Van Krevelen, 1990). It is convenient to characterize the distribution in terms of molar mass averages (Young, 1991). The number-average molar mass ( $M_n$ ) is defined as the sum of the products of the molar mass of each fraction multiplied by its mole fraction as given in Equation 1:

$$M_n = \sum X_i M_i \quad (1)$$

Where  $X_i$  is the mole fraction of molecules of molar mass  $M_i$ .

The weight-average molar mass ( $M_w$ ) is defined as the sum of the products of molar mass of each fraction multiplied by its weight fraction as shown in Equation 2:

$$M_w = \sum w_i M_i \quad (2)$$

$M_n$  is most affected by the low molecular weight fraction since a small fraction of low molecular weight molecules by weight may represent a large portion of the total number of molecules present in the polymer, skewing  $M_n$  to a lower value. On the contrary,  $M_w$  is sensitive to the higher molecular weight fraction (Rosen, 1993). The ratio of  $M_w / M_n$  is known as the polydispersity index and used as a measure of the breadth of the molecular weight distribution (Visser, 1996). Typically  $M_w / M_n$  is in the range 1.5 – 2.0 (Young, 1991).

### 2.3.2.2. Molar mass distribution

Molecular weight distribution is an important characteristic of polymers, which can significantly affect polymer properties. Gel permeation chromatography (GPC) is by far the most widely used method of determining molecular weight distribution.

The separation method involves column chromatography in which the stationary phase is a heteroporous, solvent-swollen polymer gel varying in permeability over many orders of magnitude. As the liquid phase, which contains the polymer, is passed through the gel, the polymer molecules diffuse into all parts of the gel not mechanically barred to them. The smaller molecules permeate more completely and spend more time in the pores than the larger molecules that pass through the column more rapidly (Van Krevelen, 1997). The resulting chromatogram is a weight distribution of the polymer as a function of retention volume (Dawkins, 1984). To obtain molecular weights at given retention volumes, the chromatogram may be compared with a chromatogram obtained with fractions of known average molecular weight in the same solvent and at the same temperature (Stevens, 1990). The major problem with calibrating a particular GPC column for a particular polymer is that few standard samples of narrow molecular weight distribution are available commercially. To circumvent this difficulty, the universal calibration method is employed, which is based on the independence of the product of intrinsic viscosity and molecular weight on polymer type. A plot of  $\log([\eta]M)$  versus elution volume in the solvent yields an approximately linear curve for widely disparate groups of polymers (Stevens, 1990). By using polystyrene standards, the universal calibration curve may be established to calculate the molecular weight of the polymer requiring analysis.

### **2.3.3. Polymer crystallinity**

When polymer molecules are arranged in completely random, intertwined coils, this completely disordered structure is known as the amorphous state. When polymer molecules are arranged such that each of their atoms falls into a precise position in a

tightly-packed repeating regular structure, this highly ordered structure is described as the crystalline state (Deanin, 1972). Polymers for all practical purposes never achieve 100% crystallinity so that polymers are categorized as either amorphous or semi-crystalline (Stevens, 1990).

### **2.3.3.1. Models of polymer crystallinity**

Polymer crystallinity can be explained using the fringed micelle model and the chain folded model. The fringed micelle model (Rosen, 1993), as shown in figure 4A, shows that the crystallites are small volumes in which portions of the chains are regularly aligned parallel to one another, tightly packed into a crystal lattice. The individual chains pass from one crystallite to another through amorphous areas. However, this model does not account for polymer chains folding back on themselves, which has been observed in many polymers. Figure 4B (Rudin, 1998) shows a schematic of the chain folded model of polymers in which polymer chains fold back to form lamellar crystallites interspersed in an amorphous matrix.

### **2.3.3.2. Degree of crystallinity**

The degree of crystallinity ( $X_c$ ) of a polymer is defined as the percent weight of crystalline regions per weight of a polymer sample (Tobolsky, 1971). One technique often used to determine  $X_c$  is differential scanning calorimetry (DSC). This involves determining the change in enthalpy ( $\Delta H_f$ ) during the melting (fusion) of a semi-crystalline polymer. The degree of crystallinity can then be calculated by comparing with  $\Delta H$  for a 100% crystalline sample ( $\Delta H_{100\%}$ ) (Runt, 1985).

$$X_c = \frac{\Delta H_f}{\Delta H_{100\%}} \times 100\% \quad (3)$$

### **2.3.4. Thermal properties of semi-crystalline polymers**

The glass transition and the melting transition are two important properties of semicrystalline polymers. These two properties can be rapidly and conveniently studied using DSC.

#### **2.3.4.1. Glass transition**

At sufficiently low temperatures all polymers are hard rigid solids. As the temperature rises, each polymer eventually obtains sufficient thermal energy to enable its chains to move freely enough for it to behave like a viscous liquid. The temperature at which the transition of polymer from glassy to flexible behavior takes place, is known as the “glass transition temperature”, ( $T_g$ ).  $T_g$  characterizes the amorphous phase of a polymer (Holland and Tighe, 1992) in which chain segments may perform rotational and translational motions (Flory, 1953).

A decrease in chain flexibility due to the insertion of side groups and increased intermolecular forces due to hydrogen bonding or dipole interactions will raise  $T_g$  (Jenkins, 1972). The end of a chain is less restrained than a segment in the center of a chain. Therefore, a decrease in molecular weight or presence of low molecular weight compounds will decrease  $T_g$ .

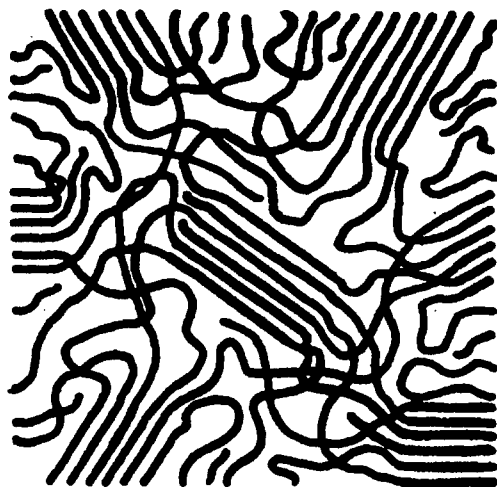
#### **2.3.4.2. Melting transition**

The temperature at which the crystalline phase of a polymer melts is the melting temperature ( $T_m$ ) (Visser et al., 1996). A melting temperature range is observed in all semi-crystalline polymers, because of variations in the sizes and perfection of crystallites (Rudin, 1998).

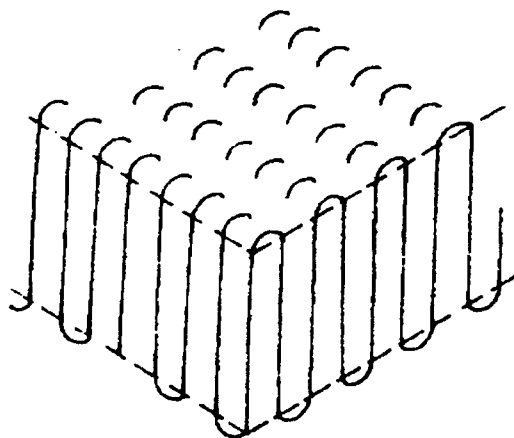
Melting points of semicrystalline polymers have been shown to decrease with decreasing chain length (Rosen, 1993). Melting points increase with an increase in the degree of crystallinity of a polymer (Rosen, 1993).

**Figure 4.** Schematic drawings of A) the fringed micelle model and B) the chain folded model of crystallinity.

A)



B)



## **2.4. Biodegradable polymers as biomaterials**

A biomaterial is a substance that is used in prostheses or in medical devices designed for contact with the living body for an intended method of application and for an intended time period (Piskin, 1994). All biomaterials must meet certain criteria, including the necessary biomechanical properties, biocompatibility, easy purification and sterilization, and suitable surface properties (Piskin, 1994). Biocompatibility may be interpreted to mean that the biomaterials and their degradation products (if they are biodegradable) should not produce undesirable host reactions (e.g., thrombosis, inflammatory reactions, tissue necrosis, toxicity, allergenic reactions, carcinogenesis) (Piskin, 1994).

Biodegradable polymers may be defined as synthetic or natural polymers which are degradable in vivo, either enzymatically or non-enzymatically, to produce biocompatible or non-toxic by-products. These can be further metabolized or excreted via normal physiologic pathways (Jalil and Nixon, 1989). In this work, PLLA, chitosan and hyaluronic acid are all biocompatible and biodegradable polymers.

### **2.4.1. Biodegradation of biodegradable polymers**

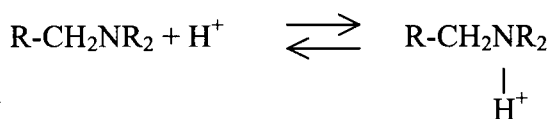
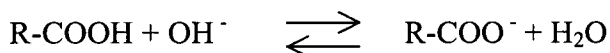
Biodegradation is defined as the conversion of materials into less complex intermediates or end products by solubilization, simple hydrolysis, or the action of enzymes and other products of the organism. Biodegradation of polymers is expected to undergo four stages: hydration, strength loss, loss of mass integrity, and mass loss (Park et al., 1993<sup>a</sup>).

### 2.4.1.1. Solubilization

In contact with an aqueous environment, the hydrophilic polymer in solid form imbibes water and swells to form a hydrogel. Once a gel is formed, water molecules diffuse freely through a rather loose network formed by swollen polymer molecules. Upon further addition of water, polymer-polymer contacts are broken and individual polymer molecules are dissolved in water. This process is generally referred to as erosion (Park et al., 1993<sup>a</sup>).

### 2.4.1.2. Ionization followed by dissolution

Some polymers are initially water-insoluble but become solubilized by ionization or protonation of pendant group. Examples are shown below:



Insoluble

Highly soluble

The solubility of the polymer is strongly pH-dependent. At high pH's, polybases are not water-soluble. As the extent of protonation gradually increases, the polymer becomes more hydrophilic, absorbs water, swells, and finally dissolves in water (Park et al., 1993<sup>a</sup>).

### 2.4.1.3. Chemical hydrolysis

For hydrolysis to occur, the polymer has to contain hydrolytically unstable bonds that should be reasonably hydrophilic for the access of water. Polyesters are degraded

mainly by simple hydrolysis. For semi-crystalline polymers, degradation starts in the amorphous regions, followed by the crystalline domains. The first stage of the degradation process involves non-enzymatic, random hydrolytic ester cleavage. Enzymes are thought to be involved in the degradation of hydrolysis products formed during the initial degradation stage (Park et al., 1993<sup>a</sup>).

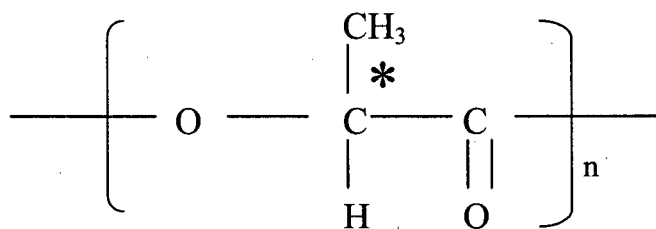
Hydrolytic degradation is more rapid for more hydrophilic polymers. Polymers with high molecular weight, extensive branching, high glass transition temperature, or high crystallinity are generally more resistant to hydrolysis due to the restricted polymer chain flexibility that reduces the diffusion of water (Park et al., 1993<sup>b</sup>).

#### **2.4.2. Poly (L-lactic acid) (PLLA)**

##### **2.4.2.1. Structure, thermal properties and applications of PLLA**

Lactic acid is a chiral molecule that exists in two stereoisomeric forms; L and D. Therefore, there are three forms of poly (lactic acid); D (-), L (+), and the racemic (D, L) forms. PLLA is a semi-crystalline polymer (up to approximately 40% crystallinity) (Figure 5) (Piskin, 1994). Depending on the molecular weight of the polymer, the glass transition appears in the range of 15–35 °C and melting endothermic peaks range from 120 to 160 °C (Huh and Bae, 1996). Since the L (+) form of lactic acid is metabolized in the body, PLLA has attracted a great deal of attention as a biodegradable biomaterial. With high mechanical strength and toughness, semi-crystalline PLLA has been used in diverse applications in orthopedic devices (Piskin, 1994; Holland and Tighe, 1986; Kulkarni et al., 1971). A wide range of drugs ranging from small molecular weight therapeutic agents to peptide hormones, antibiotics, and chemotherapeutic drugs have been evaluated using PLLA to achieve controlled drug delivery (Jalil, 1990).

**Figure 5.** The chemical structure of poly (L-lactic acid). The asterisk (\*) denotes a chiral carbon in the polymer backbone.



#### 2.4.2.2. Biocompatibility of PLLA

Typically, the biocompatibility of a material is determined through histological evaluations as a function of implantation time in a suitable animal model (Hooper et al., 1998). Poly (lactic acid) polymers are considered to be fully biocompatible in their various applications (Pistner et al., 1993). No inflammatory or foreign body reaction to PLLA rods was observed in the medullary cavity of rabbits for one year (Matsusue and Yamamuro, 1992). Only very mild inflammatory reactions in rats were observed when PLLA discs were implanted subcutaneously (Bergsma et al., 1995) or PLLA rods implanted intraosseously (Bergsma et al., 1996) over a one year period.

#### 2.4.2.3. Biodegradation of PLLA

PLLA polymer chains are cleaved by hydrolysis to the monomeric acids and are eliminated from the body through the Krebs cycle, primarily as carbon dioxide and in urine (Lewis, 1990).

A two-stage chemical hydrolysis mechanism was proposed by Chu et al. (1981). Diffusion of water into the amorphous regions of the polymer occurs, producing random hydrolytic scission at the susceptible ester linkage. When most of the amorphous regions have been eroded, the second stage commences with hydrolysis of the crystalline regions.

The hydrolysis can be catalyzed by both acid and alkaline conditions (Makino et al., 1985, 1986; Tsuji, 2000; Lu et al., 2000). The  $\text{OH}^-$  or  $\text{H}_3\text{O}^+$  attacks the ester bonds, followed by further cleavage of the initial products into fractions with lower molecular weights (Makino et al., 1985). Crystallinity, molecular weight and water uptake are key factors in determining the rates of PLLA degradation (Lewis, 1990).

Enzymatic hydrolysis of PLLA in the presence of pronase, proteinase-K and bromelain has also been reported (Williams, 1981; Leenslag et al., 1987; Iwata and Doi, 1998; Tokiwa et al., 1999). Furthermore, Makino et al. (1984, 1985) showed that the addition of carboxylic esterase promoted the degradability of PLLA by cleaving groups located in the crystalline zone directly. In addition, microbial degradation of PLLA has been demonstrated by Karjomaa et al. (1997).

### **2.4.3. Chitosan**

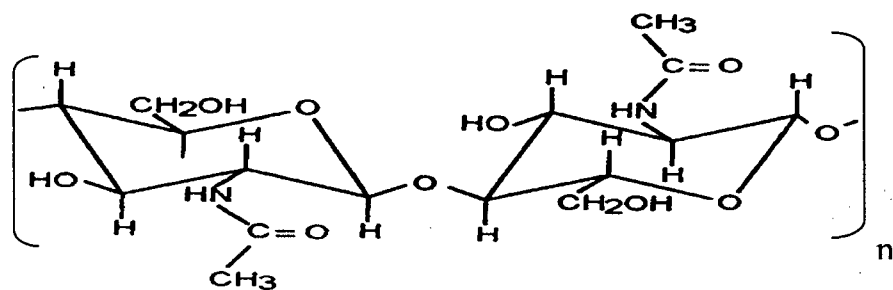
#### **2.4.3.1. Physicochemical and biological properties of chitosan**

Chitin, poly- $\beta$ -(1-4)-N-acetyl-D-glucosamine, is the main component of shells of crab, shrimp and krill. Chitosan is the deacetylated product of chitin, comprising copolymers of glucosamine and N-acetylglucosamine (Figure 6) (Hon, 1996). Chitosan is soluble in acidic solutions but is insoluble at  $\text{pH} > 6.5$  and in most organic solvents (Knapezyk et al., 1989). The degree of deacetylation is one of the most important chemical characteristics of chitosan, which determines the content of free amino groups in the polysaccharide.

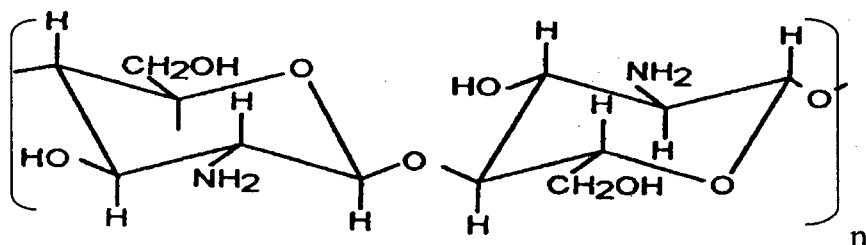
Chitosan exhibits favorable biological properties such as a lack of toxicity, biocompatibility, and biodegradability (Bhaskara Rao and Sharma, 1997; Felt et al., 1998; Jameela et al., 1995; Tomihata and Ikada, 1997; Muzzarelli, 1997). Additionally it

has good mucoadhesive properties. The mucoadhesive properties are probably mediated by ionic interactions between the positive amino groups of the polysaccharide and the negative residues of sialic acid in mucus (He et al., 1998).

**Figure 6.** The chemical structure of (1) chitin and (2) chitosan.



(1)



(2)

#### 2.4.3.2. Pharmaceutical applications of chitosan

Due to its polymeric cationic character and its gel and film-forming properties, chitosan has been extensively examined in controlled drug release systems. Kristle et al. (1993) evaluated lidocaine-loaded chitosan hydrogels, which released the drug by almost zero order kinetics. The gel-forming property of the chitosan at low pH, along with its antacid and antiulcer properties, makes it an interesting agent to prevent gastric irritation. Due to good mucoadhesive properties, chitosan is a promising candidate for the development of nasal drug delivery systems with controlled drug release characteristics.

(Illum et al., 1994; Aspden et al., 1997). Zhou and Donovan (1996) showed in a rat model that incorporating chitosan in nasal formulations resulted in a significant increase of the residence time of the formulations in the nasal cavity. Glutaraldehyde crosslinked chitosan microspheres loaded with either cisplatin (Nishioka et al., 1990) or mitoxantrone (Jameela and Jayakrishnan, 1995) have been formulated and a controlled release of drug was achieved.

#### **2.4.3.3. Biodegradation of chitosan**

Chitosan can be hydrolyzed by a number of enzymes, such as chitosanase, chitinase, lysozyme, esterases, and carboxy peptidase (Ishiguro et al., 1992; Varum et al., 1997; Bhaskara et al., 1997; Muzzarelli, 1997, Onishi and Machida, 1999). Among these enzymes, lysozyme has been extensively studied. Lysozyme is found in various body fluids and tissues of humans (Nordtveit, 1996). It was demonstrated that there was a specific interaction between lysozyme and the N-acetylated unit in the chitosan (Ishiguro et al., 1992; Nordtveit Hjerde et al., 1996; Kristiansen et al., 1998). The lysozyme hydrolysis increased with increasing N-acetylated units in the chitosan (Nordtveit Hjerde, 1996; Varum et al., 1997). In addition, as with all polysaccharides, depolymerization may occur by acid hydrolysis and an oxidative-reductive depolymerization reaction (Varum et al., 1997).

#### **2.4.3.4. Adhesion prevention effect of chitosan**

The adhesion prevention effect of a derivative of chitosan, N, O- carboxymethyl chitosan (NOCC), was studied by Kennedy et al. (1996). NOCC was administered as a sterile 2% solution or a 1% crosslinked gel in two rat models of surgical adhesions: the uterine horn model and the small bowel laceration model. It was found that NOCC

consistently reduced the size, strength and number of adhesions in both models. The mechanism of action of NOCC is still unclear. There are several possibilities by which NOCC may exert its antiadhesive activity including diluting fibrin in the original inflammatory exudates, affecting the activities of the inflammatory factors, or acting as a physical barrier by coating two surfaces (Kennedy et al., 1996).

#### 2.4.4. Hyaluronic acid (HA)

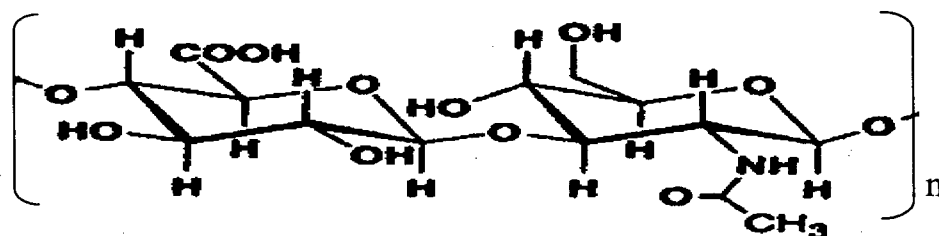
##### 2.4.4.1. Physicochemical properties of HA

HA is a water-soluble glycosaminoglycan consisting of alternating  $\beta$ D(1-4)-linked 2-acetamido-2-deoxy-D-glucose and  $\beta$ D(1-3)-linked D-glucuronic acid (Figure 7). It is widely distributed in the extracellular matrix of connective tissues, and is present in synovial fluid, the aqueous and vitreous humour of the eye, and other tissues (Goa and Benfield, 1994). HA exists in a random coil configuration, which is polyanionic at physiological pH. At high molecular weight, these random coils become entangled to form a viscoelastic gel (Goa and Benfield, 1994; Ambrosio et al., 1999).

##### 2.4.4.2. Biodegradation and crosslinking of HA

In vivo, HA is mainly degraded by two mechanisms: (1) via hyaluronidase as a specific enzyme and (2) via hydroxyl radicals as a source of active oxygen (Yui et al., 1992; Vercruyssen et al., 1997). The mechanism of HA degradation in the acute inflammatory process is probably due to the generation of hydroxyl radicals.

**Figure 7.** The chemical structure of hyaluronic acid.



HA is rapidly cleared from plasma, almost wholly by degradation to lower molecular weight products. The plasma elimination half-life for injected HA in humans is very short, at 2.5 to 5.5 minutes (Goa and Benfield, 1994). Therefore, chemical modifications of HA are required for pharmaceutical applications. HA, ranging in size from six disaccharide units (1200 Da) to very high molecular weights (> 2,000,000 Da), can be modified and crosslinked hydrogels can be formed (Prestwich et al., 1997).

Cross-linking of HA has been explored using different chemical agents (Bulpitt and Aeschlimann, 1999; Prestwich et al., 1998; Pouyani and Prestwich, 1994; Simkovic et al., 2000; Rehakova et al., 1996; Vercruyssen et al., 1997; Tomihata and Ikada, 1997<sup>ab</sup>). Tomihata and Ikada (1997<sup>b</sup>) used carbodiimide to crosslink HA in order to obtain slow degrading hydrogels. Carbodiimide caused crosslinking by the intermolecular formation of ester bonds between the hydroxyl and carboxyl groups belonging to different polysaccharide molecules. Subcutaneous implantation of the crosslinked films elicited no significant inflammatory reaction in the surrounding tissue (Tomihata and Ikada, 1997<sup>b</sup>).

#### **2.4.4.3. Clinical and pharmaceutical applications of HA**

HA possesses a high capacity for water sorption, water retention and lubrication. This property has allowed it to be applied in ophthalmic surgery as a viscoelastic material and in orthopedic surgery for the treatment of articular diseases (Tomihata and Ikada, 1997<sup>a</sup>). Its biocompatibility, water solubility, and ability to be chemically modified allow high drug loading for use in drug delivery systems (Vercruyssen et al., 1997). HA has been used as a solution for delivery of peptide growth factors (Prisell et al., 1992) or as a gel for diclofenac (Moore and Willoughby, 1995). Through the esterification of carboxyl groups of hyaluronic acid, hyaluronic acid esters have been produced. The microspheres

prepared using the hyaluronic acid esters have been evaluated as delivery devices for nerve growth factors (Ghezzi et al., 1992), hydrocortisone (Benedetti et al., 1990) and insulin (Illum et al., 1994).

#### **2.4.4.4. Adhesion prevention effect of HA**

The effectiveness of HA in preventing post-surgical adhesions has been widely studied. The gels formed from 2% sodium hyaluronate in buffer reduced the extent and severity of tendon adhesions in chicken models (Miller et al., 1997). An autocrosslinked ester of HA demonstrated greater adhesion prevention compared to oxidized regenerated cellulose in the rabbit uterine horn model (De Laco et al., 1998). Intraperitoneal instillation of 1% HA significantly minimized adhesions induced by local abrasion of the uterine surfaces (Shushan et al., 1994). The mechanism may involve inhibition of platelet aggregation. Moreover, pretreatment with HA also reduced intraperitoneal adhesion significantly (Urman et al., 1991).

### **2.5. Development of controlled release paclitaxel-loaded polymer films**

Our novel approach is to load paclitaxel-encapsulated microspheres into chitosan and HA films (hydrogel systems). To our knowledge there has been no reported work on this type of formulation approach.

#### **2.5.1. PLLA microspheres**

##### **2.5.1.1. Preparation of poly (lactic acid) microspheres**

Poly (lactic acid) microspheres have been prepared using different methods, such as solvent evaporation and solvent extraction, double emulsion, phase separation (coacervation), and spray-drying (Jain et al., 1998; Arshady, 1991, 1992; Conti et al., 1992; Pavanetto et al., 1993). The double emulsion process is essentially a water-in-oil-in

water (W/O/W) method and is best suited to encapsulate water-soluble drugs such as peptides, proteins and vaccines (Giunched et al., 1998; Soriano et al., 1995; Crotts and Park, 1995). The solvent evaporation method uses an oil-in-water (O/W) emulsion, which works best for water-insoluble drugs (Bodmeier and McGinity, 1987). In the solvent evaporation process, the active ingredient is dissolved or dispersed in a solution of the polymer in a suitable water-immiscible and volatile organic solvent. This solution or dispersion is emulsified in an aqueous medium to form microdroplets. The organic solvent then diffuses into the aqueous phase and evaporates at the water-air interface. The microdroplets solidify and solid, free-flowing microspheres are obtained after complete organic solvent evaporation, filtration, and drying (Bodmeier and McGinity, 1987; O'Donnell and McGinity, 1997). A variety of drugs, ranging from small molecular weight therapeutic agents to peptide hormones, antibiotics and chemotherapeutic agents, have been incorporated into poly (lactic acid) polymers, producing microspheres with controlled drug release characteristics (Juni and Nakano, 1987; Izumikawa et al., 1991; Tsai et al., 1986; Jalil and Nixon, 1992).

#### **2.5.1.2. Drug release from polymeric microspheres**

Drug release from polyester microspheres has been reported to be triphasic (Sanders et al., 1994; Spenlehauer et al., 1988; Liggins, 1998). Initially, a burst phase of release was observed due to release of drug located near the microsphere surface. This was followed by a period of slow release, which was attributed primarily to diffusion of the drug out of the microsphere. There was then an increase in the drug release rate, due to a combination of diffusion and degradation of the polymer matrix.

The decrease of molecular weight of a polymer results in an increased hydrophilicity of the matrix, decreased density and a lowered glass transition temperature, which allows swelling of the matrix and greater molecular mobility of the drug and polymer chains. Therefore a faster drug release rate was achieved with a lower molecular weight matrix (Spenlehauer et al., 1988; Izumikawa et al., 1991; Wakiyama et al., 1982; Jalil and Nixon, 1990<sup>a</sup>; Liggins, 1998). Decreased size of microspheres leads to faster drug release rate owing to the decreased diffusional path length and the increased surface area in contact with the release medium (Jameela and Jayakrishnan, 1995; Wakiyama et al., 1981). In addition, an increase in drug loading results in an increased drug release rate due to a decreased amount of polymer matrix as a diffusion barrier (Leelarasamee et al., 1986) and an increased drug concentration gradient as a driving force for diffusion.

#### **2.5.1.3. Selection of 2 k g/mol PLLA for microspheres**

It has been suggested that drug release from a surgical adhesion barrier should be rapid and complete in less than 4 weeks. The in vitro release profiles of paclitaxel from PLLA microspheres prepared with PLLA with increasing molecular weight from 2k to 50k g/mol showed a decrease in the rate and extent of paclitaxel release (Liggins, 1998). In our formulation, 2k g/mol PLLA was selected for microspheres preparation in order to achieve more rapid paclitaxel release properties.

#### **2.5.2. Drug release from microsphere-loaded films**

We postulate that there are two major stages of drug release from microsphere-loaded films. (1) Diffusion and degradation controlled release of paclitaxel from PLLA

microspheres into the hydrogel film (see section 2.4.2.3. and 2.5.1.2.). (2) Drug diffusion through the hydrogel to the external medium.

Solute transport through polymeric membranes is generally described in terms of two mechanisms, the pore mechanism and the partition mechanism (Zenter et al., 1978). In the pore mechanism, solutes are presumed to permeate the membrane by diffusion through microchannels or pores within the membrane structure. This is further explained by the 'free volume' theory (Yasuda et al., 1971). The free volume of a hydrated polymer membrane can be visualized as the fluctuating pores or channels inside the hydrated matrix, which are not occupied by the polymer backbone. The theory postulates that for solute diffusion within the hydrated polymer matrix, the solute must jump from one void to the next, and relates the diffusion rate to the probability of finding a void with sufficient size to accommodate the solute. In the solution-diffusion or partition mechanism, solutes transverse the membrane by a process involving solute dissolution in the membrane structure followed by solute diffusion along and between the polymer segments that make up the membrane structure.

It has been reported that the pore mechanism described the transport of many hydrophilic drugs (Domb et al., 1990; Simon et al., 1997, Papini et al., 1993; Thacharodi and Rao, 1993<sup>a</sup>). However, for the transport of hydrophobic drugs some were consistent with the pore mechanism (Kim et al., 1979; Zentner et al., 1979) and others were governed by both the pore mechanism and the partition mechanism (Hunt et al., 1990; Nakatsuka and Andradý, 1992; Thacharodi and Rao, 1993<sup>b</sup>).

## 2.6. Objectives

The overall objective of this work was to develop and characterize a paclitaxel-loaded drug delivery system composed of drug-loaded microspheres dispersed in a hydrogel matrix film for application in the prevention of post-surgical adhesions. The specific aims of this project were to:

- 1) Prepare control and paclitaxel-loaded PLLA (2k g/mol) microspheres
- 2) Characterize the physicochemical properties and release profiles of paclitaxel-loaded microspheres
- 3) Fabricate and characterize the physicochemical properties of microsphere-loaded chitosan and HA films and determine the release profiles of paclitaxel from microsphere-loaded films

### **3. EXPERIMENTAL**

#### **3.1. Materials and supplies**

##### **3.1.1. Paclitaxel**

Paclitaxel was purchased from Hauser (Boulder, CO, USA) and stored at  $-4^{\circ}\text{C}$  in a freezer.

##### **3.1.2. Chemicals and solvents**

Poly (L-lactic acid) PLLA: MW 2k g/mol, Polysciences Inc. (Warrington, PA, USA)

Chitosan: MW 70k and 150k g/mol, Fluka (Switzerland)

Sodium hyaluronate: MW  $0.8 - 1.6 \times 10^6$  g/mol, Sigma Chemical Co. (St. Louis, MO, USA)

1-Ethyl-3-(3-dimethyl amino-propyl) carbodiimide (EDAC) hydrochloride: MW 191.7, Sigma Chemical Co. (St. Louis, MO, USA)

Poly (vinyl alcohol) (PVA): 98% hydrated, MW 13k – 23k g/mol, Aldrich Chemical Company, Inc. (Milwaukee, WI, USA)

Polystyrene standards: MW 600-4000 g/mol, Polysciences Inc. (Warrington, PA, USA)

Polysorbate 80: Sigma (St. Louis, MO, USA)

Bovine serum albumin Fraction-V: Boehringer Mannheim (German)

Sodium phosphate monohydrogen ( $\text{Na}_2\text{HPO}_4$ ) and sodium dihydrogen orthophosphate ( $\text{NaH}_2\text{PO}_4 \cdot \text{H}_2\text{O}$ ): BDH Inc. (Toronto, ON, Canada)

Sodium chloride (NaCl): Acros Organics (Belgium, New Jersey, USA)

Indium standard (99.99%): Sigma (St. Louis, MO, USA)

Tetrahydrofuran (THF), dichloromethane (DCM), acetonitrile and methanol were HPLC grade, Fisher Scientific (Fairlawn, New Jersey, USA)

### **3.1.3. Glassware**

Test tubes for in vitro release studies were 15 ml and 50 ml Kimax<sup>®</sup> test tubes with Teflon<sup>®</sup>-lined screw-capped lids. Beakers, jars, Erlenmeyer flasks and graduated cylinders were Pyrex<sup>®</sup> brand. Scintillation vials (20-ml) with polypropylene-lined screw-capped lids were used for microspheres storage. All glassware was obtained from Fisher Scientific (Toronto, ON).

### **3.1.4. Phosphate-buffered saline with albumin (PBS-A), HPLC mobile phase and poly (vinyl alcohol) (PVA) solution**

PBS-A containing 0.4% albumin was prepared using sodium phosphate monobasic dihydrate, 1.26 g, sodium phosphate dibasic, 8.60 g, bovine serum albumin (Fraction v), 1.6 g, sodium chloride, 32.88 g, and distilled water, 4.0 L. All ingredients were contained in a 4 L Erlenmeyer flask and stirred at room temperature to dissolve the solids. The pH of the solution was in the range of 7.2 - 7.4. PBS-A was stored at 4 °C in a refrigerator.

The HPLC mobile phase was prepared by mixing 50 ml of methanol, 370 ml of distilled water, and 580 ml of acetonitrile in 1 L graduated cylinder and filtered through 0.45 µm Millipore<sup>®</sup> membrane filter (Millipore Corp., Massachusetts). All solvents were HPLC grade.

A 10% poly (vinyl alcohol) (PVA) solution in distilled water was prepared by combining 40 g PVA with 400 ml of distilled water in a 1 L beaker, and boiling with

stirring to dissolve the PVA. The 10% PVA solution was then cooled and stored at 4 °C in a refrigerator.

## **3.2. Equipment**

### **3.2.1. Apparatus for microsphere preparation**

The apparatus for microsphere preparation was comprised of an RZR-2000 digital stirrer (Wiarnton, Canada) with a four-blade impeller. For the 4-blade impeller, each blade was a 90° sector, which inclined 15° from horizontal. The stirrer could provide the varied stirring speed up to 2000 rpm.

### **3.2.2. HPLC**

Chromatographic analyses of paclitaxel was conducted with a Waters HPLC (Milford, MA) system, consisting of a model 717+ autosampler, a model 600 controller and pump module, a model 486 tunable absorbance detector and a model 746 data collection module. The column used was a Novo-Pak C<sub>18</sub> column (Millipore Corporation, MA).

### **3.2.3. Scanning electron microscope**

Surface morphology studies of microspheres and films were performed with a Hitachi S-2300 scanning electron microscope (Tokyo, Japan). Samples were coated using a Hummer sputter coater (Technics, Alexandria, VA).

### **3.2.4. Particle size analyzer**

The particle size distributions of microspheres were analyzed by a Coulter LS130 laser scattering particle size analyzer (Coulter Scientific, Amherst, MA) with Coulter LS130 /La130 version 1.53 software.

### **3.2.5. Differential scanning calorimeter (DSC)**

The DSC (Perkin Elmer, Norwalk, CT) was composed of a Pyris 1 DSC module and Cryo Fill model liquid nitrogen cooling system, which was controlled with Pyris Series computer software. Aluminum sample pans were from Perkin Elmer (Norwalk, CT).

### **3.2.6. X-ray powder diffractometer**

The X-ray powder diffractometer was a Geigerflex model (Rigaku Inc., Tokyo, Japan) with 4 components: a heat exchanger unit, an X-ray generator with a goniometer, a D/MAX-B controller interface, and a Dexton PCII 286 computer.

### **3.2.7. Gel permeation chromatography**

Gel permeation chromatographic analyses of polymers were conducted using a Shimadzu HPLC system (Shimadzu Corporation, Tokyo, Japan), composed of a SIL-9A auto injector and a LC-10AD HPLC pump. The refractive index detector was from Waters (Milford, MA). The system was controlled by Class VP software. The GPC column used was made of PLgel 5  $\mu\text{m}$  with a pore size of  $10^3 \text{ \AA}$  (Hewlett Packard).

### **3.2.8. Centrifuge, incubator and oven**

A centrifuge, model GS-6 (Beckman Instruments inc., Palo Alto, CA) was used during microsphere manufacture and release studies from microspheres.

An isotemp incubator (Sheldon Manufacture Inc., Portland, OR) and a culture tube rotator with a rotation speed control unit (VWR, Toronto, ON) were used for microsphere release studies. An Innova 4000 incubator shaker (New Brunswick Scientific, Edison, NJ) was used for degradation studies and release studies from films.

A Napco vacuum oven model 5831 (Precision Scientific, Chicago, IL) equipped with an Emerson vacuum pump model SA55NXGTE4870 (Emerson Motor, St. Louis, MO) was used to dry microspheres and chitosan and HA films for degradation studies.

### **3.2.9. Other equipment**

Olympus optical microscope model BH-2 (Olympus Optical, Japan)

Reacti-Therm III heating/stirring module (Pierce Inc. Rockford, IL)

Vortexer (VWR, Bohemia, NY)

Mettler balances model PJ300, AJ100, and AE163 (Mettler instruments, Zurich, Switzerland)

Accumet pH meter model 610A (Fisher Scientific Inc., Fairlawn, NJ)

Refrigerator (Caltel Scientific, Richmond, BC)

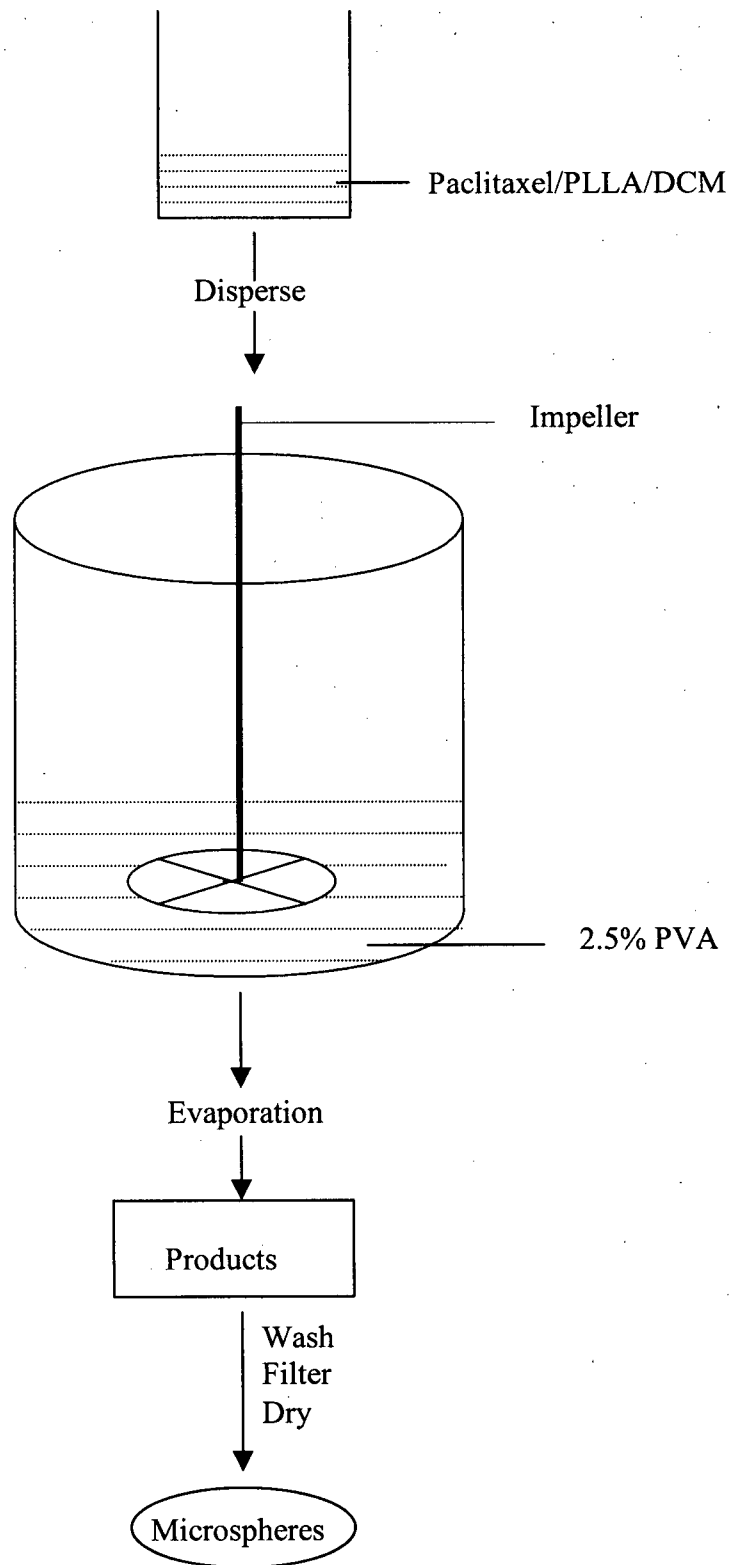
Branson ultrasonic cleaner (Branson Ultrasonics Corporation, Danbury, CT)

### **3.3. Preparation of PLLA microspheres**

The microspheres were prepared using the solvent evaporation method based on Liggins, 1998 (Figure 8). Concentrations of solutions of 5, 10, 15, and 20% (w/v) PLLA in DCM were evaluated to make paclitaxel-free control microspheres. Varied amounts of polymer (PLLA) were dissolved in 5 ml of DCM. The organic solution was dropped into 100 ml of agitated aqueous phase, 2.5% PVA solution in a glass jar. The resulting emulsion was stirred continuously at 600 rpm for 2.5 hrs at room temperature and under ambient pressure. The formed microspheres were then rinsed with distilled water by centrifugation (914 x g) 4 times for 10 min. The washed microspheres were sieved through 90  $\mu\text{m}$  and 53  $\mu\text{m}$  meshes and collected into pre-weighed 20-ml scintillation vials. The vials were left uncapped in the fume hood for 48 hrs. The yields of

microspheres prepared with different concentrations of PLLA were compared and the optimal concentration of 5% and 10% was used to prepare all subsequent batches of microspheres.

**Figure 8.** Flowchart of preparation of paclitaxel loaded microspheres (adapted from Deluca et al., 1992).



Paclitaxel loadings of 5, 10 and 25% (w/w) were obtained by varying the paclitaxel/polymer ratio. Paclitaxel and PLLA were dissolved in 5 ml of DCM. The other procedures were the same as those for making paclitaxel free microspheres.

Microspheres of 20% paclitaxel loading in different size ranges were manufactured by varying the stir speed and PVA concentrations. The conditions are given in Table 2.

**Table 2.** Conditions for preparation of PLLA (2k g/mol) microspheres in different size ranges. Polymer concentration was 5% w/v.

Size range ( $\mu\text{m}$ )	Stir speed (rpm)	PVA concentration (% w/v)
< 10	1500	5
10-50	900	2.5
50-90	600	2.5

### **3.4. Physicochemical characterization of PLLA (2k g/mol) microspheres**

#### **3.4.1. Particle size analysis**

Particle size distributions of microspheres were determined using a laser diffraction particle size analyzer. In a 20-ml scintillation vial, 5-10 mg of microspheres samples were suspended in 15 ml of distilled water with two drops of 1% polysorbate 80 and sonicated for 2 minutes to prevent aggregation of microspheres. The suspension was then transferred to the measurement cell for analysis.

#### **3.4.2. Surface morphology of microspheres**

SEM was used to characterize the surface morphology of microspheres. The dried samples were spread on the conductive adhesive surface of the sample holder. The sample holders were placed into a coater with a high vacuum. When a vacuum pressure reached  $10^{-5}$  torr, argon gas was turned on and sputtered. Samples were coated with gold-palladium for 30 seconds. For some samples a second coating was added at an angle of  $45^{\circ}$ . After coating, samples were placed into the SEM and observed at 20 kV.

#### **3.4.3. Evaluation of the water-soluble fraction of PLLA**

To 100 mg 2k g/mol PLLA in 20-ml scintillation vials were added 1 ml of DCM. The vials were rotated to spread a thin layer of polymer against the wall. After the evaporation of DCM, 20 ml of distilled water were then added and the vials were agitated in an incubator at 100 rpm 37 °C to leach out the water-soluble fraction of PLLA. The leaching process was conducted for 14 hours and then the material was dried under vacuum at room temperature. The weights of the original material and the final material after the leaching process were recorded. The water-soluble fraction of PLLA was then calculated as the difference between the original weight of the polymer and the final weight of the material.

#### **3.4.4. Recovery assays for total content of paclitaxel in microspheres**

One ml of 1 mg/ml paclitaxel in acetonitrile and 1 ml of 4 mg/ml PLLA in DCM were mixed in a 16-ml test tube. To the solution, 15 ml of 60: 40 acetonitrile: water were added. The volumes of the upper and lower phases were measured and the paclitaxel content was determined in both phases by HPLC. Percent recoveries in each phase and the total percent recovery were determined based on four replicates of samples.

#### **3.4.5. Determination of the total content of paclitaxel in microspheres**

An accurately weighed quantity of 5 mg of microspheres were dissolved in 1 ml of DCM in a 16-ml tube and left for 5 minutes. To the solution, 15 ml of 60: 40 acetonitrile: water were added. The tube was shaken vigorously and then centrifuged at 228 x g for 5 minutes. Two phases were produced and PLLA was precipitated at the interface. The paclitaxel content of the upper phase and lower phase was determined by HPLC. Values

of total content of paclitaxel were based on triplicates for each formulation and were reported as the mean  $\pm$  standard deviation.

#### **3.4.6. X-ray powder diffraction**

The X-ray powder diffraction patterns of paclitaxel, PLLA and PLLA microspheres were measured using a Geigerflex X-ray diffractometer. Two hundred to 400 mg samples were loaded into the sample holder for studies. The X-ray source was CuK $\alpha$  radiation (40 kV, 20 mA). The  $2\theta$  range scanned was from  $5^\circ$  to  $50^\circ$  at a rate of  $1^\circ$   $2\theta$ /min.

#### **3.4.7. Thermal analysis**

Approximately 5 mg of paclitaxel, PLLA and microsphere samples were accurately weighed into aluminum open pans. Scanning rates from 5 to  $40^\circ\text{C}/\text{min}$  were evaluated and  $20^\circ\text{C}/\text{min}$  was chosen to study the thermal properties of samples.

#### **3.4.8. Paclitaxel analysis**

##### **3.4.8.1. Extraction of paclitaxel from PBS-A release medium**

To 15 ml of paclitaxel in PBS-A release medium, were added 1 ml of DCM and shaken vigorously. After 5 minutes, the two phases were separated, an upper phase and lower phase. The upper phase was discarded and the lower phase was analyzed further.

##### **3.4.8.2. Reconstitution of paclitaxel**

The organic phase was evaporated to dryness in a Reacti Therm-III module at  $60^\circ\text{C}$  under a gentle stream of nitrogen gas. To the residue was added 1 ml of acetonitrile: water 60: 40 and vortexed to reconstitute the paclitaxel.

#### **3.4.8.3. Quantitative analysis of paclitaxel using HPLC**

The reconstituted paclitaxel solution was transferred into 1ml HPLC sample vials. Paclitaxel was assayed at ambient temperature with an injection volume of 20  $\mu$ l. The Nova-Pak C<sub>18</sub> column was employed as stationary phase and acetonitrile: water: methanol 58: 37: 5 as mobile phase, flowing at 1 ml/min. The detection absorbance wavelength was set at 232 nm.

#### **3.4.9. Validation of the paclitaxel standard curves used for HPLC analysis**

The validation procedures were based on the recommendations of Shah et al. (1992). A standard curve for paclitaxel was prepared by dissolving paclitaxel in acetonitrile: water 60: 40 in the range of 0.3 to 20  $\mu$ g/ml. The injection volume was 20  $\mu$ l and the mobile phase was acetonitrile: water: methanol 58: 37: 5 flowing at 1 ml/min through a Novo-Pak C<sub>18</sub> column. Limit of quantitation is the lowest concentration of an analyte that can be measured with a stated level of confidence (Shah et al., 1992), which was estimated at 0.07  $\mu$ g/ml. For each day, 4 standard curves were constructed, and this was conducted successively for 3 days. Intra-and inter-day precision and accuracy were determined with single-factor ANOVA. For all precision and accuracy data, values were reported as the mean  $\pm$  standard deviation.

Intra-day precision was expressed by relative standard deviation (RSD) of the average of the four replicate data points on each day. Inter-day precision was expressed by RSD of the average of the twelve replicate data points over three days. Values of RSD of less than 10% were considered an acceptable level for precision at each concentration. Inter-day precision was also determined as the significance level of ANOVA tests between each of the three days' sets of four replicate data points for each concentration.

A p-value less than 0.05 suggested a significant difference between days in the means of a given concentration.

Accuracy values were expressed by the average percent bias based on three replicate spiked paclitaxel solutions. Bias is the average deviation from the predicted value of paclitaxel concentrations measured from spiked samples for each of the concentration data points. Sufficient accuracy for each concentration was defined as a bias of less than 10%.

Linearity was expressed as the coefficient of determination ( $R^2$ ) of the curves.

### **3.5. Casting of chitosan and HA films**

#### **3.5.1. Casting of chitosan films**

##### **3.5.1.1.1. Preparation of chitosan solutions**

Chitosan samples with MW 70k and subsequently, 150k g/mol, were employed due to the lack of availability of 70k material as studies progressed. Chitosan dispersions were prepared by dissolving chitosan in 1% (v/v) acetic acid at 37 °C with agitation at 100 rpm for 24 hours. The dispersions were filtered through 40-60 µm Pyrex® filters to remove undissolved substances.

##### **3.5.1.1.2. Casting chitosan films without microspheres**

A chitosan solution (4 g) was poured into a 2.5 cm level Petri dish and left in the fume hood for 3 days where it evaporated to dryness at room temperature.

##### **3.5.1.1.3. Casting chitosan films containing microspheres**

Chitosan films with MW 70k g/mol were prepared by first dispersing a certain amount of 20% paclitaxel-loaded microspheres in different size ranges (< 10, 10-50 and

50-90  $\mu\text{m}$ ) in 500  $\mu\text{l}$  of 0.01% polysorbate 80, then mixing the resulting dispersion with 1% chitosan solutions to obtain drug-loaded dispersion. 4 g of the resulting dispersion were cast into a 2.5 cm Petri dish.

Chitosan films with MW 150k g/mol were cast by adding 20% w/w microspheres with 5, 10 and 25% paclitaxel loadings to a 1% chitosan solution to obtain final paclitaxel loading in the films of 1, 2 and 5% (Table 3).

**Table 3.** Theoretical loadings of paclitaxel in MW 150k g/mol chitosan films loaded with 50-90  $\mu\text{m}$  PLLA (2k g/mol) microspheres of different drug loadings.

% paclitaxel in microspheres	% microspheres in films	% paclitaxel in films	Amount of microspheres in films (mg)	Amount of paclitaxel in films ( $\mu\text{g}$ )
5	20	1	8	400
10	20	2	8	800
25	20	5	8	2000

### 3.5.2. Casting crosslinked hyaluronic acid films without and with microspheres

A one percent hyaluronic acid (HA) solution was prepared by adding sodium hyaluronate to distilled water and shaking at 100 rpm at 37  $^{\circ}\text{C}$  for a few hours. To 1% HA solution was added glycerol to give a final glycerol concentration of 10%. 1-ethyl-3-(3-dimethylamino-propyl) carbodiimide (EDAC) was added to give a final concentration of 0.2 mM. To cast HA films without microspheres, 4 g of the resulting HA solution were poured in 2.5 cm Petri dishes. To fabricate microsphere-loaded HA films, accurately weighed quantities of microspheres were dispersed in 500  $\mu\text{l}$  of 0.01% polysorbate 80 and added into the HA solution. Microspheres of 5, 10 and 25% paclitaxel loadings were used to obtain 1,2 and 5% drug loadings in HA films (Table 4). The suspension was vortexed thoroughly and 4 g were cast into a 2.5 cm Petri dish. The cast films were left in a fume hood at room temperature for 3 days.

**Table 4.** Theoretical loadings of paclitaxel in HA films incorporated with 50-90  $\mu\text{m}$  PLLA (2k g/mol) microspheres of different drug loadings.

% paclitaxel in microspheres	% microspheres in films	% paclitaxel in films	Amount of microspheres in films (mg)	Amount of paclitaxel in films ( $\mu\text{g}$ )
5	20	1	8	400
10	20	2	8	800
25	20	5	8	2000

### **3.6. Characterization of chitosan and HA films**

#### **3.6.1. Measurement of the thickness of the films**

The thicknesses of both chitosan and HA films with control and paclitaxel-loaded microspheres were measured using a Digimatic Outside Micrometer (Mitutoyo, Japan). Four different locations on the films were measured and the values were reported as means  $\pm$  standard deviations.

#### **3.6.2. Surface morphology and cross-sectional view of chitosan films with control and 25% paclitaxel-loaded microspheres**

The surface morphology of films was studied as in section 3.4.2. For cross-sectional view, the films were first embedded in resin, then ground and polished using a series of milling stones. The films with a flattened cross-section were then placed in sample holders and observed as in 3.4.2.

### **3.7. In vitro degradation studies**

#### **3.7.1. Degradation of PLLA microspheres**

PLLA microspheres (10 mg) with or without paclitaxel loading were dispersed in a 15-ml tube containing 15 ml of PBS-A, pH 7.4 and tumbled end-over-end in an oven at 37  $^{\circ}\text{C}$ . The medium was replaced every day for the first 2 weeks and alternate days for

the latter period of 4 weeks. At predetermined periods, the microsphere samples were centrifuged at 914x g for 10 min. The pellets were washed with distilled water three times and dried under vacuum and then stored in a desiccator at room temperature. The degraded PLLA microspheres were characterized in terms of their molecular weight, thermal events, surface morphology, and mass.

### **3.7.1.1. Molecular weight**

#### **3.7.1.1.1. Calibration of the GPC column**

A GPC column (pore size  $10^3$  Å) was calibrated using polystyrene molecular weight standards with molecular weights between 600 and 4000. Polystyrene standards were analyzed as 0.3% w/v solutions in tetrahydrofuran (THF) through the column. A mobile phase of THF flowing at 1 ml/min and a refractive index detector at 40 °C were employed throughout the analyses. A calibration curve was generated by plotting the log of the molecular weights of polystyrene standards against the retention times on the chromatographs.

#### **3.7.1.1.2. Molecular weight of microspheres**

The collected microspheres were dissolved in THF and filtered through a 0.45 µm membrane filter. The solutions were analyzed under the same conditions as for polystyrene standards.

#### **3.7.1.2. Thermal properties**

Thermal events of degraded microsphere samples were studied in aluminum open pans using a heat-cool cycle, then a reheat-recool cycle over a temperature range of -20 to 170 °C at a scan rate of 20 °C/min. The first cycle was heating from -20 to 170 °C and

holding for 5 min, then cooling to  $-20^{\circ}\text{C}$ . The second cycle was reheating from  $-20$  to  $170^{\circ}\text{C}$  and holding for 5 min, then recooling to  $-20^{\circ}\text{C}$ .

### **3.7.1.3. Surface morphology**

The collected microsphere samples were prepared and observed for SEM analysis as in 3.4.2.

### **3.7.1.4. Mass loss of degraded microspheres**

The microsphere samples were weighed after week 1, 2, 3, 4 and 5. The mass loss (%) was determined based on the following Equation:

$$\text{Mass loss (\%)} = (M_0 - M_t) / M_0 \times 100\% \quad (6)$$

Where,  $M_0$  is the weight of microspheres before degradation, and  $M_t$  is the weight after a degradation time,  $t$ .

## **3.7.2. Degradation of chitosan and hyaluronic acid films**

### **3.7.2.1. Mass loss of films**

Accurately weighed 10 mg chitosan films without microspheres and 12.5 mg control microsphere-loaded chitosan films were incubated in PBS-A, pH 7.4 in 15 ml tubes at  $37^{\circ}\text{C}$  with stirring at 100 rpm. The media were replaced with fresh PBS-A every day for the first week and alternate days for the latter 5 weeks. After 2 hours, week 1, 2, 3, 4, 5 and 6, the medium was removed and the films were washed with distilled water three times and dried under vacuum.

Accurately weighed quantities of hyaluronic acid films without microspheres and with control microspheres were incubated in 5 ml of PBS-A, pH 7.4 in 2.5 cm Petri dishes at  $37^{\circ}\text{C}$  with 100 rpm. After 4, 12 and 20 hours, the films were collected as described for chitosan films and the percent mass losses determined.

### **3.7.2.2. Surface morphology**

The surface morphology of degraded samples of films was studied as in section 3.4.2.

## **3.8. In vitro release studies**

### **3.8.1. In vitro release of paclitaxel from microspheres**

In vitro release profiles of paclitaxel from the microspheres were obtained by the tumbling method at 37 °C. Triplicate samples of 5 mg microspheres were suspended in 50-ml test tubes containing 50 ml of pre-warmed 0.15 M PBS-A, pH 7.4. The test tubes were screw-capped and tumbled at 15 rpm at 37 °C in a thermostatically controlled oven. Tumbling was stopped and samples of the media (45 ml) were withdrawn at predetermined time intervals after the microsphere pellet had been centrifuged. The paclitaxel in 15 ml of the supernatant was extracted with 1 ml of DCM, followed by evaporation to dryness and analyzed using HPLC. The sample volumes were immediately replaced with fresh pre-warmed PBS-A to maintain the original volume.

### **3.8.2. In vitro release of paclitaxel from microsphere-loaded films**

#### **3.8.2.1. In vitro release of paclitaxel from microsphere-loaded chitosan films**

Approximately 10 mg chitosan films were placed in 15-ml test tubes containing 15 ml of PBS-A solution. These films contained various amounts (5, 12.5 and 25% w/w) of 20% paclitaxel-loaded microspheres in three different size ranges (<10, 10-50, and 50-90 µm). The tubes were tumbled at 15 rpm at 37 °C in a thermostatically controlled oven. At predetermined time points, tumbling was stopped and samples of media (14 ml) were withdrawn and 14 ml fresh pre-warmed PBS-A was replaced. The paclitaxel released in the media was measured using the extraction and analysis methods as in 3.4.8.

Alternatively, accurately weighed 25 mg chitosan films were suspended in 50 ml of PBS-A solution. These films contained 20% by weight of PLLA microspheres, which all were in 50-90  $\mu\text{m}$  size range but with different loadings of paclitaxel (5, 10 and 25% w/w). The tubes were left in a 37  $^{\circ}\text{C}$  incubator shaking at 100 rpm. At predetermined periods, 48 ml of medium was taken and the same volume of fresh pre-warmed PBS-A was replaced. Fifteen ml of the medium containing released paclitaxel was measured using the extraction and analysis methods as in 3.4.8. The amount of paclitaxel in 50 ml of the medium was then calculated.

#### **3.8.2.2. In vitro release of paclitaxel from microsphere-loaded HA films**

Accurately weighed approximately 25 mg microsphere-loaded HA films were contained in  $1 \times 3 \text{ cm}^2$  stainless steel sieve cages with a 60  $\mu\text{m}$  pore size mesh and then placed at the bottom of 50-ml tubes containing PBS-A, pH 7.4. As HA dissolved into the medium, the films would begin to disintegrate. The cages held the film pieces together and the dissolved HA could travel freely through the mesh of the cages. The tubes were left in a 37  $^{\circ}\text{C}$  incubator shaking at 100 rpm. At predetermined periods, 48 ml of medium were taken while the cages remained in the tubes. Forty-eight ml of fresh pre-warmed PBS-A was added to the tubes for the continuing release study. Fifteen ml of the medium containing released paclitaxel was measured using the extraction and analysis methods as in 3.4.8. The amount of paclitaxel in 50 ml of the medium was then calculated.

#### **3.9. Statistical treatment of data**

Data collected by measurement of several samples from single or different batches of material were presented as mean  $\pm$  standard deviation. The data were analyzed

using ANOVA and t-tests. The level of significance was at  $\alpha$  level of 0.05 and the null hypothesis was that there was no difference between samples.

Particle size analyses of microspheres were determined based on triplicate samples. Particle size distributions of microspheres made with 5% w/v PLLA were measured in single batches for each size range. Particle size distributions of microspheres prepared with 10% w/v PLLA were studied based on 3 batches for each drug loading. The data were reported as the mean  $\pm$  standard deviation.

Total content of paclitaxel in microspheres made with 5% w/v PLLA was determined based on 3 measurements of each batch. Values are reported as mean  $\pm$  standard deviation. Total content of paclitaxel in microspheres made with 10% w/v PLLA was measured based on triplicates of 3 different batches. Data are reported as mean  $\pm$  standard deviation. The difference between batches was examined with ANOVA. ANOVA p values less than 0.05 were interpreted to mean variability exists between batches.

For in vitro release studies, measurements were made based on three samples for microspheres and chitosan films containing 5% paclitaxel loaded microspheres, and four samples for 50-90  $\mu$ m microsphere loaded films. Values of the mean and standard deviation were calculated from cumulative amounts of paclitaxel released from each sample. In figures showing release studies, the mean values were plotted as a function of time and the error bars represented the standard deviations.

## **4. RESULTS**

### **4.1. Characterization of PLLA microspheres**

#### **4.1.1. Effect of PLLA concentrations on yields of control microspheres**

The polymer concentration is one of the variables affecting microsphere formation. PLLA solutions of 5, 10, 15 and 20% w/v PLLA were evaluated. The microspheres were collected in three size ranges (using 53 and 90  $\mu\text{m}$  sieves); smaller than 50  $\mu\text{m}$ , 50-90  $\mu\text{m}$ , and greater than 90  $\mu\text{m}$ . The percent yields of control microspheres prepared using different PLLA concentrations are shown in Table 5. Percent yields for smaller than 50  $\mu\text{m}$  microspheres were the highest for 5% w/v PLLA. Percent yields for 50-90  $\mu\text{m}$  microspheres made with 5% and 10% w/v PLLA were statistically significantly higher than those prepared with 15% and 20% PLLA. Percent yields for greater than 90  $\mu\text{m}$  microspheres were the highest for 15 and 20% w/v PLLA. All microspheres in subsequent studies were prepared using 5% PLLA and 10% PLLA. Microspheres prepared using 5% PLLA were all 20% paclitaxel loaded and in the size ranges of smaller than 10  $\mu\text{m}$ , 10-50  $\mu\text{m}$ , and 50-90  $\mu\text{m}$ . Microspheres prepared using 10% PLLA were mostly in the size range 50-90  $\mu\text{m}$  with different paclitaxel loadings of 5, 10 and 25% w/w. Some of microspheres with all different paclitaxel loadings was greater than 90  $\mu\text{m}$ .

**Table 5.** Percent yields of control microspheres in different size ranges prepared using between 5 and 20% w/v PLLA (2k g/mol). Data are mean values based on measurements of four batches at each PLLA concentration  $\pm$  standard deviation.

Size Range ( $\mu\text{m}$ )	% Yield with different PLLA (% w/v) concentration				ANOVA p value
	5% PLLA	10% PLLA	15% PLLA	20% PLLA	
>90	4.0 $\pm$ 1.1	14.2 $\pm$ 8.3 <sup>a</sup>	43.5 $\pm$ 8.6 <sup>a b</sup>	46.2 $\pm$ 6.6 <sup>a b</sup>	< 0.01
50-90	40.8 $\pm$ 6.4	41.4 $\pm$ 6.2	27.3 $\pm$ 5.4 <sup>a b</sup>	20.7 $\pm$ 1.1 <sup>a b</sup>	< 0.01
<50	23.8 $\pm$ 6.6	13.5 $\pm$ 3.1 <sup>a</sup>	5.7 $\pm$ 2.3 <sup>a b</sup>	5.3 $\pm$ 0.9 <sup>a b</sup>	< 0.01

<sup>a</sup> p < 0.05 vs 5% PLLA

<sup>b</sup> p < 0.05 vs 10% PLLA

#### 4.1.2. Surface morphology of microspheres

The surface morphology of microspheres was observed using SEM and is shown in Figure 9. Control and paclitaxel-loaded microspheres (5 to 25%) were all spherical in shape and the external surfaces appeared smooth and non-porous. No effects of paclitaxel loading on the surface morphology of microspheres were observed. No paclitaxel crystals were detected on the surface of drug-loaded microspheres over the range studied.

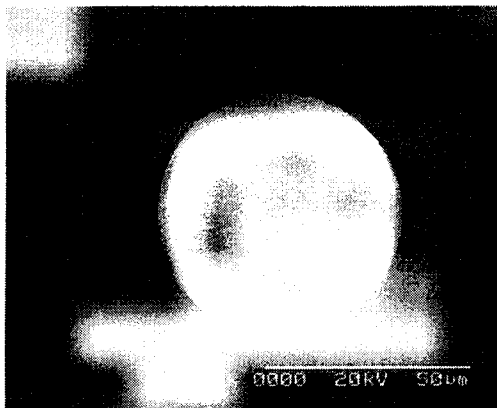
#### 4.1.3. Particle size distributions of microspheres

Microspheres loaded with 0 to 25% paclitaxel were manufactured in 3 size ranges. The particle size ranges of 20% paclitaxel-loaded microspheres prepared using 5% w/v PLLA were less than 10  $\mu\text{m}$ , 10-50  $\mu\text{m}$ , and 50-90  $\mu\text{m}$ . The microspheres prepared using 10% w/v PLLA and different drug loadings were all in the size range of 50-90  $\mu\text{m}$ . The particle size distributions of microspheres prepared using 5% and 10% w/v PLLA concentration are shown in Figure 10 A and B, respectively. The mean size values of microspheres are summarized in Table 6. ANOVA showed no significant

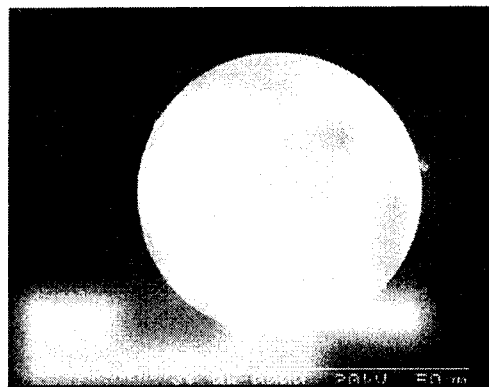
difference in the mean particle size values of 50-90  $\mu\text{m}$  microspheres with either 5, 10 or 25% paclitaxel loading.

**Figure 9.** SEM micrographs of 50-90  $\mu\text{m}$  PLLA (2k g/mol) microspheres with paclitaxel loadings of A) 0, B) 5, C) 10 and D) 25%. (Magnification of all micrographs is 1000x.)

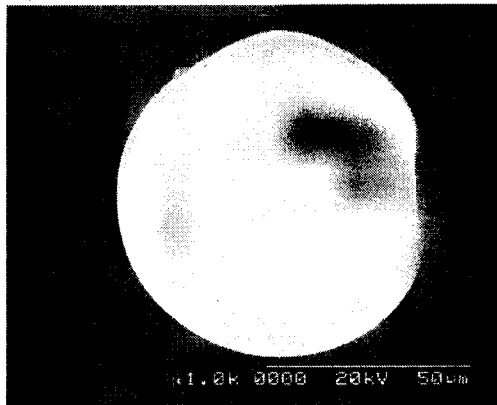
A)



B)



C)



D)

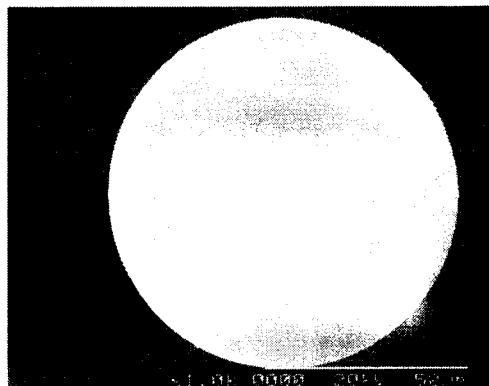


**Table 6.** Particle size distributions of paclitaxel-loaded microspheres prepared using 5% and 10% w/v PLLA (2k g/mol). For microspheres prepared using 5% w/v PLLA, values are the mean  $\pm$  standard deviation of three measurements from single batches. For microspheres prepared using 10% w/v PLLA, data are mean  $\pm$  standard deviation of three measurements from three batches.

Microspheres prepared using 5% w/v PLLA		
Drug loading (% w/w)	Size range ( $\mu\text{m}$ )	Mean value ( $\mu\text{m}$ )
20%	< 10	$2 \pm 1$
	10 - 50	$26 \pm 4^a$
	50 - 90	$60 \pm 3^{a,b}$
ANOVA p value		< 0.01
Microspheres prepared using 10% w/v PLLA		
5%	50 - 90	$69 \pm 3$
10%		$68 \pm 12$
25%		$62 \pm 6$
ANOVA p value		< 0.51

<sup>a</sup>  $p < 0.05$  vs < 10  $\mu\text{m}$  microspheres

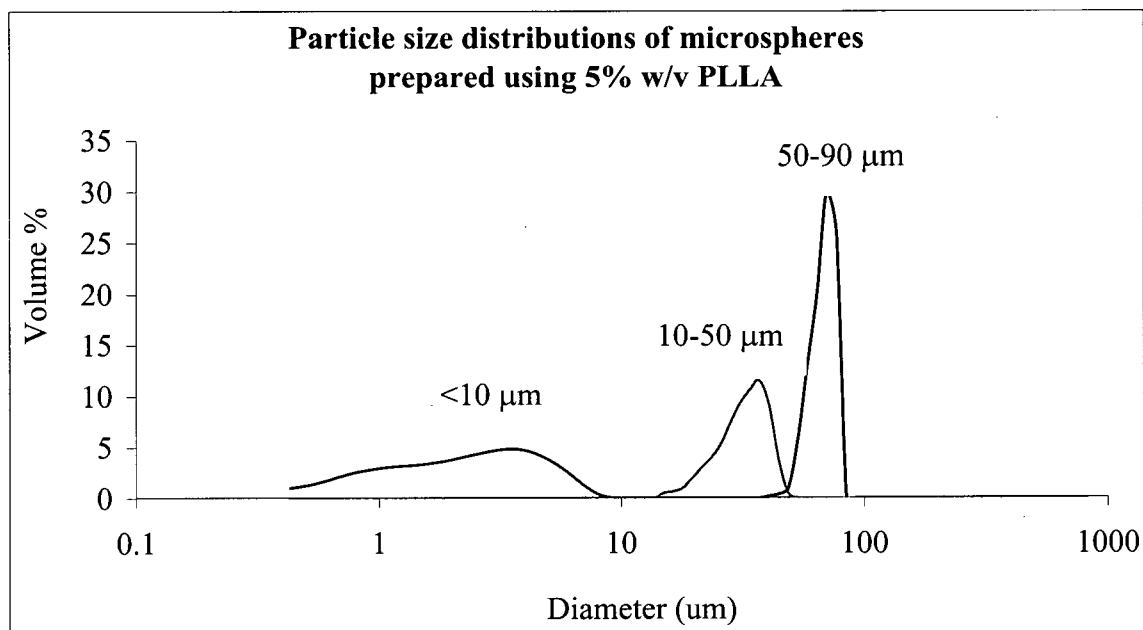
<sup>b</sup>  $p < 0.05$  vs < 10-50  $\mu\text{m}$  microspheres

#### 4.1.4. Determination of paclitaxel content in PLLA microspheres

The recovery of paclitaxel from spiked solutions of PLLA in DCM is given in Table 7. Total recovery of paclitaxel was 99.2% with 97.4% paclitaxel in the organic phase. Drug content analysis of paclitaxel-loaded microspheres is given in Table 8. A higher than expected content was observed in all types of microspheres prepared using 5 and 10% w/v PLLA. Hence it appears that the extent of incorporation of PLLA must have been less than that of paclitaxel into the formed microspheres.

**Figure 10.** Particle size distributions of A) 20% paclitaxel-loaded microspheres prepared using 5% w/v PLLA (2k g/mol) in different size ranges and B) 5-25% paclitaxel-loaded microspheres prepared using 10% w/v PLLA (2k g/mol) (50-90  $\mu\text{m}$ ).

A)



B)

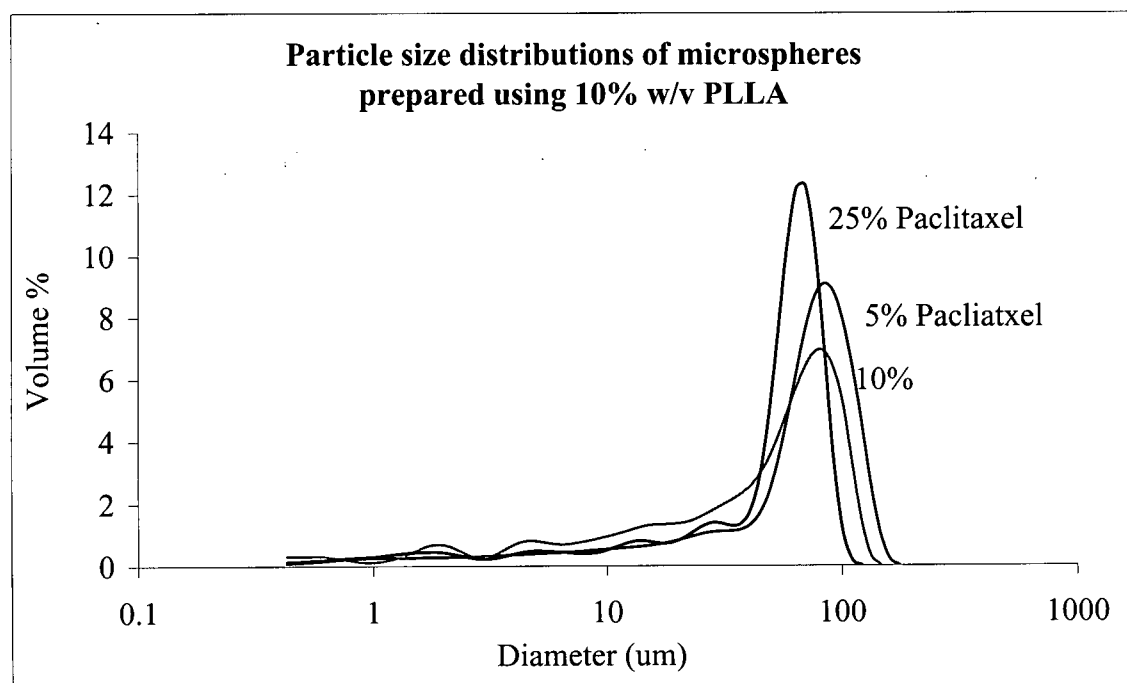


**Table 7.** Precision and efficiency of extraction of paclitaxel from spiked solutions and precision of organic-aqueous phase separation in the total content assay. Values of mean  $\pm$  standard deviation are determined based on four measurements.

	Mean $\pm$ standard deviation	RSD (%) <sup>a</sup>
Volume of upper phase	7.5 $\pm$ 0.4 ml	5.6
Volume of lower phase	8.0 $\pm$ 0.0 ml	0.0
Percent of paclitaxel in upper phase	97.4 $\pm$ 5.5%	0.6
Percent total recovery of paclitaxel	99.2 $\pm$ 8.4%	0.9

<sup>a</sup> RSD (Relative standard deviation) is the ratio of the standard deviation to the mean value, expressed as a percentage.

**Table 8.** Total content of paclitaxel in PLLA (2k g/mol) microspheres prepared using a) 5% w/v PLLA and b) 10% w/v PLLA. Analyses of microspheres prepared using 5% w/v PLLA were determined in single batches for each size range. For microspheres prepared using 10% w/v PLLA, values were measured based on 3 batches for each drug loading.

a) Total content of paclitaxel in microspheres prepared using 5% w/v PLLA

Particle size ranges ( $\mu\text{m}$ )	Theoretical drug loading (% w/w)	Drug content (% w/w)
<10	20%	26 $\pm$ 3
10-50		24 $\pm$ 1
50-90		27 $\pm$ 1
ANOVA p value		0.26

b) Total content of paclitaxel in microspheres prepared using 10% w/v PLLA

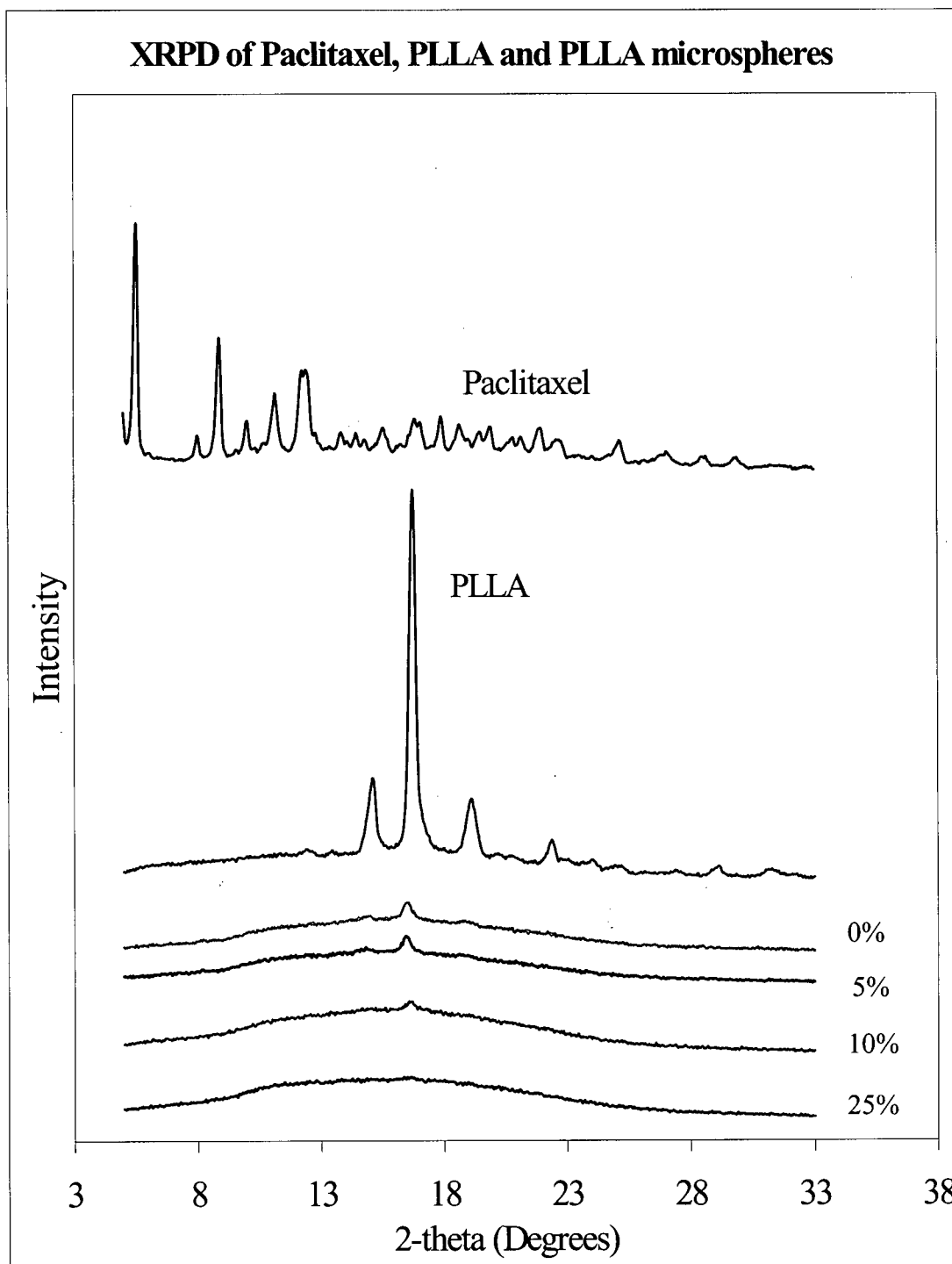
Particle size range ( $\mu\text{m}$ )	Theoretical drug loading (% w/w)	Drug content (% w/w)	ANOVA p value
50-90	5%	5 $\pm$ 0	0.038
	10%	11 $\pm$ 1	0.016
	25%	29 $\pm$ 1	< 0.01

In order to estimate the loss of a water-soluble fraction of PLLA out of the microspheres during the microsphere manufacture process, 100 mg PLLA was incubated in distilled water to dissolve water-soluble components. About 93% PLLA remained after 14 hours incubation, indicating that at least 7% of the original material was water-soluble and not incorporated into microspheres.

#### **4.1.5. X-ray powder diffraction patterns (XRPD) of microspheres**

The XRPD patterns of microspheres with different drug loadings were obtained and compared to paclitaxel and PLLA alone (Figure 11). There were several strong diffraction peaks for paclitaxel between  $5-15^{\circ} 2\theta$ . Three peaks were characterized for PLLA in the range of  $14.5$  to  $20^{\circ} 2\theta$ . One characteristic peak between  $16.3$  and  $16.5^{\circ} 2\theta$  was found in control PLLA microspheres and its intensity was decreased significantly compared to PLLA alone. With the increase in paclitaxel loading, the intensity of the peak reduced further. No peaks due to crystalline paclitaxel were detected in any paclitaxel-loaded microspheres.

Figure 11. XRPD patterns of paclitaxel, PLLA (2k g/mol) and PLLA (2k g/mol) microspheres with paclitaxel loadings of 0, 5, 10 and 25%.



#### 4.1.6. Thermal properties of paclitaxel, PLLA and microspheres

Thermal properties of paclitaxel were studied over a temperature range of 0 to 300 °C (Figure 12). No glass transition was detected and an endothermic melting peak was found around 231 °C, which suggests that paclitaxel was crystalline. Further heating caused the decomposition of paclitaxel at higher temperatures.

PLLA was scanned over temperature range of -20 to 300 °C with decomposition occurring at 250 °C. Thus, a two-cycle scan over a temperature range of -20 to 170 °C was employed and DSC heating/reheating scans are shown in Figure 13. In the first cycle the glass transition was not well defined, while an endothermic melting peak at 135 °C was observed which corresponded to the crystalline component of PLLA. The degree of crystallinity,  $X_c$ , was calculated using equation 3 and found to be 23%. A value for the heat of fusion for 100% PLLA crystallinity used in the calculations was 93.7 J/g (Furukawa et al., 2000). The polymer exhibited a broad melting peak with a shoulder at a lower temperature of the melting peak.

In the second cycle a glass transition was evident at 26 °C and the melting peak temperature was 138 °C. Compared to the first cycle, the  $X_c$  of PLLA subjected to a second heating cycle was only 6%.

Thermal properties of 50–90 µm microspheres with paclitaxel loading between 0 and 25% were studied over a temperature range of -20 to 170 °C. The reason for selecting a temperature range lower than paclitaxel's melting point is that paclitaxel-loaded microspheres were found to begin decomposing around 180 °C. DSC scans of microspheres are shown in Figure 14 and the transitions are summarized in Table 9. Control microspheres showed a  $T_g$  around 51 °C accompanied with a small enthalpy

relaxation peak. The amorphous component of the PLLA in 25% paclitaxel-loaded microspheres showed a statistically significantly elevated T<sub>g</sub> compared to control microspheres (Figure 14 A and Table 9). Above T<sub>g</sub>, a crystallization exotherm (T<sub>c</sub>) was observed in control microspheres around 105 °C as the polymer chains gained more mobility and were able to crystallize. Further heating resulted in melting of the crystallites within the polymer matrices. Compared to control microspheres, a melting temperature (T<sub>m</sub>) depression of PLLA was observed in all paclitaxel-loaded microspheres and the magnitude of the melting point depression increased with increasing paclitaxel loading. PLLA exhibited a 7 °C melting point depression when comparing control to 10% paclitaxel-loaded microspheres (Table 9). Control microspheres possessed a degree of crystallinity (X<sub>c</sub>) of about 24%. The degrees of crystallinity of paclitaxel-loaded microspheres decreased from 12% to 8% with an increase in paclitaxel loading (first cycle), which is consistent with XRPDs of microspheres. In the second cycle (Figure 14B) T<sub>g</sub> showed a similar trend to the first cycle. No crystallization exotherm was evident in control microspheres. Melting endotherms became less significant in all microspheres.

**Table 9.** Thermal properties of 50-90  $\mu\text{m}$  microspheres prepared using 10% w/v PLLA. Values are means of measurements from each of three batches  $\pm$  standard deviation. Thermal properties were obtained from heat-cool-reheat-recool cycles at a scan rate of 20  $^{\circ}\text{C}/\text{min}$ . The first cycle was to heat from  $-20$  to  $170$   $^{\circ}\text{C}$  and hold for 5 min, then cool back to  $-20$   $^{\circ}\text{C}$ . The second cycle was to reheat from  $-20$  to  $170$   $^{\circ}\text{C}$  and hold for 5 min, then recool back to  $-20$   $^{\circ}\text{C}$ .

a) First cycle

Microspheres	Tg ( $^{\circ}\text{C}$ )	Tc ( $^{\circ}\text{C}$ )	Tm ( $^{\circ}\text{C}$ )	$\Delta\text{H}_f$ (J/g)	Xc (%)
0% paclitaxel	$51 \pm 3.1$	$105 \pm 1.2$	$148 \pm 0.7$	$23 \pm 3.8$	$24 \pm 4.0$
5% paclitaxel	$51 \pm 2.0$	-	$145 \pm 1.3^a$	$12 \pm 4.3$	$12 \pm 4.6^a$
10% paclitaxel	$53 \pm 2.2$	-	$141 \pm 1.5^{ab}$	$7 \pm 3.3$	$8 \pm 2.5^a$
25% paclitaxel	$58 \pm 0.2^{abc}$	-	-	-	-
ANOVA p value	0.01		< 0.01		< 0.01

b) Second cycle

Microspheres	Tg ( $^{\circ}\text{C}$ )	Tm ( $^{\circ}\text{C}$ )	$\Delta\text{H}_f$ (J/g)
0% paclitaxel	$44 \pm 0.7$	$145 \pm 2.3$	$7 \pm 3.1$
5% paclitaxel	$45 \pm 0.1$	-	-
10% paclitaxel	$48 \pm 2.5^{ab}$	-	-
25% paclitaxel	$55 \pm 0.6^{abc}$	-	-
ANOVA p value	0.0004		

- unavailable

<sup>a</sup> p < 0.05 vs 0% paclitaxel loaded microspheres

<sup>b</sup> p < 0.05 vs 5% paclitaxel loaded microspheres

<sup>c</sup> p < 0.05 vs 10% paclitaxel loaded microspheres

**Figure 12.** DSC scan of paclitaxel over a temperature range of 0 to 300 °C at a scan rate of 20 °C/min.

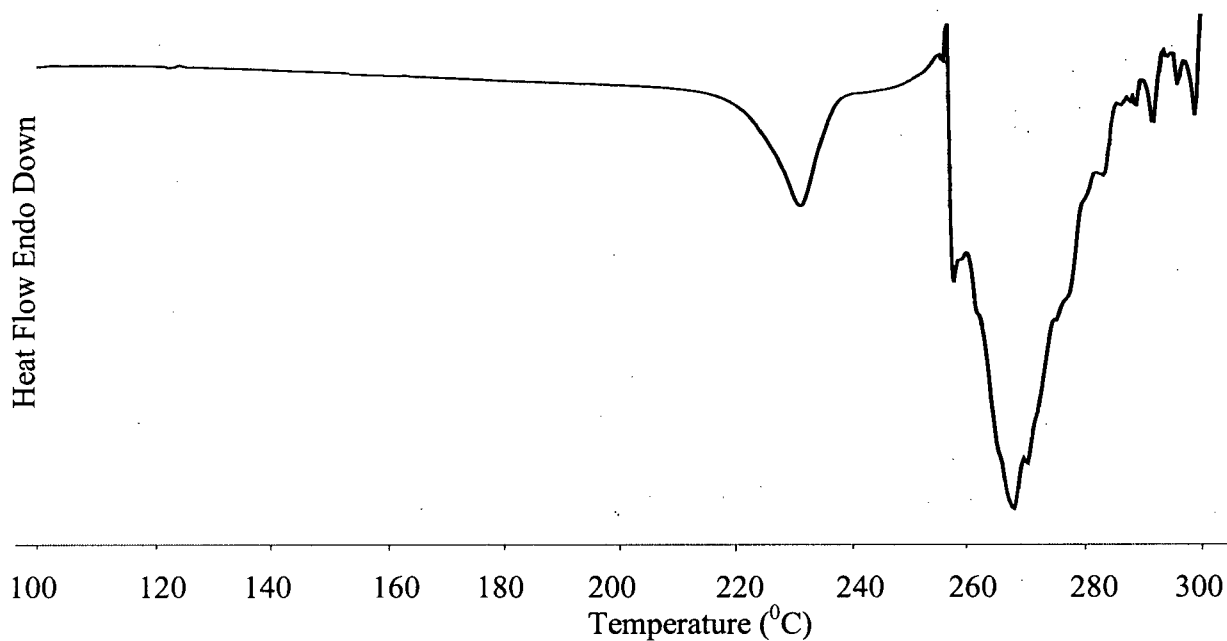


**Figure 13.** DSC heating/reheating scans of PLLA (2k g/mol) following two cycles of heat-cool-reheat-recool at a scan rate of 20 °C/min. A) The first cycle: heating from -20 to 170 °C and holding for 5 min, then cooling to -20 °C; B) the second cycle: reheating from -20 to 170 °C and holding for 5 min, then cooling to -20 °C.

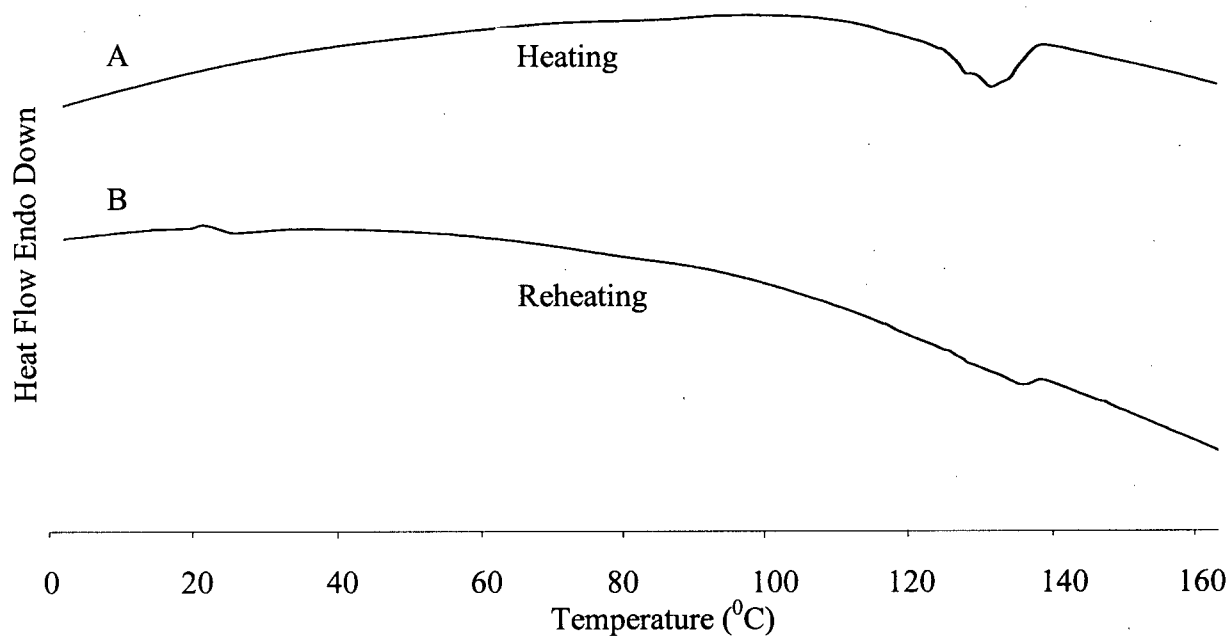
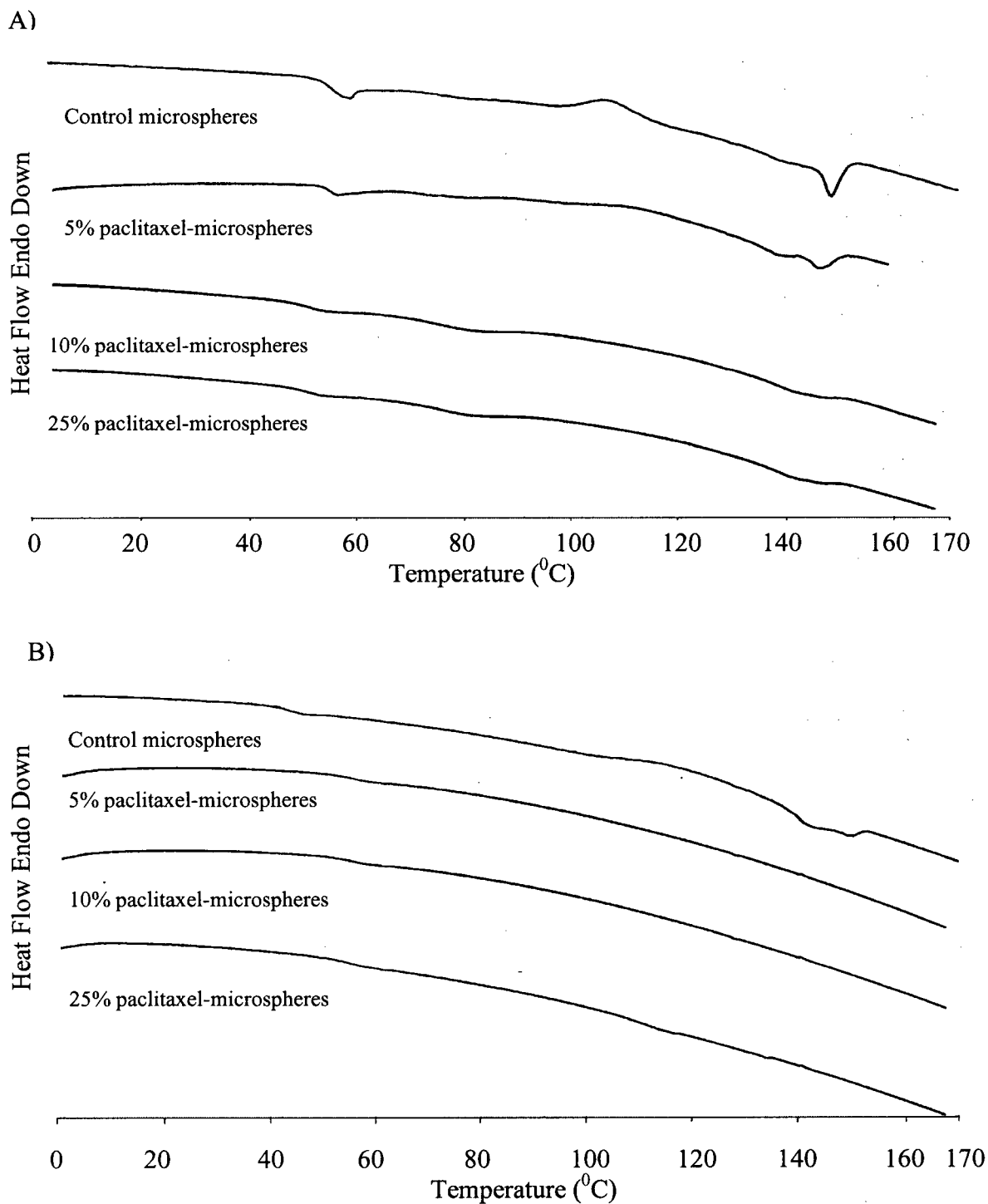


**Figure 14.** DSC heating/reheating scans of PLLA (2k g/mol) microspheres with paclitaxel loadings between 0 and 25% following two cycles of heat-cool-reheat-recool at a scan rate of 20 °C/min. A) The first cycle: heating from -20 to 170 °C and holding for 5 min, then cooling to -20 °C; B) the second cycle: reheating from -20 to 170 °C and holding for 5 min, then recooling to -20 °C.



## 4.2. Characterization of chitosan and HA films

### 4.2.1. Thickness of films

The thickness of cast films was between 80 and 97  $\mu\text{m}$  (Table 10). Statistical analyses showed that control and 1% paclitaxel-loaded chitosan films were thicker than 2% and 5% paclitaxel-loaded chitosan films. Control hyaluronic acid films were generally thicker than drug-loaded films. There was no significant variability in thickness for each microsphere-loaded chitosan or HA films.

**Table 10.** Thickness of PLLA (2k g/mol) microsphere loaded A) chitosan and B) HA films containing between 0 and 5% paclitaxel. Measurements were conducted on four locations for each film. For each drug loading, four films were measured. Values are means of four film samples  $\pm$  standard deviation.

A)

Paclitaxel loading (% w/w)	1% Chitosan films ( $\mu\text{m}$ )	RSD (%) <sup>d</sup>
0%	92 $\pm$ 3	3
1%	97 $\pm$ 3	4
2%	89 $\pm$ 2 <sup>ab</sup>	3
5%	88 $\pm$ 1 <sup>ab</sup>	1
ANOVA p value	< 0.01	

B)

Paclitaxel loading (% w/w)	1% HA films ( $\mu\text{m}$ )	RSD (%) <sup>d</sup>
0%	96 $\pm$ 4	4
1%	87 $\pm$ 6 <sup>c</sup>	7
2%	86 $\pm$ 7 <sup>c</sup>	8
5%	80 $\pm$ 3 <sup>c</sup>	3
ANOVA p value	< 0.01	

<sup>a</sup> p < 0.05 vs 0% paclitaxel-loaded chitosan film

<sup>b</sup> p < 0.05 vs 1% paclitaxel-loaded chitosan film

<sup>c</sup> p < 0.05 vs 0% paclitaxel-loaded HA film

<sup>d</sup> RSD (Relative standard deviation) is the ratio of the standard deviation of four film samples for each concentration to the mean value, expressed as a percentage.

#### **4.2.2. Surface morphology and cross-sectional views of chitosan films without and with microspheres**

The surface of chitosan films without microspheres was observed with SEM and is shown in Figure 15. SEM revealed no obvious features on the surface of the films at up to 1000× magnification, indicating that the surface of the films was smooth.

The surface features and cross-sectional views of chitosan films loaded with control microspheres and 25% paclitaxel-loaded microspheres are shown in Figure 16 and 17. The surface features revealed that all films had a smooth surface. Microspheres were uniformly dispersed throughout the film matrix and no aggregates were found. The cross-sectional views suggested that all microsphere surfaces were entrapped within the matrices of the films. All microspheres in the films were intact with a smooth surface and there were no pores or cracks on the microsphere matrix.

**Figure 15.** SEM micrograph of surface feature of chitosan film without microspheres.  
(Magnification is 1000x.)

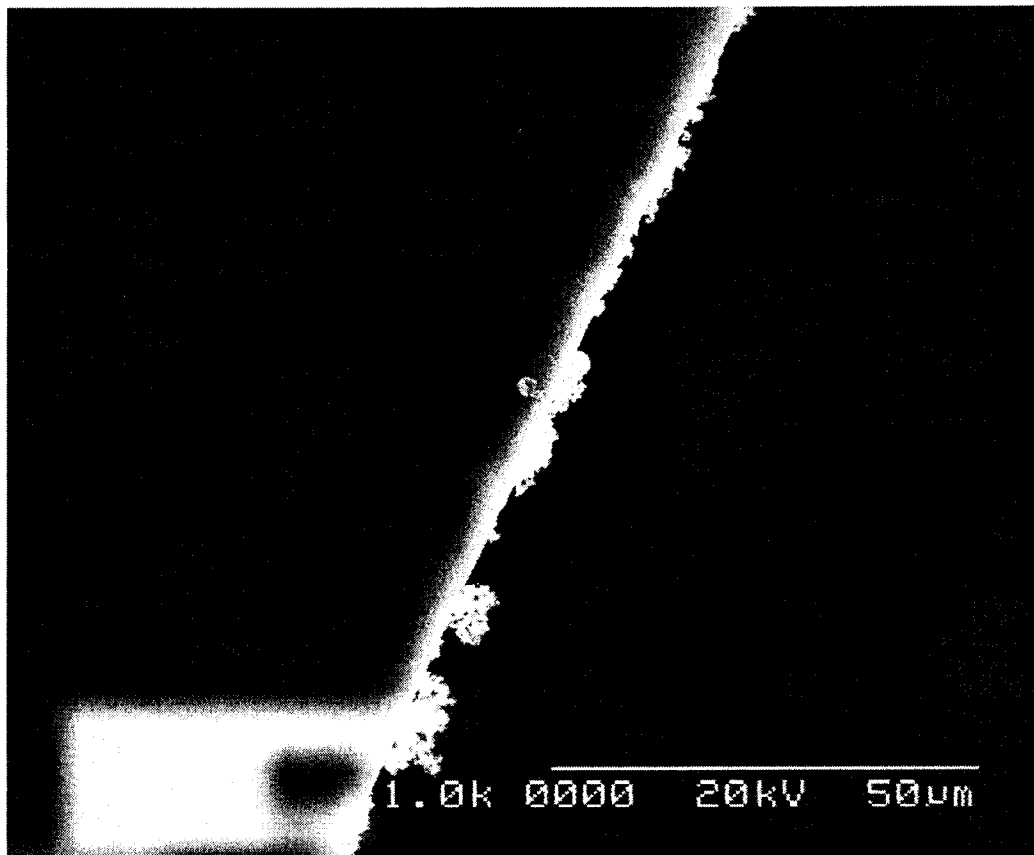
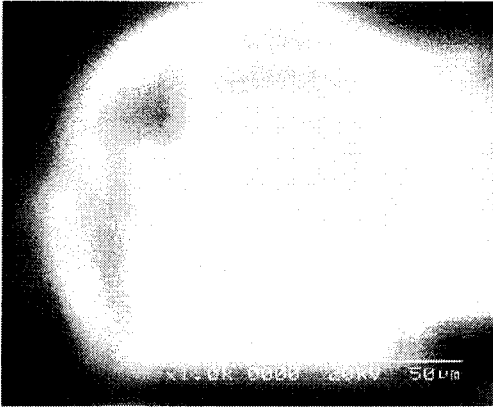
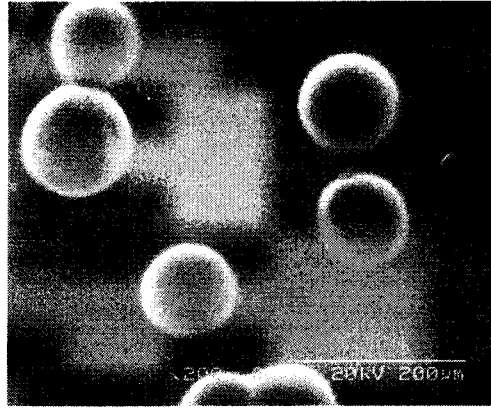


**Figure 16.** SEM micrographs of chitosan films loaded with control microspheres. A) The surface features. (Magnification of micrographs is 1000x and 200x.) B) The cross-sectional view. (Magnification of the micrograph is 1000x.)

A) (1000x)



A) (200x)



B)

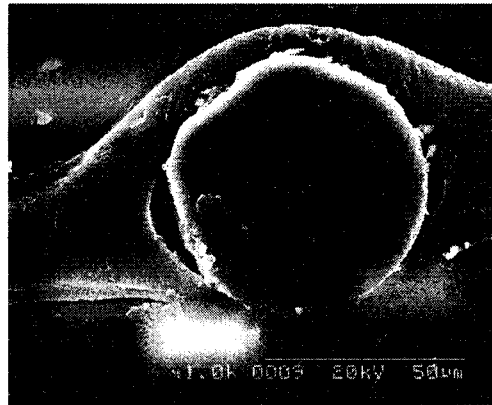
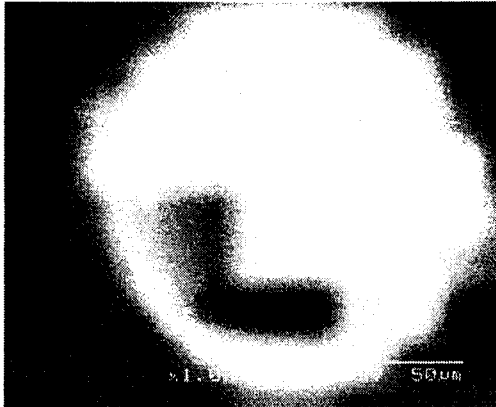
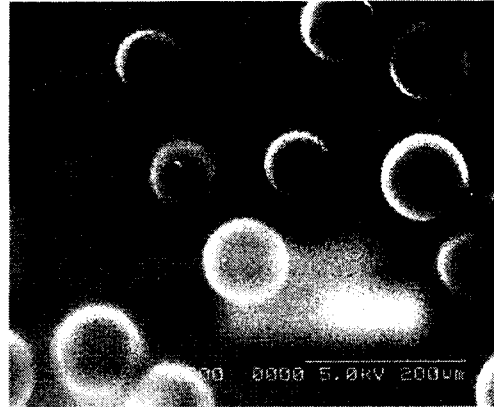


**Figure 17.** SEM micrographs of chitosan films loaded with 25% paclitaxel-loaded PLLA (2k g/mol) microspheres. A) The surface features. (Magnification of micrographs is 1000x and 200x.) B) The cross-sectional view. (Magnification of the micrograph is 1000x.)

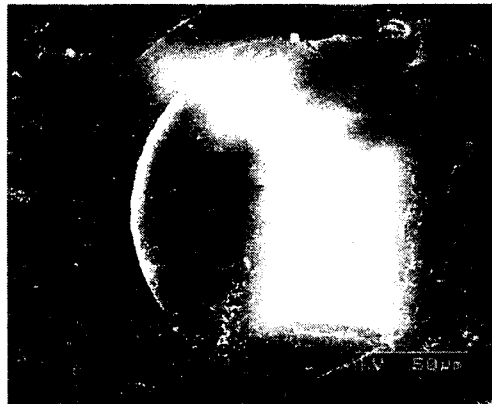
A) (1000x)



A) (200x)



B)



### **4.3. Degradation of PLLA microspheres and microsphere-loaded films**

#### **4.3.1. Degradation of PLLA (2k g/mol) microspheres**

##### **4.3.1.1. GPC analysis**

###### **4.3.1.1.1. Validation of GPC column**

The GPC column with a pore size of  $10^3 \text{ \AA}$  was validated using polystyrene standards as there were no PLLA standards available. The molecular weight ranges of polystyrene standards were between 600 and 4000. The GPC elution profiles of polystyrene are shown in Figure 18. The plot of log MW against retention time of elution peak (Figure 19) showed a linear relationship with a regression  $R^2$  of 0.9915.

###### **4.3.1.1.2. GPC analysis of degradation of microspheres**

The retention times of PLLA from microspheres incubated in PBS-A, pH 7.4 were measured using the validated column and are given in Table 11. The data showed that the retention times of PLLA from microspheres were increasing as a function of time over 6 weeks, indicating the progressive degradation of polymer chains in the microspheres. An elution profile of PLLA after 4 weeks incubation is shown in Figure 20, indicating a monomodal chromatogram.

In general, universal calibration curves allow for the calculation of MW from retention times. The product of intrinsic viscosity  $[\eta]$  and molecular weight is independent of polymer type and a plot of  $\log([\eta] \text{ MW})$  versus retention time in the solvent yields a linear curve for a widely disparate group of polymers. The  $\log([\eta] \text{ MW})$  may be considered a constant for all polymers for a given column, temperature and retention time (Stevens, 1990). If the intrinsic viscosity of known molecular weight

polystyrene for a given retention time could be determined,  $\log([\eta] \text{ MW})$  would be obtained, and therefore the molecular weight of PLLA might be calculated. However, in this case we were unable to establish a universal calibration curve due to the difficulty of obtaining the intrinsic viscosity  $[\eta]$  of very low molecular weight 2k g/mol polystyrene standard. Therefore, the molecular weights of PLLA could not be calculated. The data are shown only as retention times.

**Table 11.** GPC retention times of degraded PLLA (2k g/mol) microspheres with 0 to 25% paclitaxel loadings incubated in PBS-A at 37 °C. Values are one set of data from single samples running at one time.

Time (weeks)	Retention times of PLLA in microspheres with different paclitaxel loadings (min)			
	Control	5% paclitaxel	10% paclitaxel	25% paclitaxel
0	7.28	7.28	7.27	7.29
1	7.43	7.30	7.29	7.30
2	7.44	7.33	7.39	7.30
3	7.47	7.36	7.28	7.34
4	7.62	7.45	7.58	7.47
5	7.72	7.51	7.79	7.49
6	7.78	7.55	7.79	7.55

#### 4.3.1.1.3. PLLA stability during storage

PLLA samples removed from incubation in PBS-A, pH 7.4 were dried and stored in desiccators at room temperature. In order to determine whether degradation of PLLA samples actually occurred during storage in the desiccator, two PLLA samples that had 3 months difference in desiccator storage time were evaluated simultaneously using GPC. These PLLA samples had both been incubated in PBS-A, pH 7.4 for 2 weeks. The GPC chromatograms showed that degraded PLLA samples with different desiccator storage times eluted at the same retention time, 7.20 min. These results indicated that the

molecular weight of degraded PLLA remained unchanged with storage in the desiccator over the course of the study.

**Figure 18.** GPC elution profiles of polystyrene standards with molecular weights ranging from 600 to 4000 g/mol at 40 °C. (Solvent: THF. Solvent flow rate: 1.0 ml/min. Injection volume: 50  $\mu$ l).

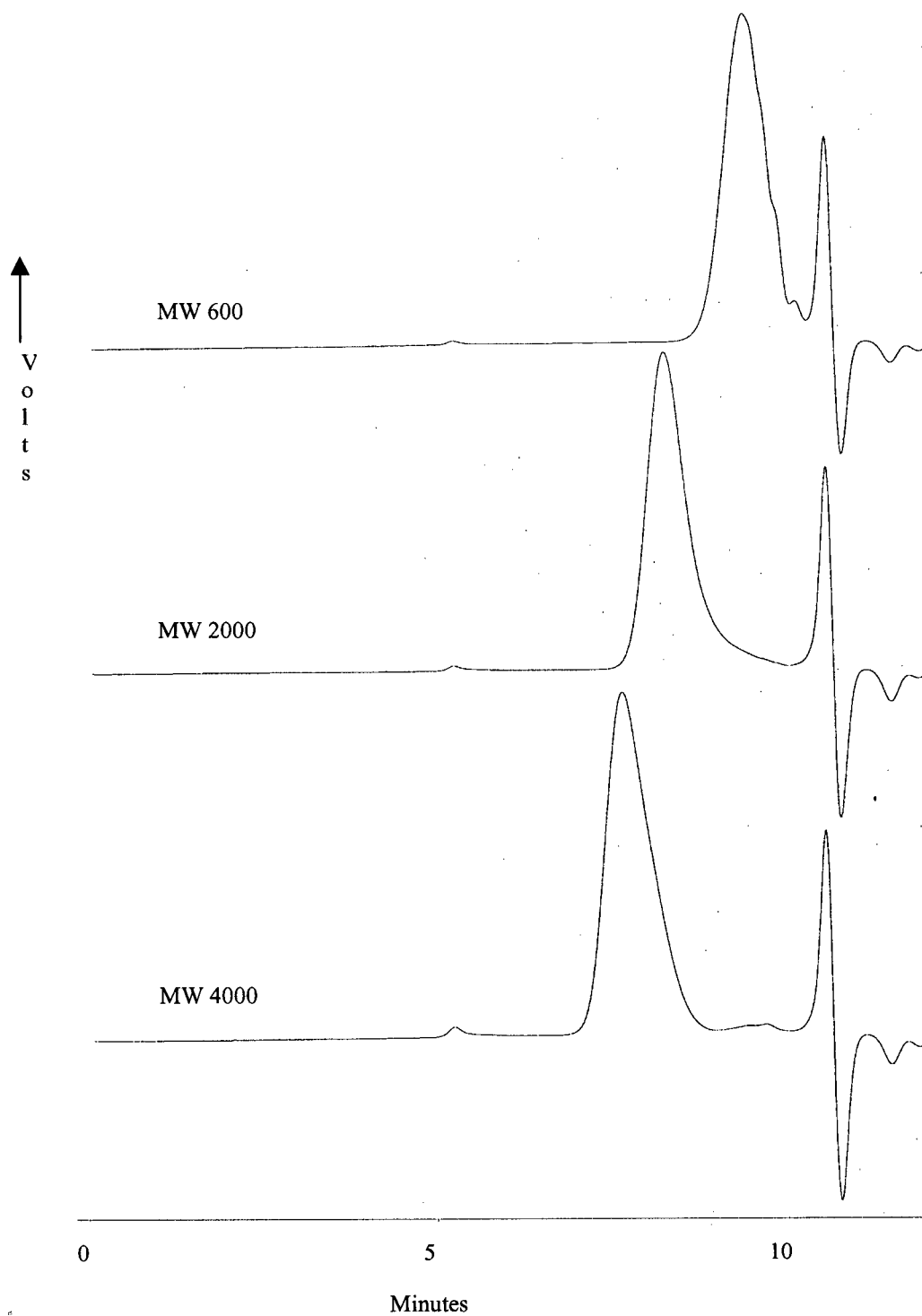


**Figure 19.** GPC standard curve for polystyrene standards with molecular weights from 600 to 4000 g/mol on a column with a nominal pore size of  $10^3 \text{ \AA}$  at  $40^\circ\text{C}$ . (Solvent: THF. Solvent flow rate: 1.0 ml/min. Injection volume: 50  $\mu\text{l}$ ).

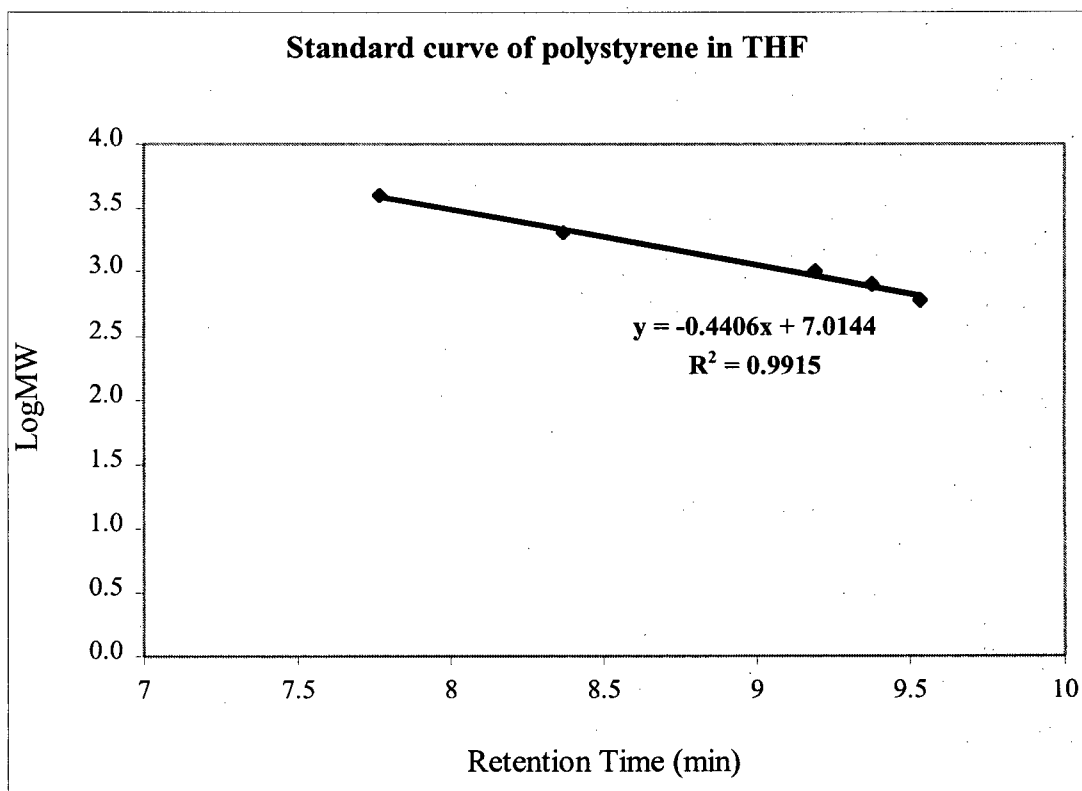
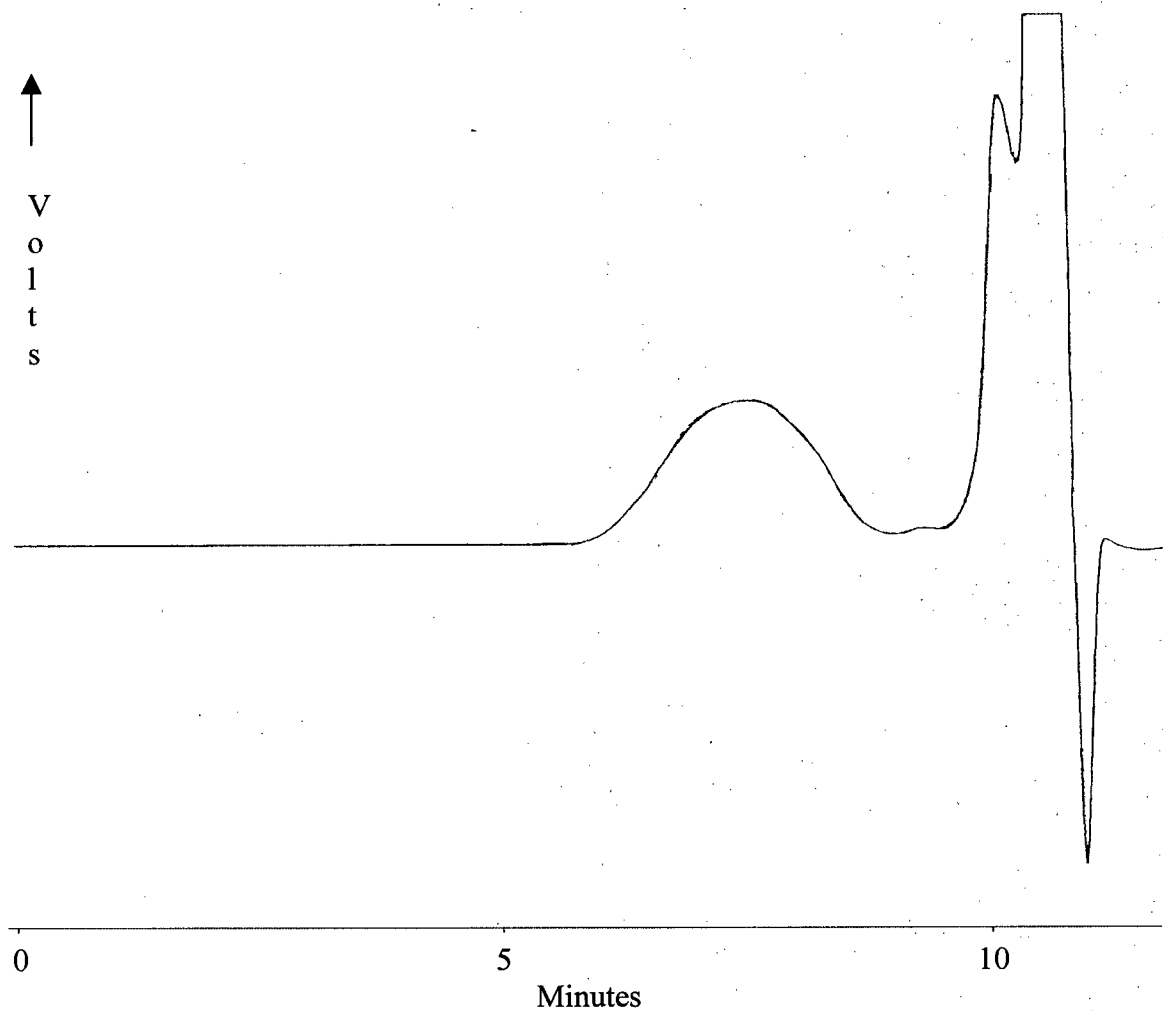


**Figure 20.** GPC elution profile of degrading PLLA (2k g/mol) control microspheres after 4 weeks incubation in PBS-A at 37 °C. (Solvent: THF. Solvent flow rate: 1.0 ml/min. Injection volume: 50  $\mu$ l).



#### 4.3.1.2. Thermal properties

Table 12 outlines the thermal properties of non-degraded and degraded PLLA microspheres. Table 12a summarizes the thermal properties of control microspheres over 4 weeks incubation in PBS-A at 37 °C. The data showed that the Tg of PLLA had increased from 51 to 65 °C. No significant change in Tm and crystallinity was detected in PLLA. DSC scans of control microspheres (Figure 21A) showed that the melting peak of PLLA became less well defined after 4 weeks incubation in PBS-A at 37 °C.

Table 12b presents the thermal properties of 25% paclitaxel-loaded PLLA microspheres. Figure 21B shows the DSC scans of 25% paclitaxel-loaded microspheres. Tg of PLLA increased about 9 °C in 4 weeks. Tm of PLLA could not be readily identified before degradation, while after 4 weeks of degradation it was observed to be 147 °C and Xc had increased up to 10%.

Table 12c shows the thermal properties of PLLA microspheres with different paclitaxel loadings after 2 weeks incubation in PBS-A at 37 °C. Figure 22 shows the DSC scans of these microspheres. Tg showed no significant change with the increase in drug loading in the microspheres. Tm of PLLA in 25% paclitaxel-loaded microspheres decreased 4 °C compared to control microspheres. The melting peaks of PLLA became broadened and Xc decreased with the increase in drug loading.

**Table 12.** Thermal properties of non-degraded and degraded PLLA (2k g/mol) control microspheres and paclitaxel-loaded microspheres. Samples were scanned at 20 °C/min over a temperature range of -20 to 170 °C. For control microspheres and 25% paclitaxel-loaded microspheres, values are means of measurements from each of three batches  $\pm$  standard deviation. For 5% and 10% paclitaxel-loaded microspheres, values are from each single batch.

a) Thermal properties of control microspheres incubated in PBS-A at 37 °C after 0, 2 and 4 weeks.

	Tg (°C)	Tc (°C)	Tm (°C)	Xc (%)
At week 0	51 $\pm$ 3.1	104 $\pm$ 1.2	148 $\pm$ 0.7	24 $\pm$ 4.0
After 2 weeks	65 $\pm$ 0.7 <sup>a</sup>	112 $\pm$ 0.2 <sup>a</sup>	148 $\pm$ 0.7	22 $\pm$ 3.1
After 4 weeks	64 $\pm$ 0.3 <sup>a</sup>	112 $\pm$ 0.2 <sup>a</sup>	148 $\pm$ 0.2	21 $\pm$ 4.0
ANOVA p value	< 0.01	< 0.01	0.37	0.87

<sup>a</sup> p < 0.05 vs at week 0

b) Thermal properties of 25% paclitaxel-loaded microspheres incubated in PBS-A at 37 °C after 0, 2 and 4 weeks.

	Tg (°C)	Tm (°C)	Xc (%)
At week 0	58 $\pm$ 0.2	-	-
After 2 weeks	64 $\pm$ 0.4 <sup>a</sup>	144 $\pm$ 1.8	6 $\pm$ 2.0
After 4 weeks	67 $\pm$ 0.3 <sup>ab</sup>	147 $\pm$ 1.7	10 $\pm$ 1.4
ANOVA p value	< 0.01	0.11 <sup>c</sup>	0.08 <sup>c</sup>

<sup>a</sup> p < 0.05 vs at week 0

<sup>b</sup> p < 0.05 vs after 2 weeks

<sup>c</sup> ANOVA tests of samples between 2 weeks and 4 weeks

c) Thermal properties of microspheres with 0 to 25% paclitaxel loadings incubated in PBS-A at 37 °C after 2 weeks.

	Tg (°C)	Tc (°C)	Tm (°C)	Xc (%)
0% paclitaxel	65 $\pm$ 0.7	112 $\pm$ 1.2	148 $\pm$ 0.7	22 $\pm$ 3.1
5% paclitaxel	64	116	151	18
10% paclitaxel	64	-	149	15
25% paclitaxel	64 $\pm$ 0.4	-	144 $\pm$ 1.8	6 $\pm$ 1.2
ANOVA p value	0.055 <sup>d</sup>		0.015 <sup>d</sup>	< 0.01 <sup>d</sup>

<sup>d</sup> ANOVA tests of samples between 0% and 25% paclitaxel loadings

**Figure 21.** DSC scans of A) degrading control PLLA (2k g/mol) microspheres and B) degrading 25% paclitaxel-loaded PLLA (2k g/mol) microspheres incubated in PBS-A at 37 °C after 0, 2 and 4 weeks.

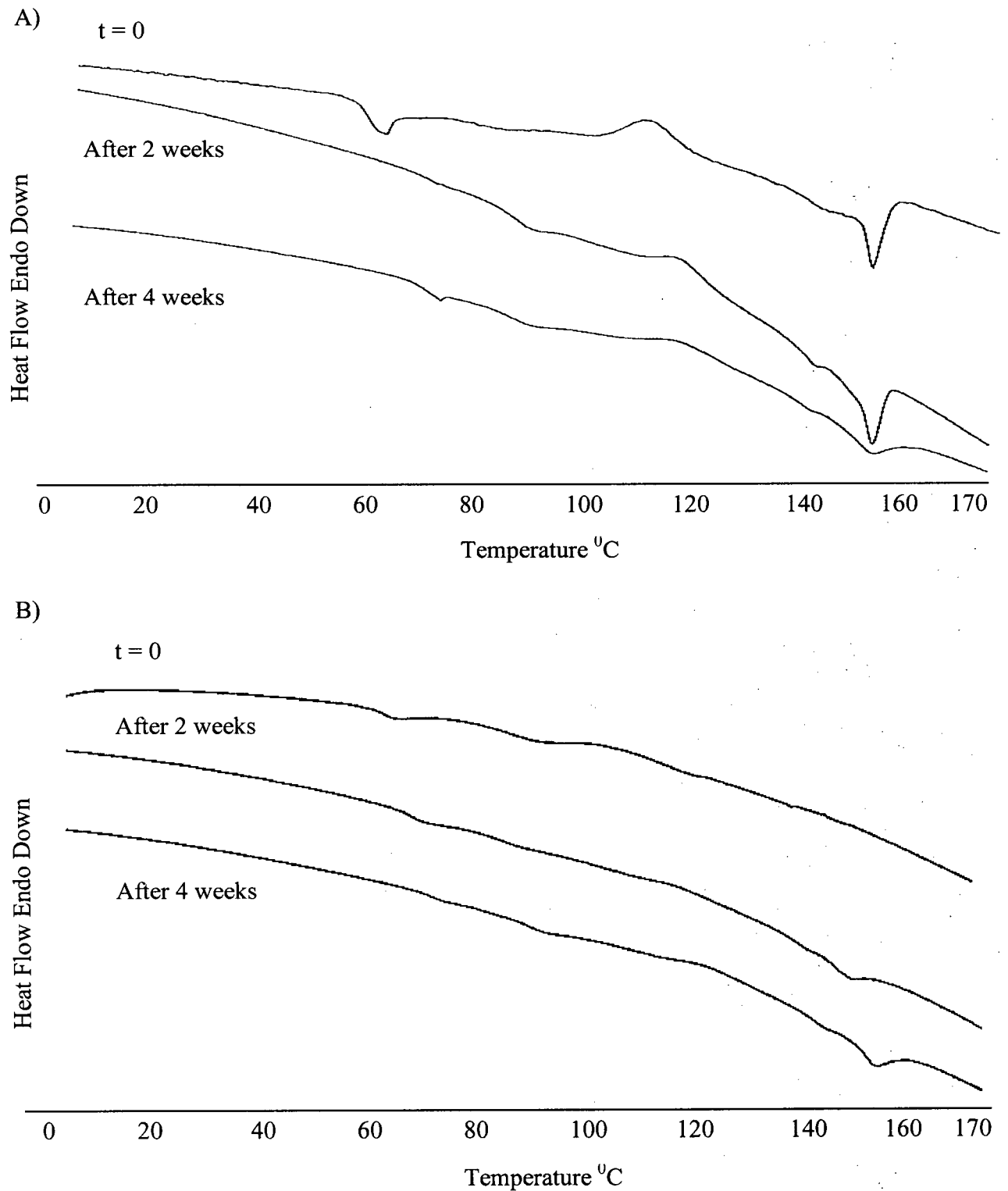
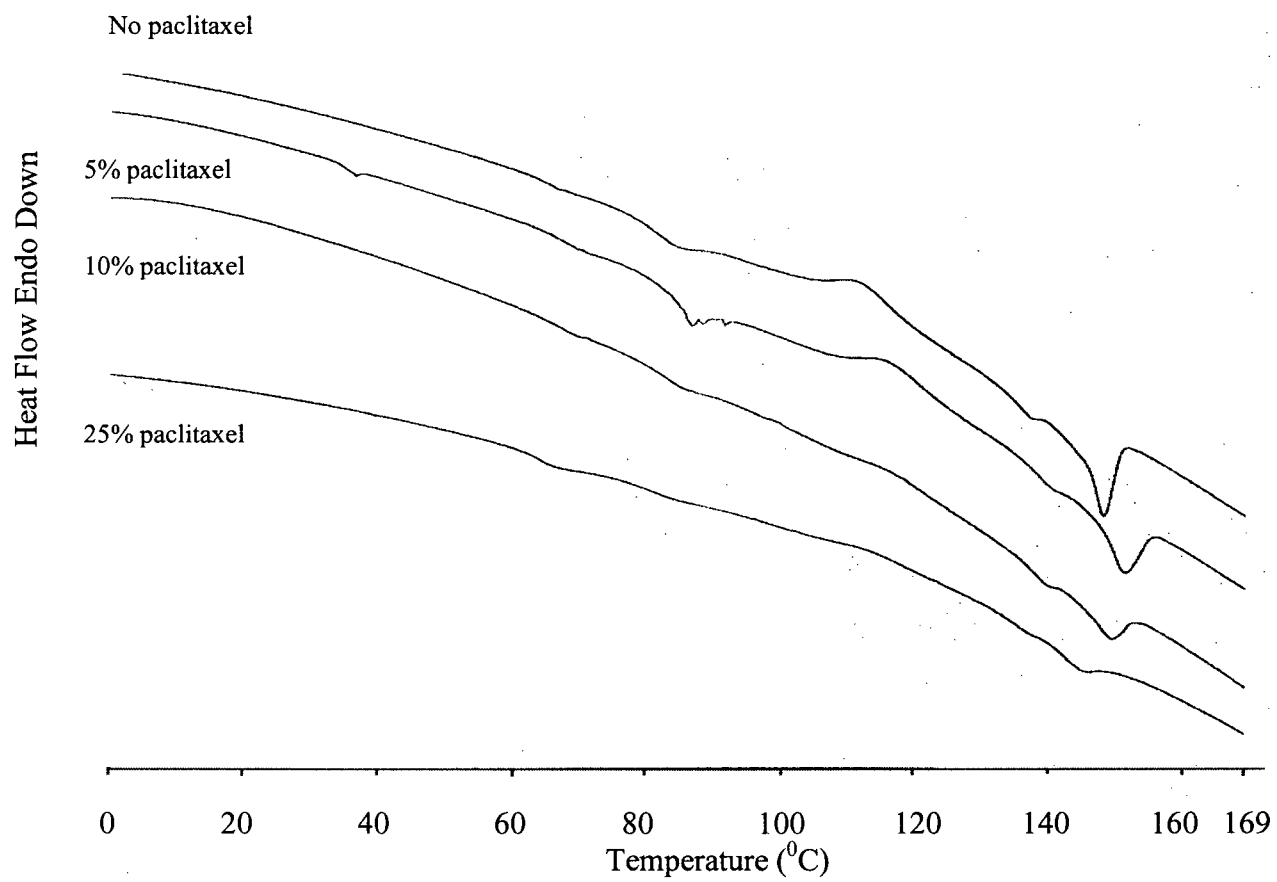


**Figure 22.** DSC scans of PLLA (2k g/mol) microspheres with paclitaxel loadings between 0 and 25% incubated in PBS-A at 37 °C after 2 weeks.



#### **4.3.1.3. Surface morphology**

Figure 23 shows the SEM micrographs of control microspheres degraded in PBS-A at 37 °C over 5 weeks. The surface of the microspheres became rough after 2 hours. After 1 week part of the outer layer of the microspheres started to erode and this process became more evident during the successive 3 weeks. After 5 weeks there was evidence of disintegration of the microspheres.

The SEM micrographs of 25% paclitaxel-loaded microspheres (Figure 24) showed a similar trend to those of control microspheres. However, they started losing structural integrity after 4 weeks and there was evidence of recrystallized paclitaxel within the matrix.

#### **4.3.1.4. Mass loss**

The mass loss is an indicator of the content of water-soluble oligomers formed by hydrolytic degradation, which are then released from the microspheres into the surrounding medium. Mass loss data for control microspheres over 5 weeks are presented in Figure 25. There was a rapid mass loss of up to 15% of their initial mass in the first week followed by a slower rate of mass loss. After 3 weeks, the rate increased and there was a total of 60% mass loss over 5 weeks.

**Figure 23.** SEM micrographs of control PLLA (2k g/mol) microspheres incubated in PBS-A at 37 °C after A) 2 hours, B) 1, C) 2, D) 3, E) 4 and F) 5 weeks. Magnification of micrographs is 200x (right hand top picture) and 1000x (all others).

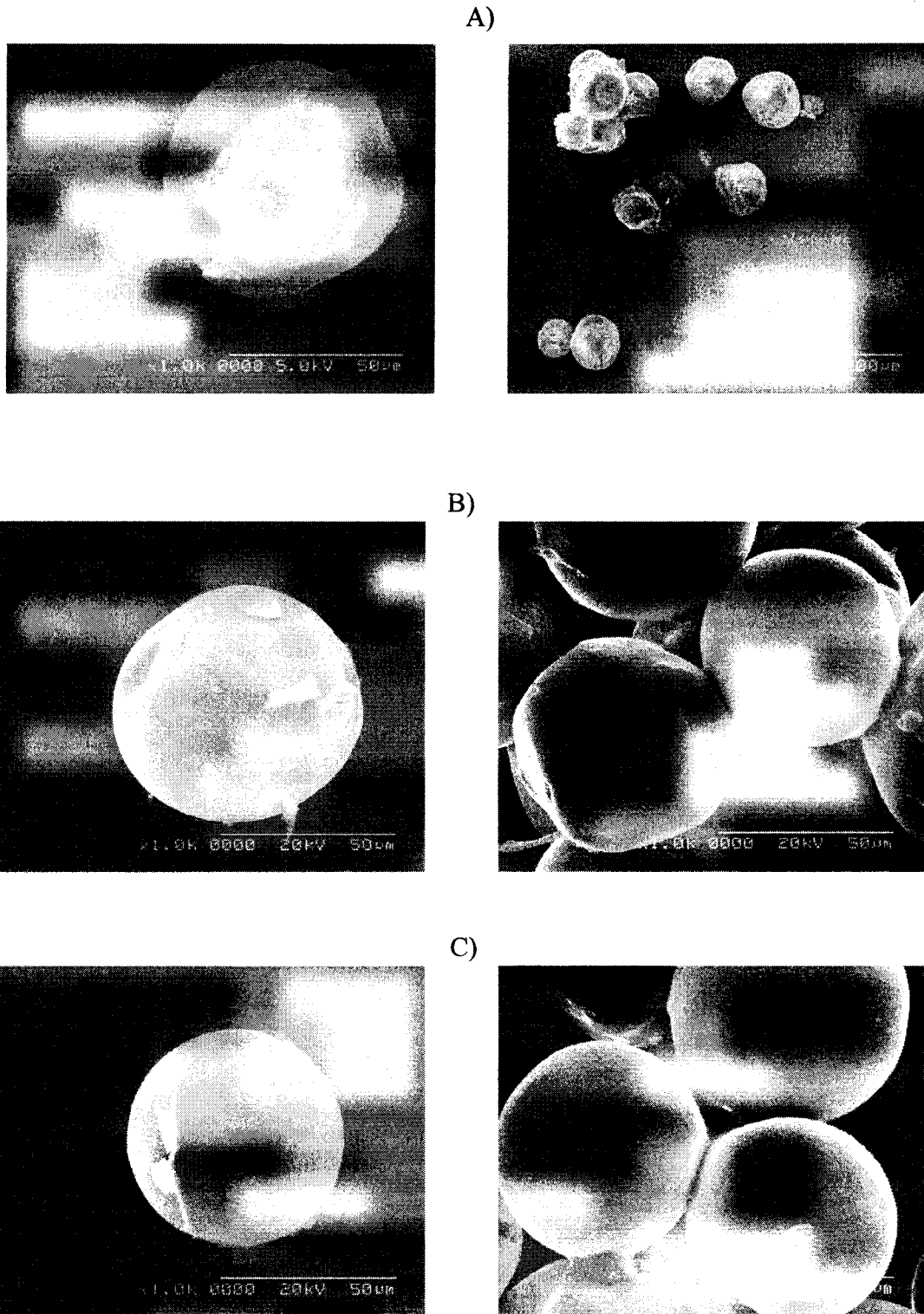


**Figure 23.** SEM micrographs of control PLLA (2k g/mol) microspheres incubated in PBS-A at 37 °C after A) 2 hours, B) 1, C) 2, D) 3, E) 4 and F) 5 weeks. Magnification of micrographs is 1000x.

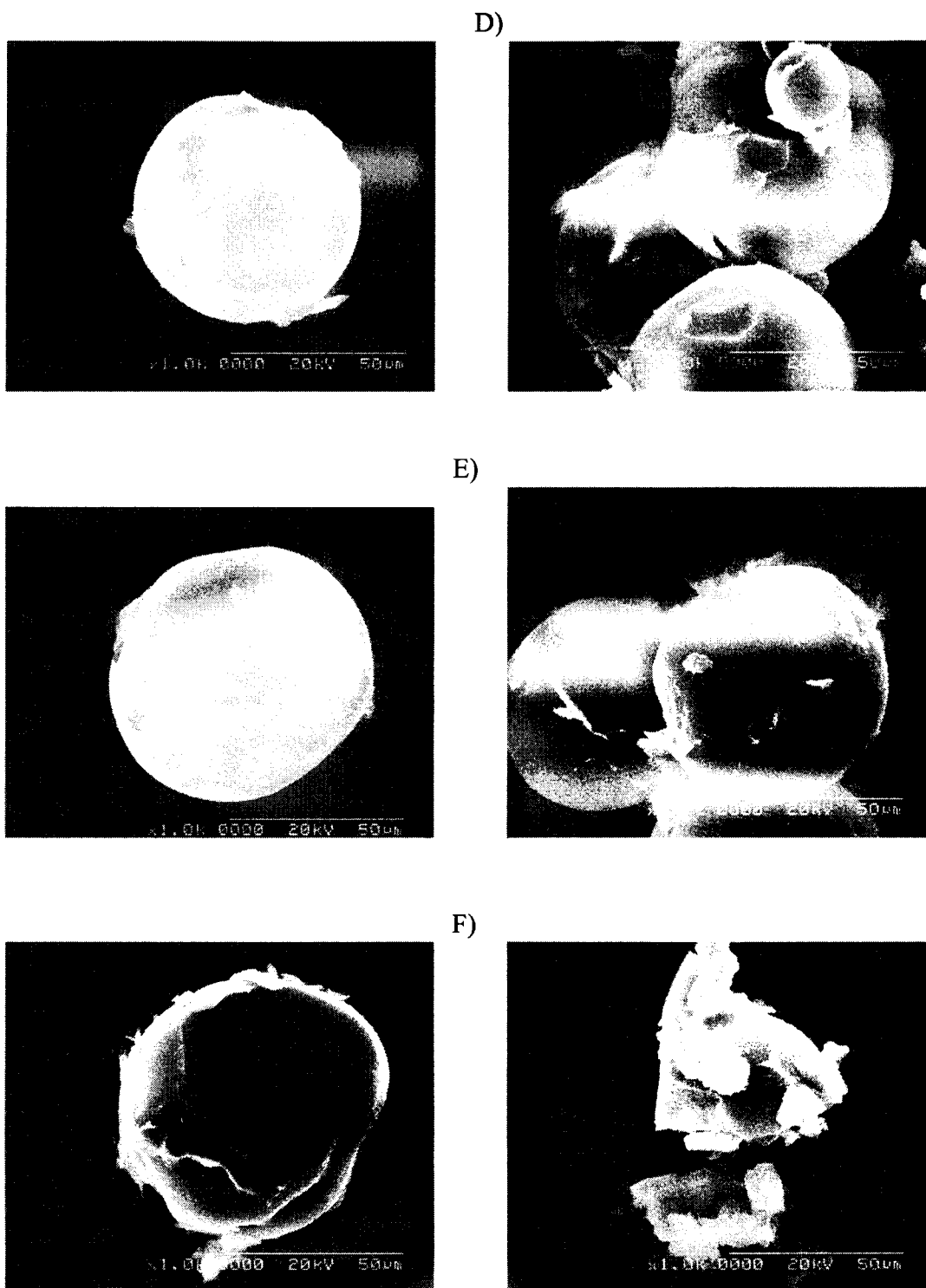


**Figure 24.** SEM micrographs of 25% paclitaxel-loaded PLLA (2k g/mol) microspheres incubated in PBS-A at 37 °C after A) 2 hours, B) 1, C) 2, D) 3, E) 4 and F) 5 weeks. Magnification of micrographs is 1000x (left hand pictures) and 500x (right hand pictures).

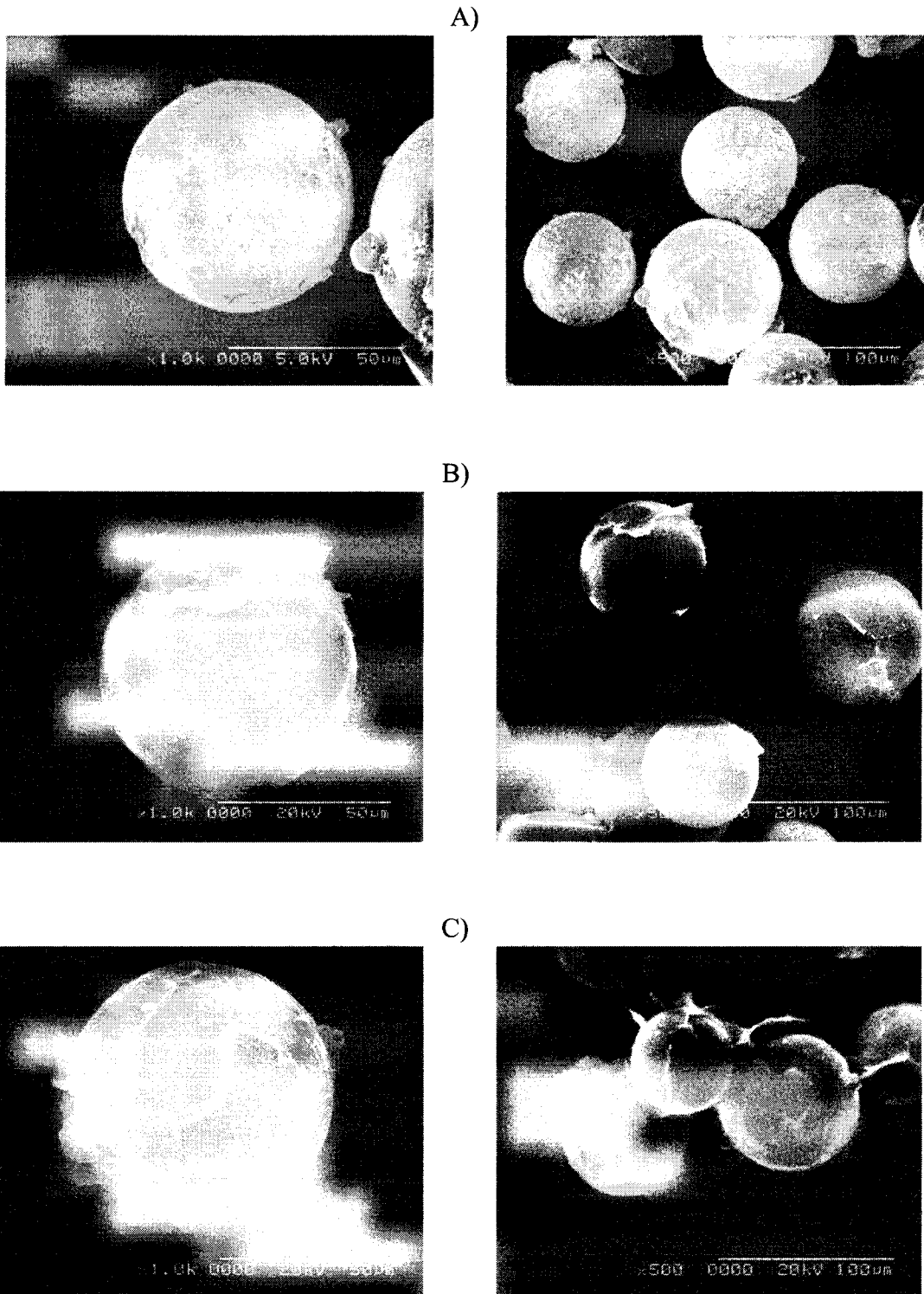


**Figure 24.** SEM micrographs of 25% paclitaxel-loaded PLLA (2k g/mol) microspheres incubated in PBS-A at 37 °C after A) 2 hours, B) 1, C) 2, D) 3, E) 4 and F) 5 weeks. Magnification of micrographs is 1000x (left hand pictures) and 500x (right hand pictures).

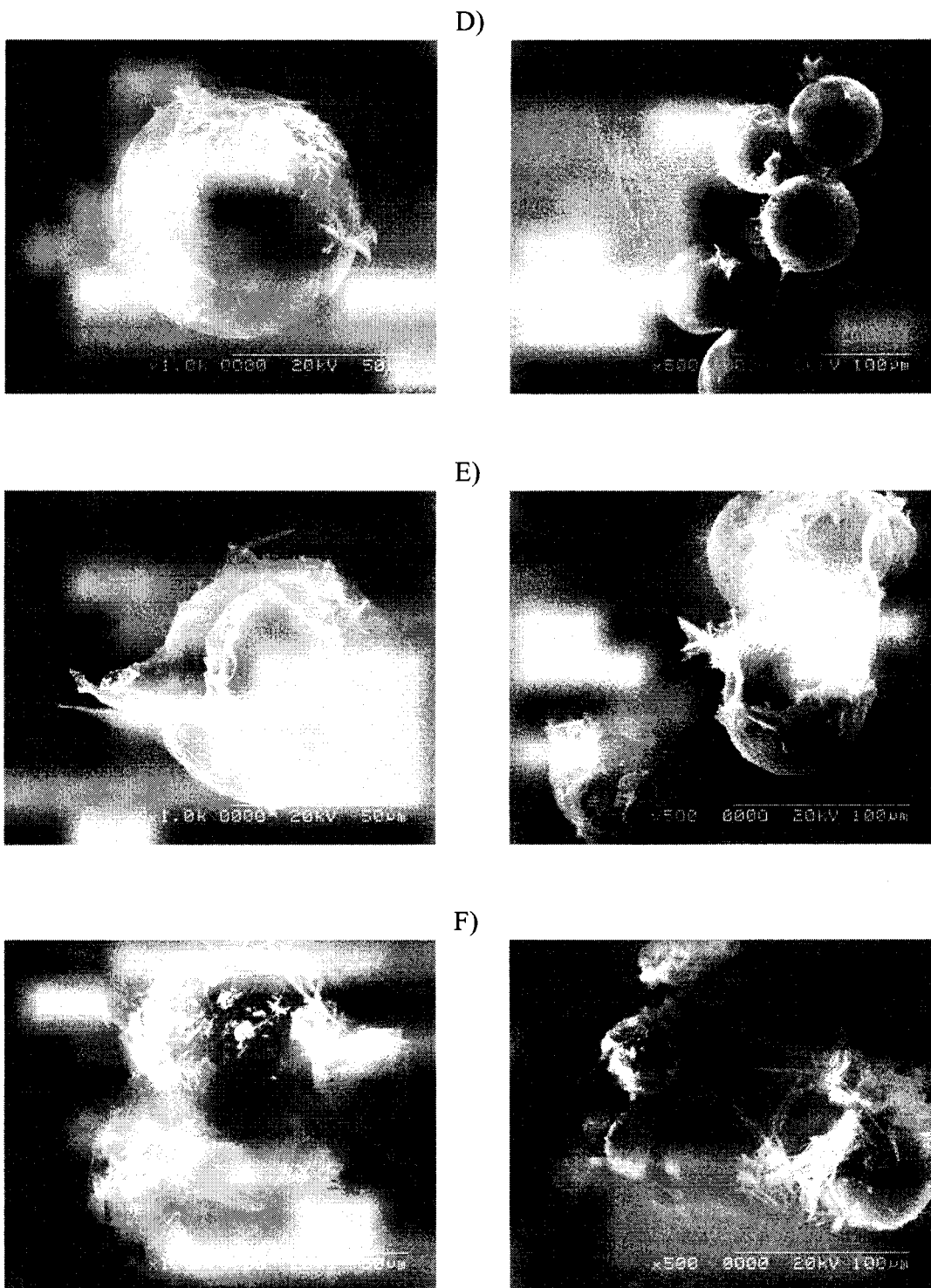
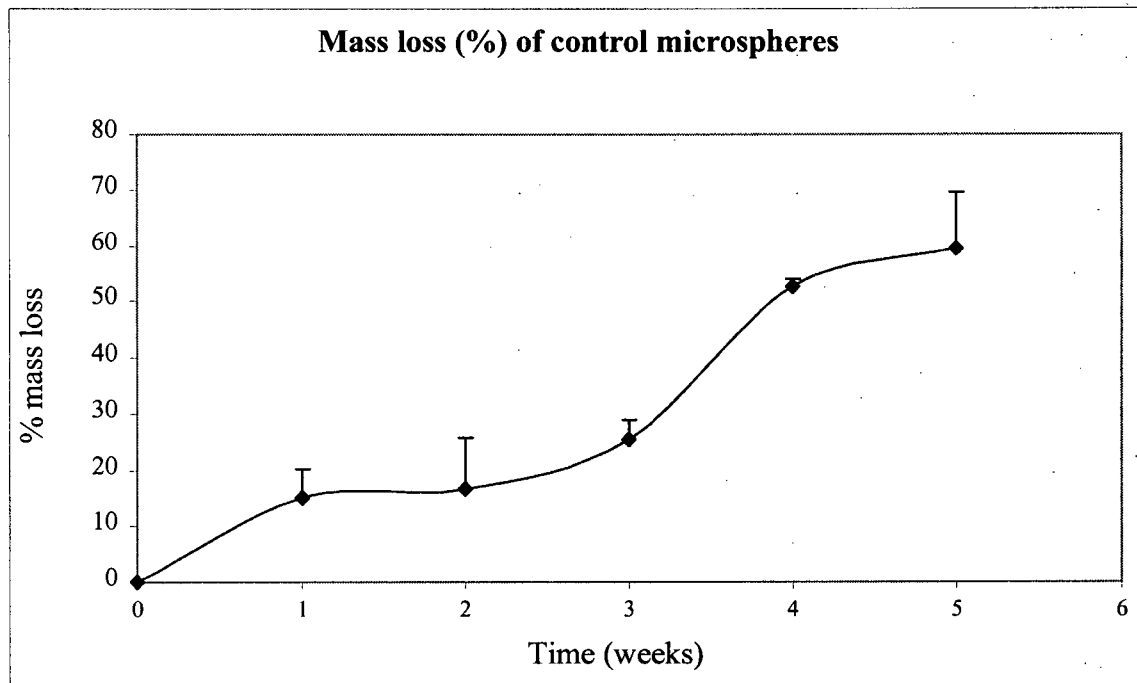


**Figure 25.** Mass loss (%) of control PLLA (2k g/mol) microspheres incubated in PBS-A at 37 °C over 5 weeks.



### **4.3.2. Degradation of films without and with microspheres**

#### **4.3.2.1. Surface morphology of films**

The SEM micrographs of chitosan films without microspheres incubated in PBS-A are shown in Figure 26. They show that after 1 week incubation, the surfaces of films became rough and dimpled. After 6 weeks, irregular pores were found on the surface. The appearance of the films also changed during incubation. Initially, the films were completely transparent, but turned white after several weeks of degradation.

The SEM micrographs of chitosan films loaded with either control microspheres (Figure 27) or 25% paclitaxel-loaded microspheres incubated in PBS-A (Figure 28) showed similar patterns. Microsphere surfaces became rough after 2 hours of incubation. After 6 weeks, the breakdown of microspheres within the chitosan films was observed.

The SEM micrographs of HA films loaded with control microspheres (Figure 29) showed that microspheres in the films began to surface erode after 4 hours of incubation.

**Figure 26.** SEM micrographs of chitosan films incubated in PBS-A at 37 °C after A) 1 and B) 6 weeks. (Magnification of micrographs is 600x and 500x.)

A) (600x)



B) (500x)



**Figure 27.** SEM micrographs of chitosan films with control PLLA (2k g/mol) microspheres incubated in PBS-A at 37 °C after A) 2 hours, B) 2, C) 3 and D) 6 weeks. Magnification of micrographs is 1000x (left hand pictures) and 200x (right hand pictures).

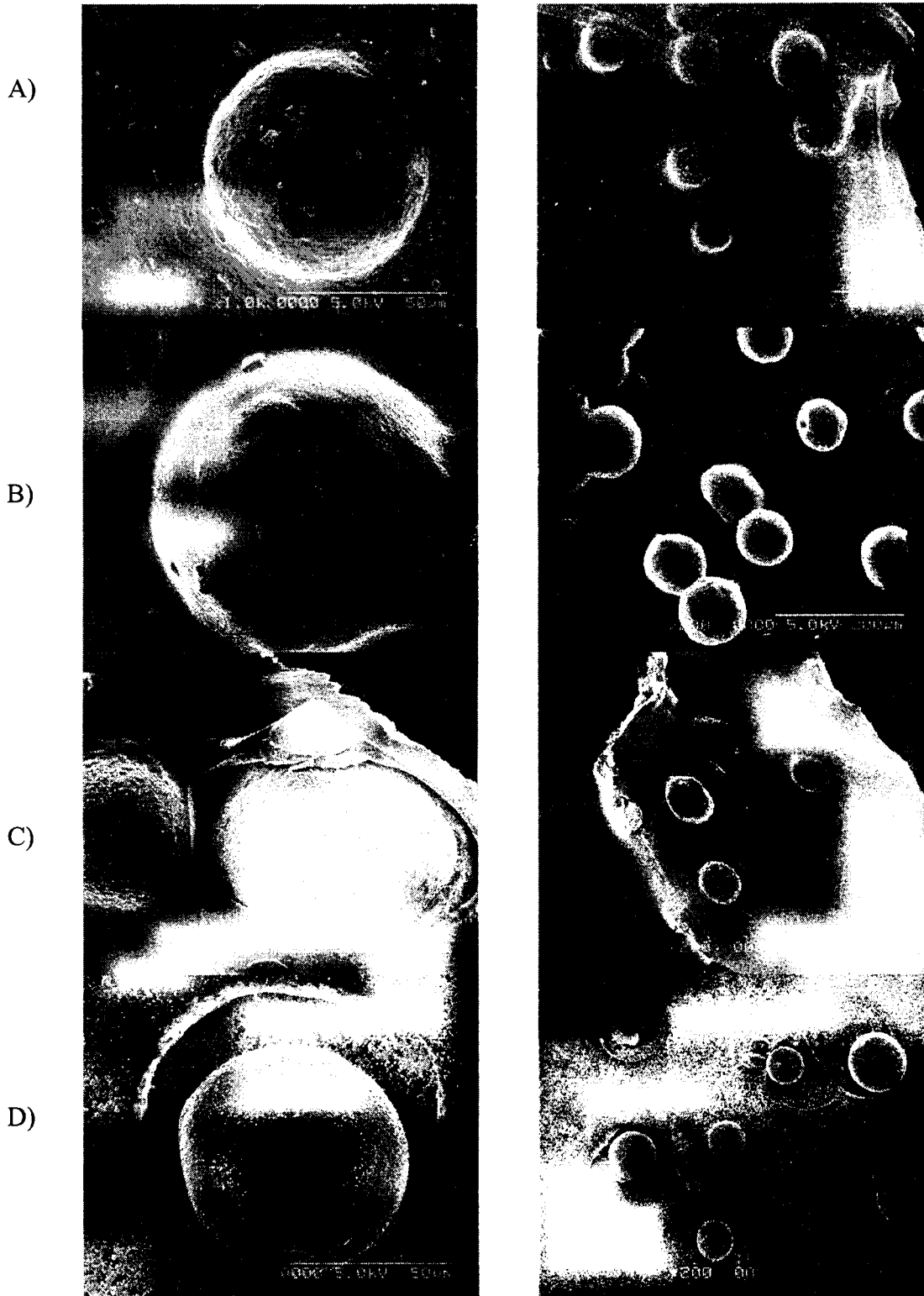


**Figure 28.** SEM micrographs of chitosan films with 25% paclitaxel-loaded PLLA (2k g/mol) microspheres incubated in PBS-A at 37 °C after A) 2 hours, B) 1, C) 2 and D) 6 weeks. Magnification of micrographs is 1000x (left hand picture) and 200x (right hand picture).

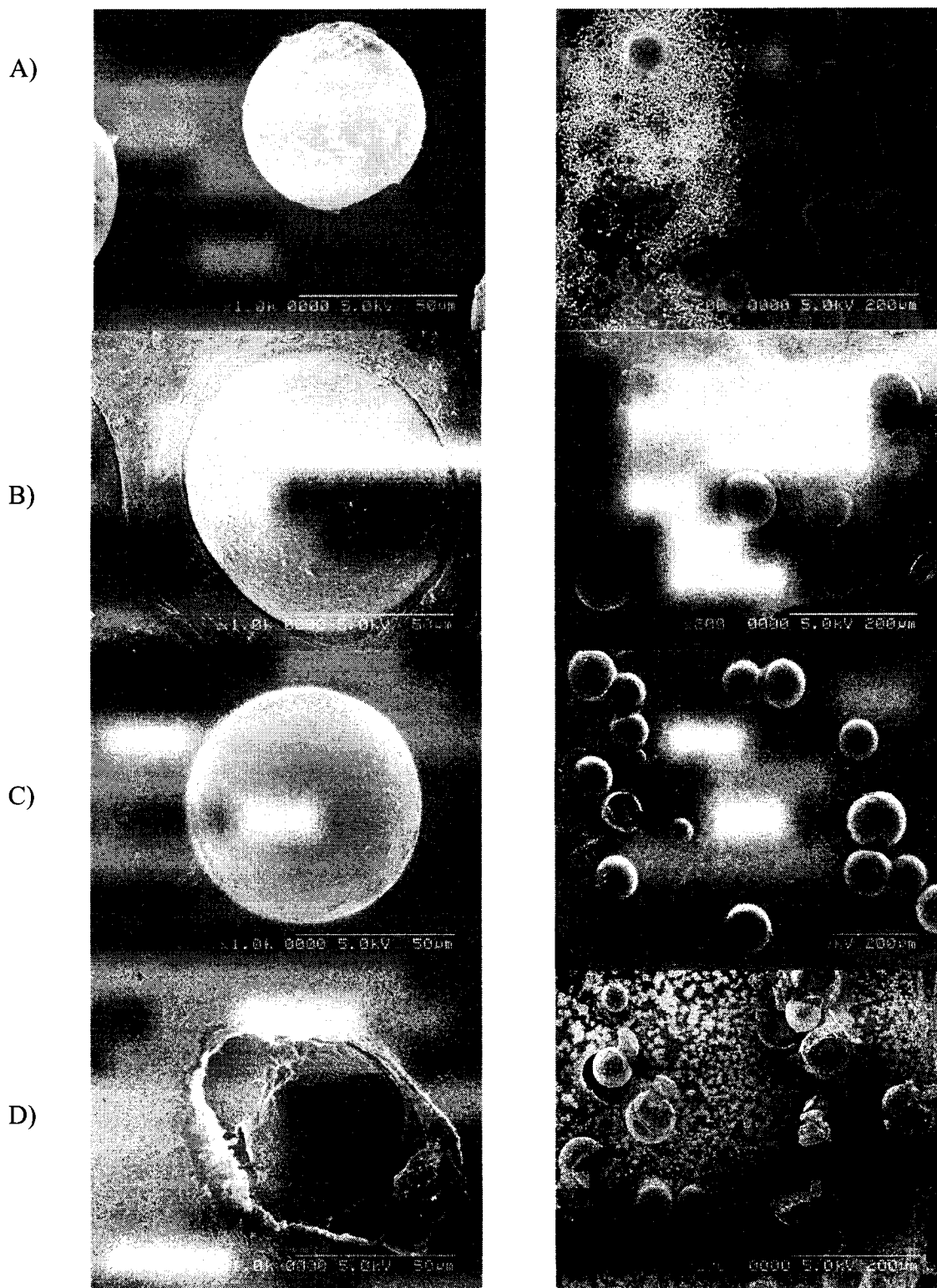
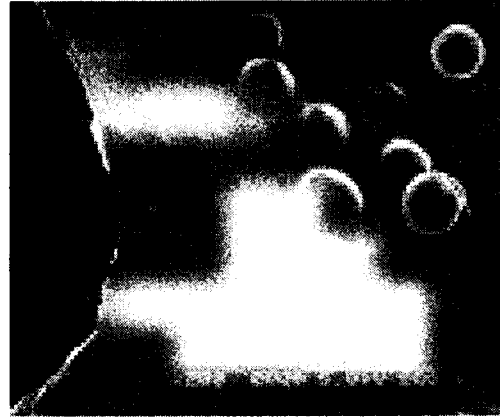
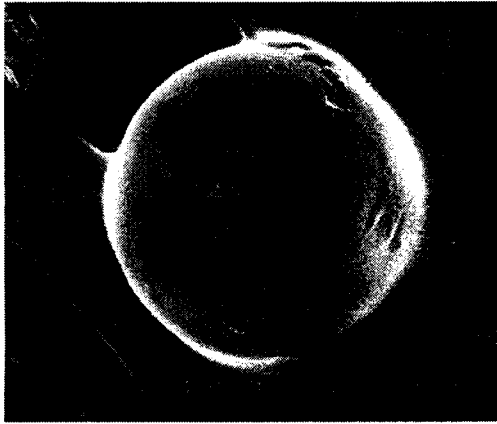
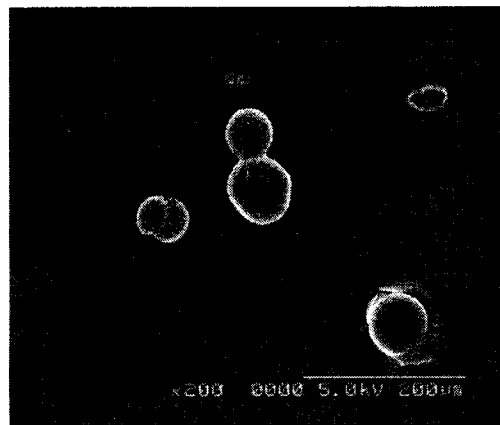
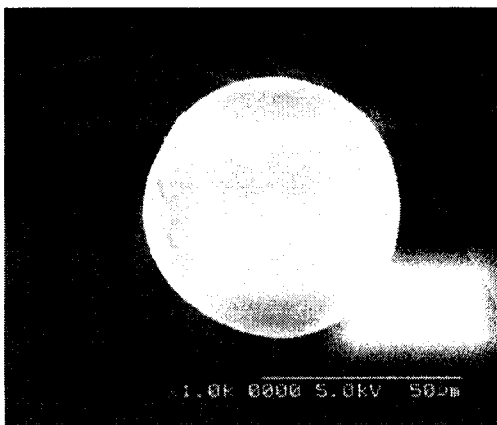


**Figure 29.** SEM micrographs of HA films with control PLLA (2k g/mol) microspheres incubated in PBS-A at 37 °C after A) 4, B) 12 and C) 20 hours. Magnification is 1000x (left hand pictures) and 200x (right hand pictures).

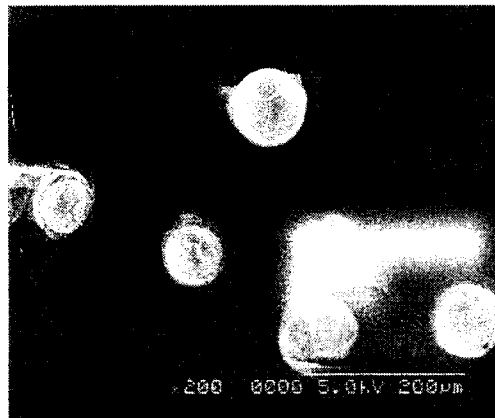
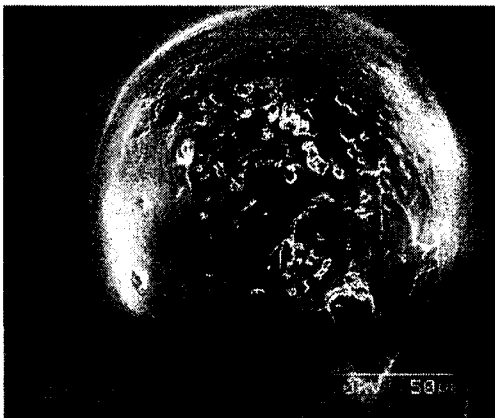
A)



B)



C)



#### **4.3.2.2. Mass loss of films**

##### **4.3.2.2.1. Mass loss of chitosan films**

Mass losses of chitosan films with and without control microspheres are shown in Figure 30. About 20% mass loss occurred in the first week and in total about 30% mass loss occurred over 6 weeks. Incorporation of microspheres into chitosan films had no significant effect on the mass loss profile of chitosan films.

##### **4.3.2.2.2. Mass loss of HA films**

Mass losses of HA films (Figure 31) were rapid for both non microsphere-loaded and control microsphere-loaded films. They both lost about 26% by weight in 4 hours and about 83% in 20 hours. Statistical analysis showed that there was no significant difference in mass loss between microsphere-loaded and non microsphere-loaded HA films.

**Figure 30.** Mass loss (%) of chitosan films without and with control PLLA (2k g/mol) microspheres incubated in PBS-A at 37 °C over 6 weeks.

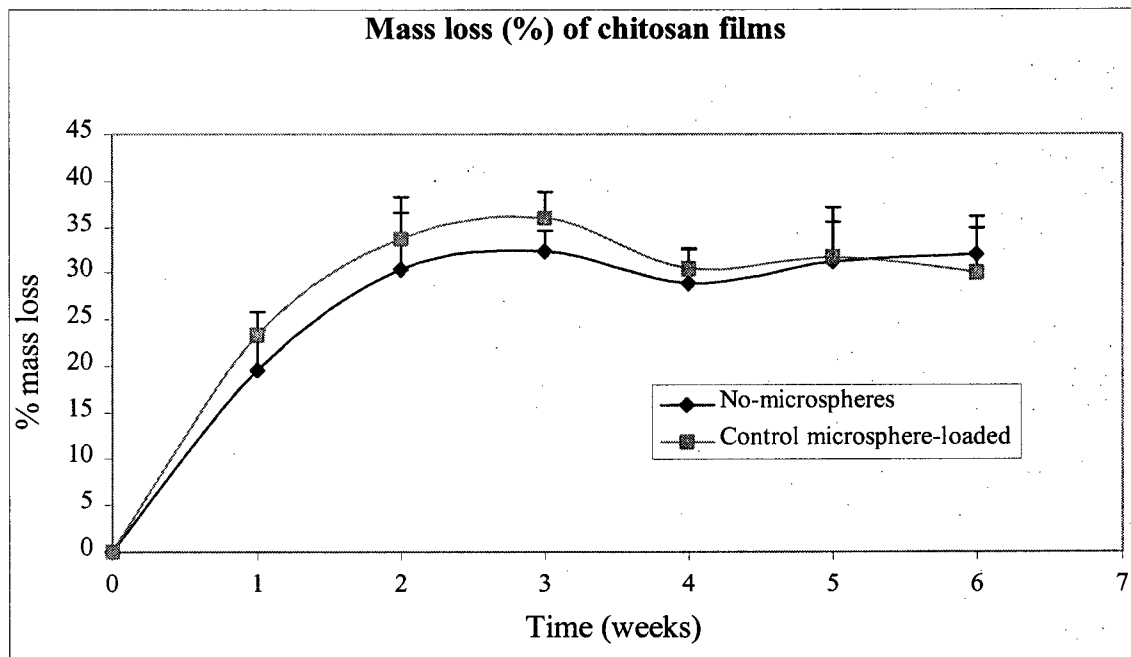
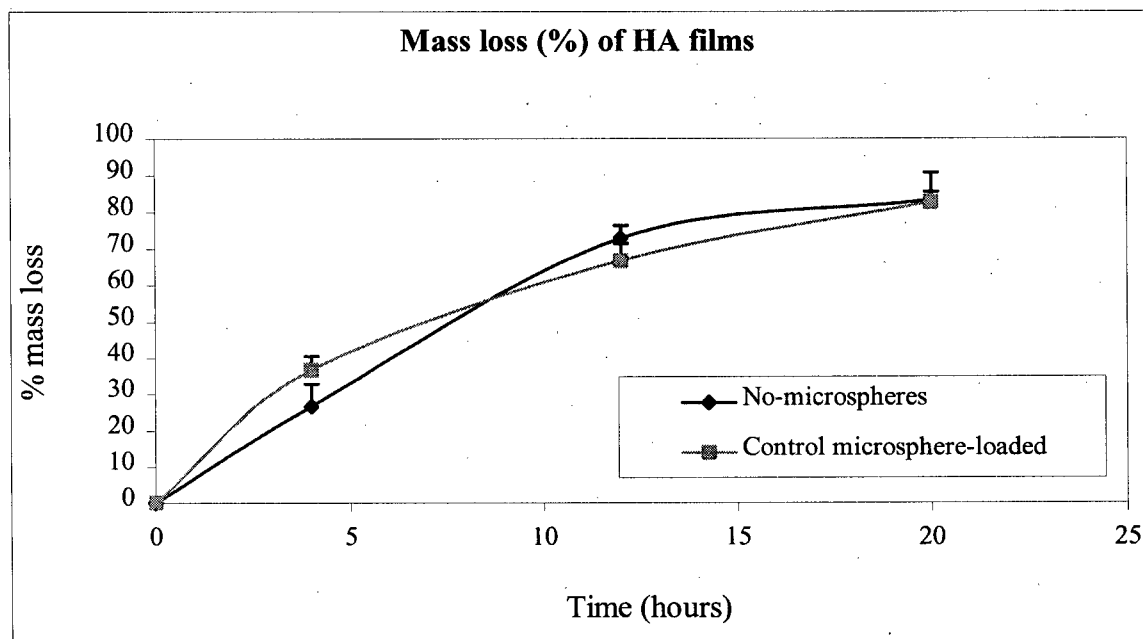


**Figure 31.** Mass loss (%) of HA films without and with control PLLA (2k g/mol) microspheres incubated in PBS-A at 37 °C over 20 hours.



#### **4.4. Validation of paclitaxel standard curves in acetonitrile: water 60: 40**

The paclitaxel standard curves in acetonitrile: water 60: 40 in the range of 0.3 to 20 µg/ml were validated. The precision data in Table 13 showed sufficient precision within each day and between 3 days. The accuracy results (Table 14) indicated sufficient accuracy at concentrations down to 0.6 µg/ml on all three days. The regression coefficient  $R^2$  of all standard curves was 0.9998 or greater.

#### **4.5. In vitro release studies**

In all in vitro release studies, the sampling intervals were chosen so that sink conditions (paclitaxel concentrations no greater than 15% of its solubility) would not be exceeded. Based on a solubility value for paclitaxel in the release medium of 1.4 µg/ml at 37 °C (Winterniz, 1999), 10.5 µg in 50 ml of PBS-A would be the maximum value allowed to maintain sink conditions. Previous work in our lab had shown that paclitaxel was stable in PBS-A for 3 days. Therefore, sampling intervals were maintained in all release studies at 3 days or less, except at the very late stage with little drug released. It was observed that when paclitaxel was present in PBS-A for 3 days or more, a second peak corresponding to 7-epitaxol appeared due to epimerization of paclitaxel (Figure 32). Its peak was included in the determination of paclitaxel released.

##### **4.5.1. Paclitaxel release profiles from PLLA (2k g/mol) microspheres**

The in vitro release profiles of paclitaxel from 50-90 µm microspheres with different loadings are shown in Figure 33. In general, all microspheres at 5% and 10% paclitaxel loading showed a phase of rapid drug release followed by a slower release phase. However, microspheres with 25% paclitaxel loading showed release profiles in which the rate of paclitaxel release was almost constant up to day 15 and then the rate of

release decreased slightly. The total amounts of paclitaxel released after 27 days were  $155 \pm 3 \mu\text{g}$ ,  $260 \pm 28 \mu\text{g}$  and  $418 \pm 13 \mu\text{g}$  for 5, 10 and 25% paclitaxel-loaded microspheres, respectively. The percent paclitaxel released values were 57%, 47% and 30% for 5, 10 and 25% paclitaxel-loaded microspheres.

After the release study was completed, the residual paclitaxel in the remaining material was assayed by extraction with DCM and quantification with HPLC. The percent residual paclitaxel was less than 1% for both 5 and 10% paclitaxel-loaded microspheres and 2% for 25% paclitaxel-loaded microspheres. The recovery (the sum of percent released and percent residual) of paclitaxel was less than expected, which could be attributed primarily to the loss of paclitaxel during the sampling procedures.

The microspheres were observed to be freely dispersed in the release medium for the first three days of release study. By the end of the first week, the microspheres had begun to aggregate and adhere to the bottom of the tube.

#### **4.5.2. Release study of paclitaxel from microsphere-loaded films**

##### **4.5.2.1. Release study of paclitaxel from chitosan films incorporated with microspheres of different size ranges**

Figure 34 shows the in vitro release profiles of paclitaxel from chitosan films containing 20% paclitaxel-loaded microspheres prepared using 5% PLLA. The cast chitosan films contained 1% paclitaxel loading and the incorporated microspheres were in the following size ranges, <10, 10-50 and 50-90  $\mu\text{m}$ . The release profiles over 72 days were biphasic with an initial burst phase over about 2 days followed by sustained slow release. The initial release rates ( $V_0$ , defined as the release rate during the first 31 hours of studies) and total extent of paclitaxel released (total amount released over 72 days,

$M_{72}$ ) were  $6 \pm 1.3 \mu\text{g/day}$  and  $30 \pm 5.9 \mu\text{g}$ ,  $8 \pm 0.2 \mu\text{g/day}$  and  $43 \pm 4.8 \mu\text{g}$ , and  $11 \pm 2.0 \mu\text{g/day}$  and  $61 \pm 4.9 \mu\text{g}$  for chitosan films loaded with less than 10, 10-50 and 50-90  $\mu\text{m}$  microspheres. Both the initial release rate and total extent of release increased significantly with the increase in the microsphere sizes (ANOVA  $p < 0.01$ ).

#### **4.5.2.2. Release study of paclitaxel from chitosan films and HA films loaded with microspheres of different drug loadings**

The paclitaxel release profiles from chitosan and HA films with different drug loadings are shown in Figure 35 and 36 respectively. Both chitosan and HA films were incorporated with 50–90  $\mu\text{m}$  microspheres of different paclitaxel loadings, 5, 10 and 25%. By loading 20% by weight microspheres in films, 1, 2 and 5% paclitaxel-loaded films were obtained. For both chitosan and HA films containing microspheres, biphasic release profiles were characterized by a 2 to 3 day burst phase followed by sustained slow release for a period of 38 days. The initial release rates of paclitaxel ( $V_0$ , defined as the release rate during the first 24 hours of studies) for 1, 2 and 5% paclitaxel-loaded films were  $70 \pm 7.0$ ,  $66 \pm 6.4$ , and  $60 \pm 3.3 \mu\text{g/d}$  for chitosan films compared to  $37 \pm 4.4$ ,  $42 \pm 3.5$ , and  $39 \pm 7.5 \mu\text{g/d}$  for HA films. The total extent of paclitaxel released (total amount released over 38 days,  $M_{38}$ ) for 1, 2 and 5% paclitaxel-loaded films were  $123 \pm 8.8$ ,  $170 \pm 8.8$  and  $307 \pm 13.4 \mu\text{g}$  for chitosan films compared to  $100 \pm 8.0$ ,  $168 \pm 11.4$  and  $379 \pm 8.6 \mu\text{g}$  for HA films. The initial release rates ( $V_0$ ) of paclitaxel from chitosan films for each drug loading were statistically significantly higher than from HA films (ANOVA  $p < 0.01$  for each comparison). For both chitosan and HA films, paclitaxel was released significantly faster from 5% paclitaxel-loaded films than from 1% and 2% paclitaxel-

loaded films. The extent of release ( $M_{38}$ ) statistically significantly increased with the increase in paclitaxel loading in the films (ANOVA  $p < 0.01$ ).

A comparison of the in vitro release profiles of paclitaxel from 5% paclitaxel loaded microspheres (50-90  $\mu\text{m}$ ) and chitosan and HA films containing the same microspheres is shown in Figure 37. In the first 3 days of the release study, 22%, 41% and 27% paclitaxel was released from PLLA microspheres alone, chitosan and HA films containing PLLA microspheres, respectively. After 27 days release, 57% paclitaxel was released from microspheres alone compared to 45% and 36% from chitosan and HA films containing microspheres.

**Table 13.** Inter- and intra-day precision of standard curves of paclitaxel in acetonitrile:water 60:40

PTX conc (µg/ml)	Day 1		Day 2		Day 3		All days		ANOVA P Value
	Peak area	RSD (%)							
0.3	17092	4.3	16269	3.8	16690	9.6	16685	6.2	0.58
0.6	31076	2.1	29933	6.6	29528	4.7	30179	4.9	0.34
1.2	59089	1.2	57648	4.5	57026	4.4	57921	3.7	0.41
2.5	115745	1.0	110775	5.2	109314	5.7	111945	4.5	0.17
5	221948	1.9	215768	5.3	214271	5.1	217329	4.3	0.50
10	437155	1.5	424035	4.3	420737	5.9	427309	4.2	0.44
20	852800	1.7	816513	6.1	864900	6.7	844738	5.4	0.33

Peak area is the average calculated from four standards at each concentration (n=12 for all days)

RSD (Relative standard deviation) is the ratio of the standard deviation to the average, expressed as a percentage.

A value less than 10% indicates sufficient precision at each concentration.

ANOVA P values are level of significance for single factor ANOVA tests between each day's peak areas at each concentration.

P < 0.05 indicates a significant difference between peak areas on different days.

**Table 14.** Accuracy of standard curves of paclitaxel in acetonitrile: water 60: 40

PTX Conc. (µg/ml)	Day 1			Day 2			Day 3		
	Predicted Value	RSD (%)	Bias (%)	Predicted Value	RSD (%)	Bias (%)	Predicted Value	RSD (%)	Bias (%)
0.3	0.27	5.6	13.3	0.27	7.2	18.0	0.35	12.6	13.1
0.6	0.59	3.2	6.1	0.61	10.0	2.6	0.63	2.2	1.1
1.2	1.24	1.1	0.9	1.30	6.1	4.2	1.24	2.2	0.4
2.5	2.54	1.3	1.5	2.63	5.4	5.4	2.40	3.7	4.1
5	4.97	2.2	0.6	5.28	6.6	5.7	4.75	3.9	5.1
10	9.89	1.0	1.1	10.55	5.2	5.5	9.32	4.7	6.8
20	19.40	1.3	3.0	20.05	6.6	0.3	19.10	5.0	4.5

Predicted value is the average (n = 3 for each day) of values of concentration calculated from one standard curve on each day.

RSD (Relative standard deviation) is the ratio of the standard deviation to the average, expressed as a percentage.

A value less than 10% indicates sufficient accuracy at each concentration.

Bias is the ratio of the deviation of predicted value from the actual concentration measured, expressed as a percentage.

**Figure 32.** HPLC chromatogram of paclitaxel and 7-epitaxol. (Column: Novo-Pak C<sub>18</sub> column. Mobile phase: acetonitrile: water: methanol 58: 37: 5. Mobile phase flow rate: 1 ml/min.)

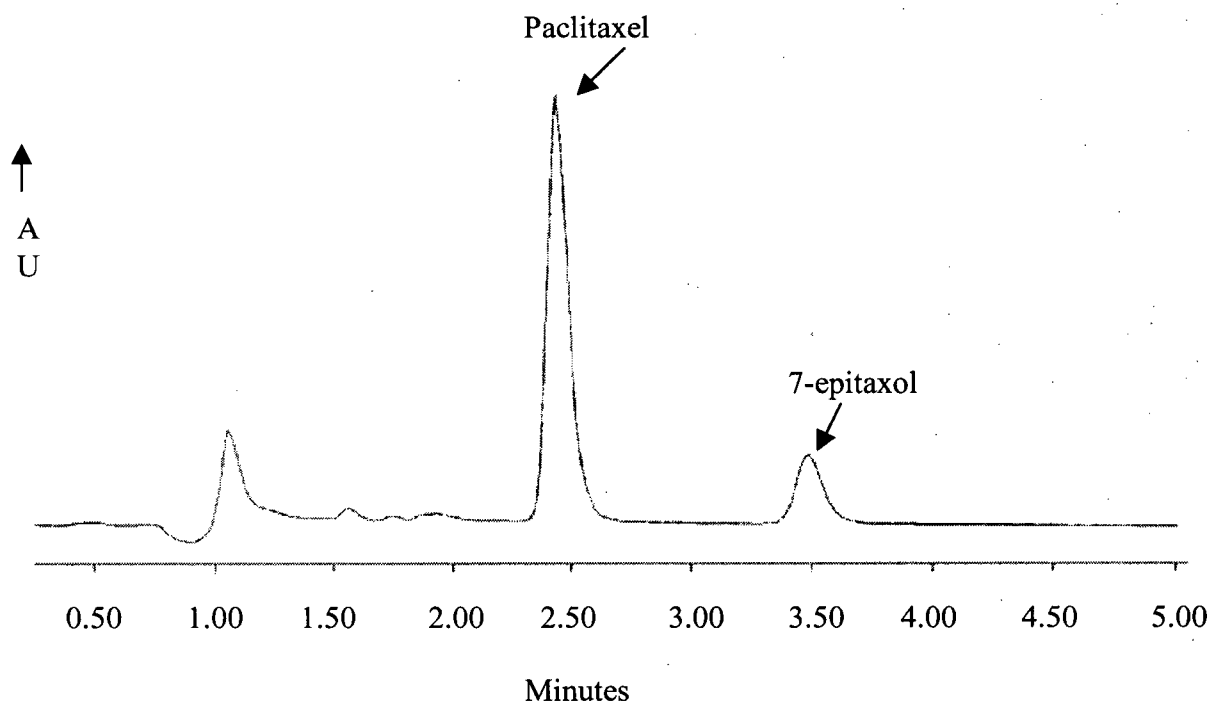
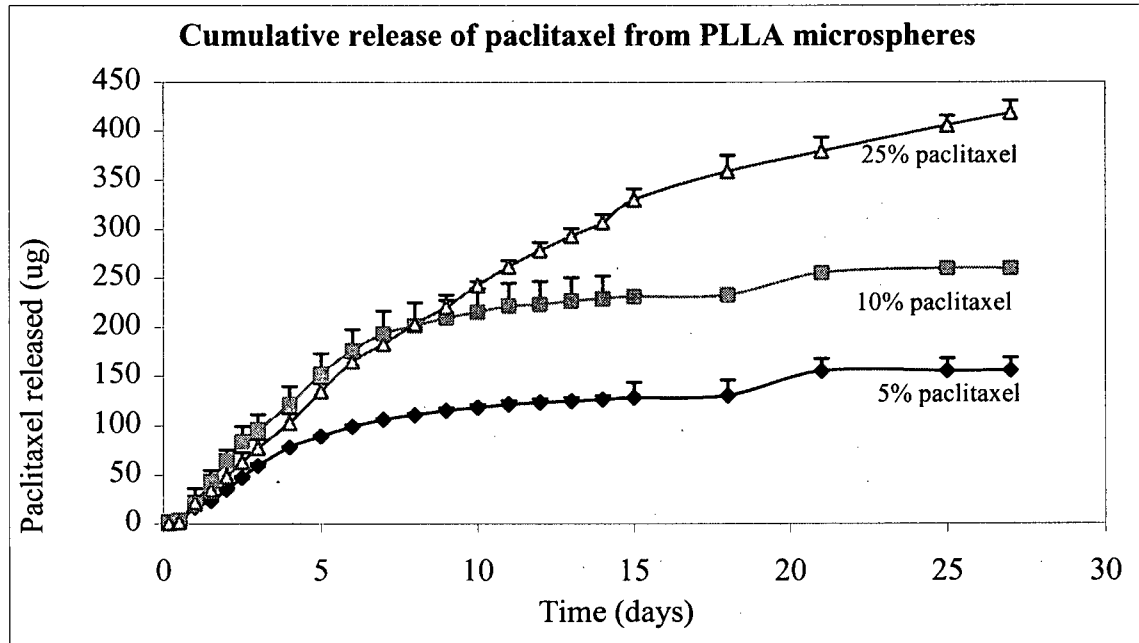


**Figure 33.** In vitro release profiles of paclitaxel from 50-90  $\mu\text{m}$  PLLA (2k g/mol) microspheres with 5, 10 and 25% paclitaxel loadings. (A: Cumulative release of paclitaxel vs. time; B: Cumulative percent release of paclitaxel vs. time)

A.



B.

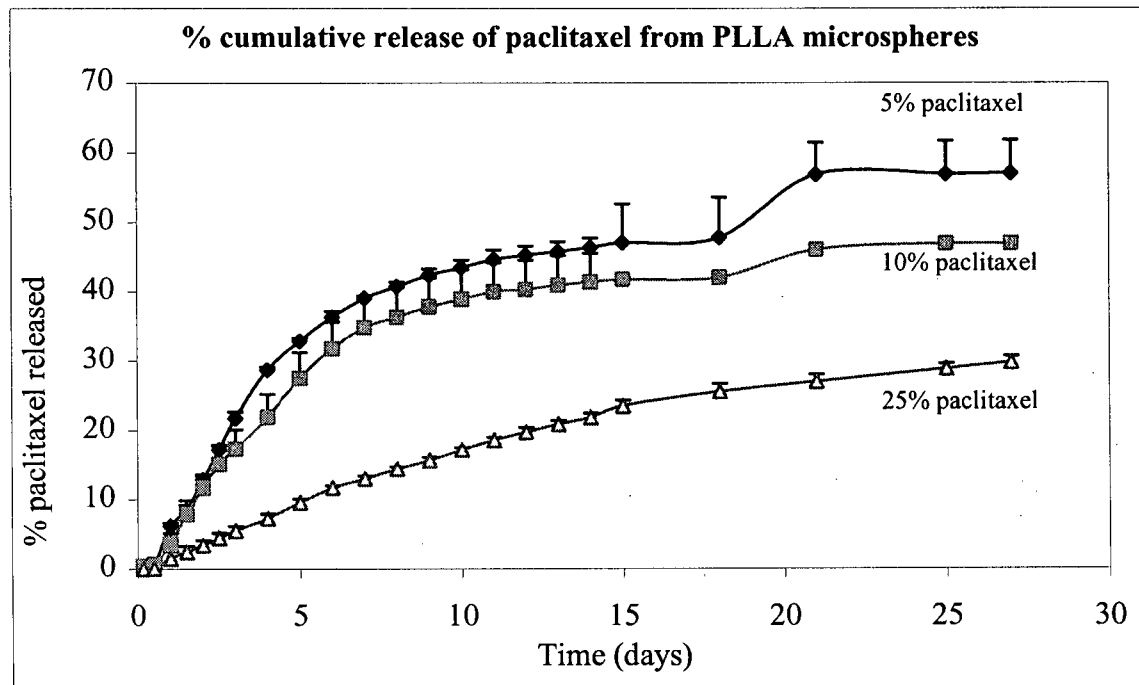
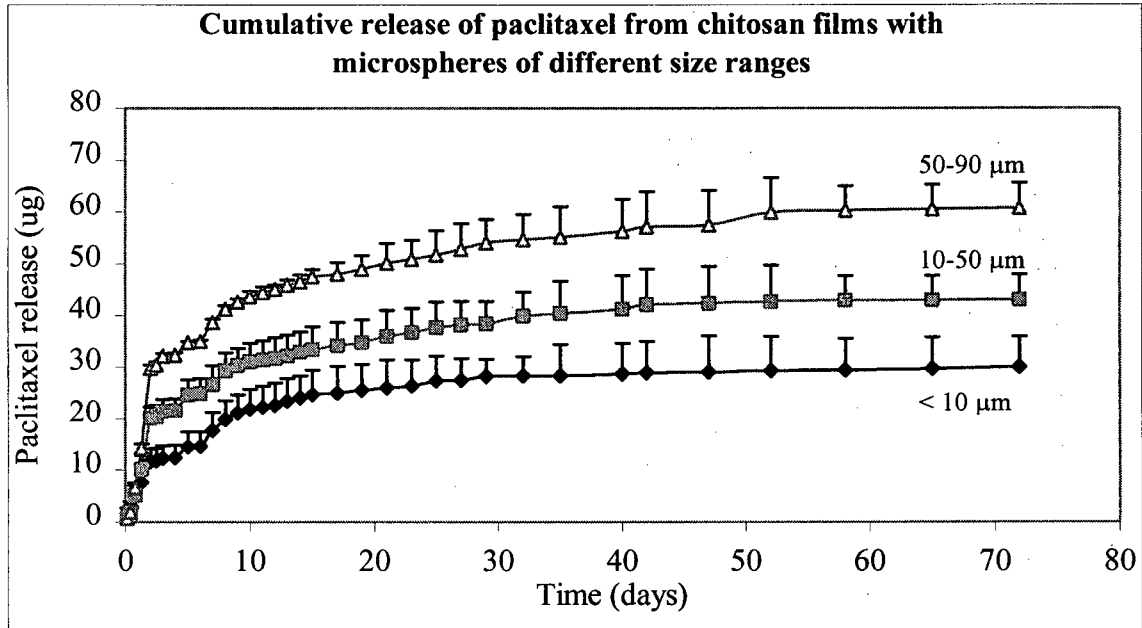


**Figure 34.** In vitro release profiles of paclitaxel from chitosan films containing 20% paclitaxel-loaded PLLA (2k g/mol) microspheres. Microspheres were in different size ranges: < 10, 10-50 and 50-90  $\mu\text{m}$  and paclitaxel loading was 1% in all chitosan films. (A: Cumulative release of paclitaxel vs. time; B: Cumulative percent release vs. time.)

A.



B.

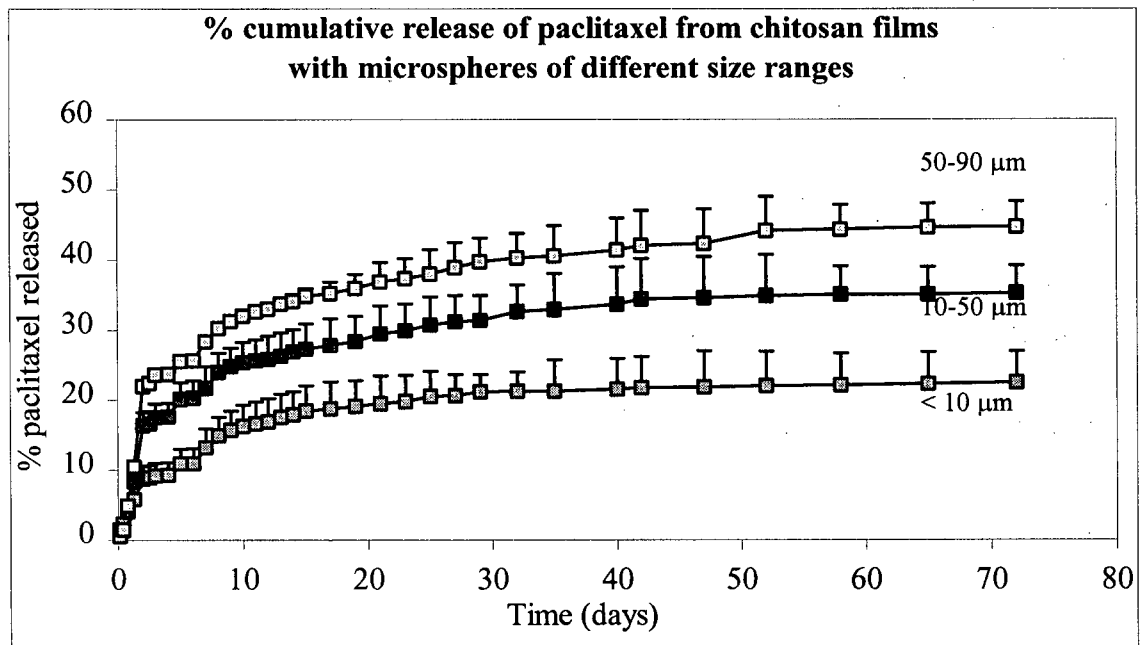
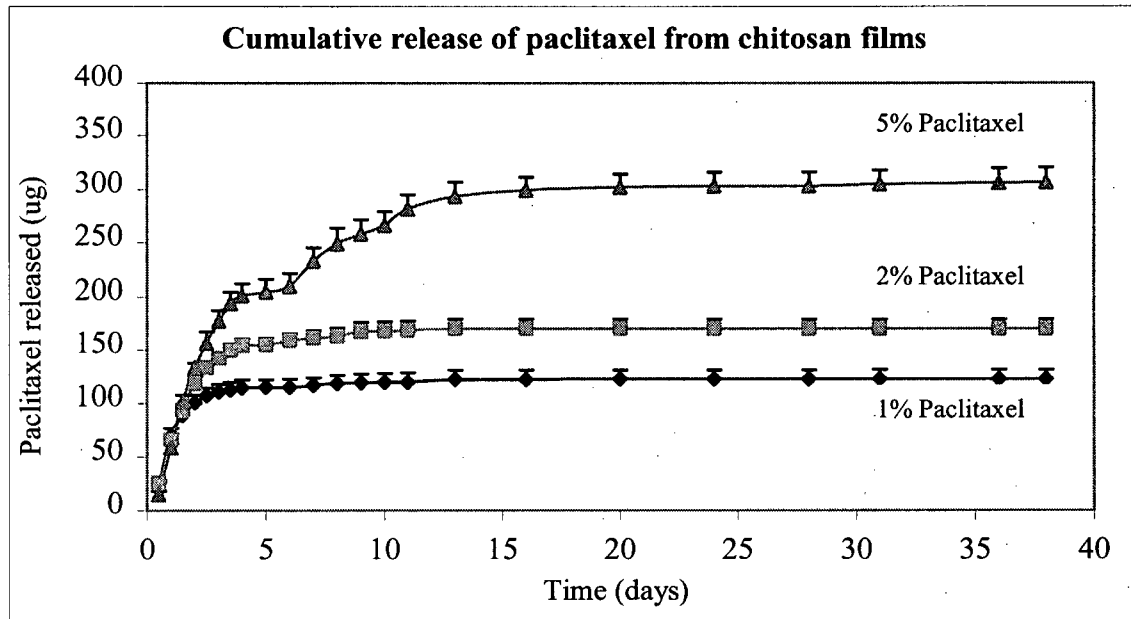


**Figure 35.** In vitro release of paclitaxel from chitosan films containing 50-90  $\mu\text{m}$  PLLA (2k g/mol) microspheres with different drug loadings. Chitosan films possessed 1, 2 and 5% loadings by loading 5, 10 and 25% paclitaxel-loaded microspheres. (A: Cumulative amount released vs. time; B: Cumulative percent released vs. time).

A.



B.

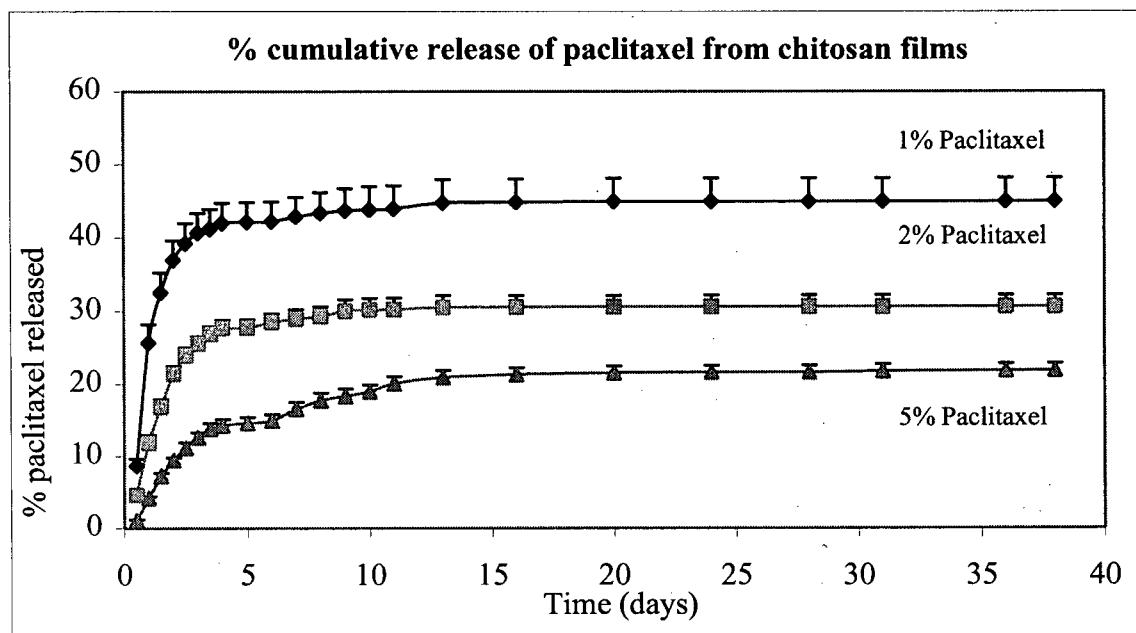
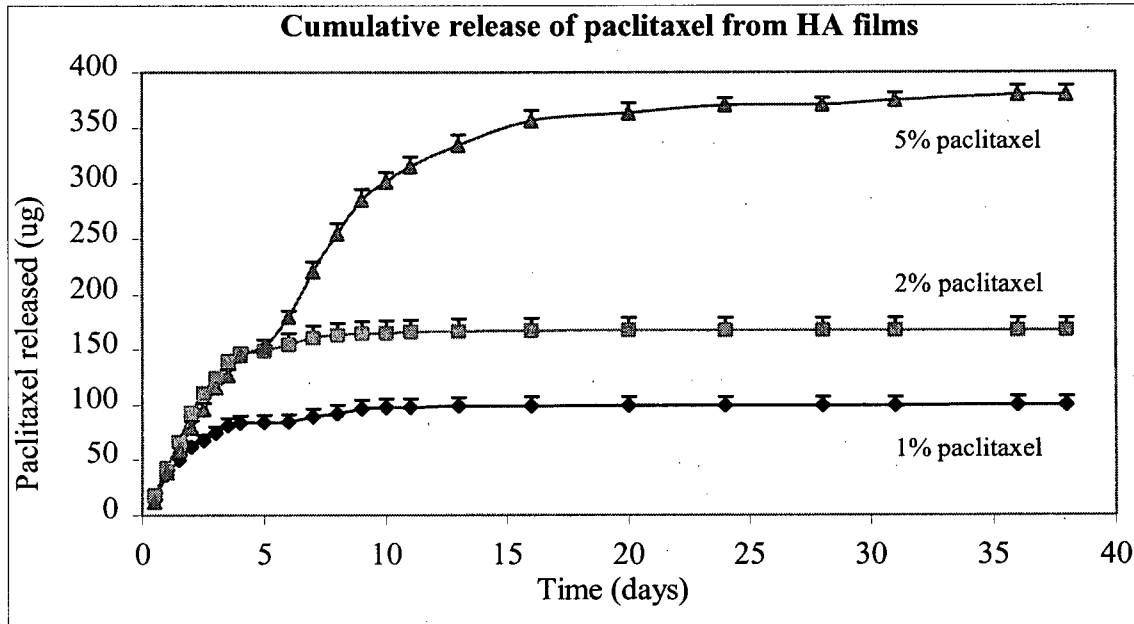


**Figure 36.** In vitro release of paclitaxel from HA films containing 50-90  $\mu\text{m}$  PLLA (2k g/mol) microspheres with different drug loadings. HA films possessed 1, 2 and 5% loadings by loading 5, 10 and 25% paclitaxel-loaded microspheres. (A: Cumulative amount released vs. time; B: Cumulative percent released vs. time).

A.



B.

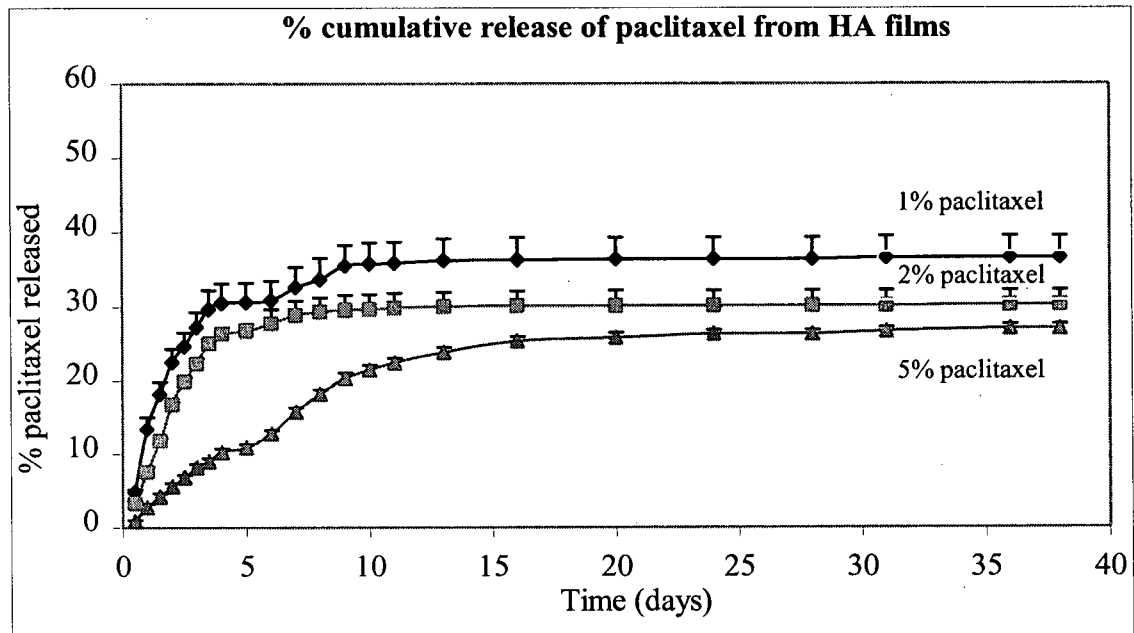
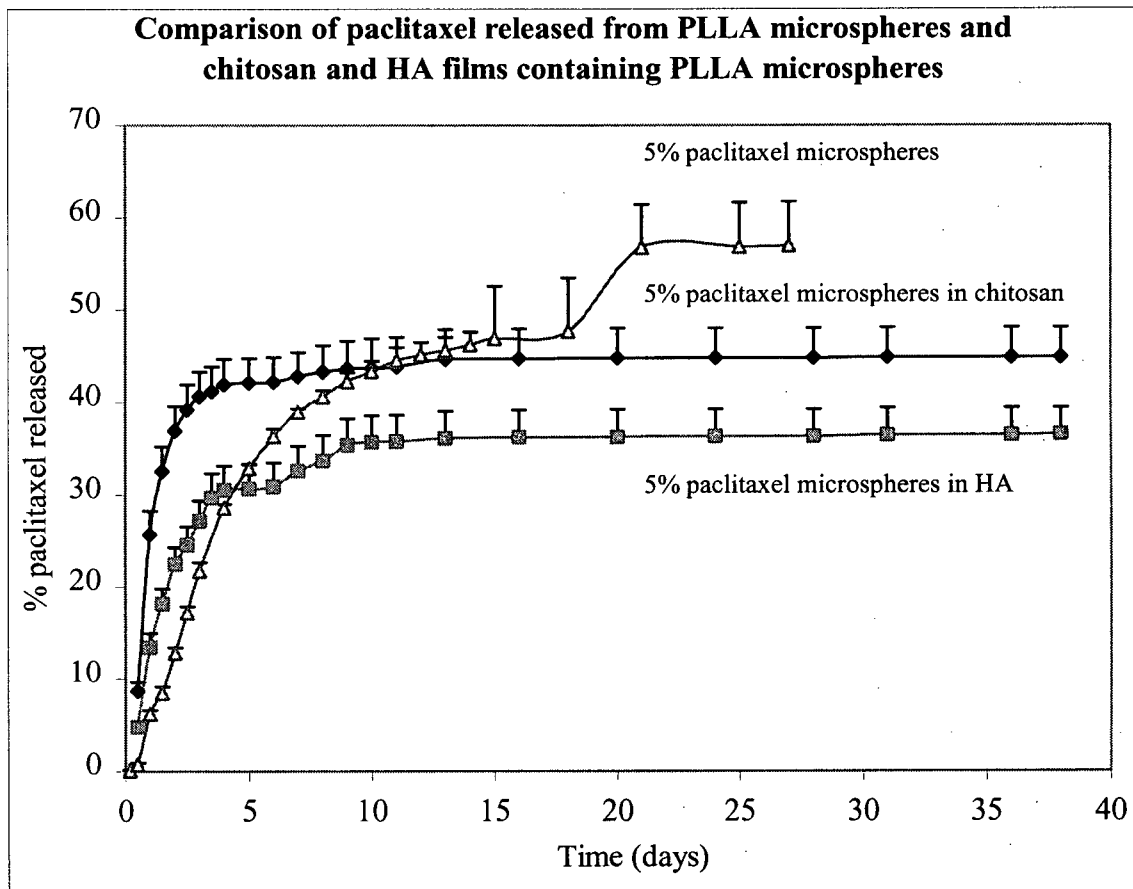


**Figure 37.** Comparison of the in vitro release of paclitaxel from 50-90  $\mu\text{m}$ , 5% paclitaxel-loaded PLLA (2k g/mol) microspheres and chitosan and HA films containing the same microspheres. Both chitosan and HA films possessed a total paclitaxel content of 1%, obtained by loading 5% paclitaxel-loaded PLLA microspheres.



## **5. DISCUSSION**

### **5.1. Preparation and characterization of microspheres**

#### **5.1.1. Effect of stir speed and emulsifier concentration on microsphere size**

The sizes of microspheres prepared using the solvent evaporation method are affected both by emulsification stir speed and PVA concentration (Conti et al., 1995). The smaller size microspheres were manufactured with the higher stirring rate and higher PVA concentration (refer to Table 2). A similar effect was also reported by other authors (Mumper and Jay, 1992). The stirring rate provides the energy, and PVA decreases the interfacial tension between the organic droplets and the aqueous medium. High levels of PVA concentrations and rapid stirring rates are appropriate for the maximum division of the organic phase, so that small mean particle sizes are obtained (Sansdrap and Moes, 1993).

#### **5.1.2. Effect of PLLA concentration on particle size distribution**

The polymer type, its molecular weight, and concentration used strongly influence the characteristics of the final microspheres (Jain et al., 1998). To evaluate the effect of PLLA concentration on the particle size distribution, microspheres were fabricated keeping the stirring rate at 600 rpm and a constant PVA concentration of 2.5%, while varying PLLA concentrations between 5% and 20% w/v. The microspheres formed were collected in three size ranges:  $< 53 \mu\text{m}$ ,  $53\text{-}90 \mu\text{m}$  and  $> 90 \mu\text{m}$ . The data showed that the percentage of larger microspheres increased with higher PLLA concentration (refer to Table 5). The observed relationship may be attributed to the increased total solid content in the system. Jalil and Nixon (1990) prepared PLLA (MW 2400 g/mol) microcapsules using a w/o emulsion system, light liquid paraffin as the continuum and a solution of

PLLA in acetonitrile as the dispersed phase. The data suggested that when the PLLA concentration was increased, there was increased collision and fusion of 'immature' microcapsules, resulting in larger 'final' microcapsules (Jalil and Nixon, 1990<sup>b</sup>). Another explanation is provided by a viscosity effect. The higher viscosity of the polymer/DCM phase with the higher polymer concentration leads to a less effective emulsifying process resulting in larger droplets producing larger microspheres (Ghaderi et al., 1996).

### **5.1.3. Surface morphology and cross-sectional views of microspheres**

The rate of solvent removal depends on the temperature, pressure, and the solubility parameter of the polymer, solvent, and dispersion medium and strongly influences the characteristics of the final microspheres (Arshady, 1991). Very rapid solvent evaporation may cause local "explosions" inside the droplets and lead to formation of porous structures on the microsphere surface (Arshady, 1991). The porous structure due to rapid removal of solvent has been demonstrated by using a reduced pressure or high temperature during microsphere preparation (Jalil and Nixon, 1990<sup>c</sup>). In this work, DCM removal under atmospheric pressure and room temperature was slow enough to give no evidence of defects on the microsphere surface (Figure 9).

It is known that polymers with high molecular weight will precipitate quickly at the surface of the droplet in the oil-in-water emulsion during the preparation of microspheres (Shukla and Price, 1991). On the contrary, low molecular weight polymers tend to precipitate slowly and thus produce non-porous microspheres (Jalil and Nixon, 1990<sup>d</sup>). The microspheres prepared using low molecular weight 2k g/mol PLLA in this formulation exhibited smooth surfaces and non-porous cross-sectional features (Figure 9, 16 and 17), indicative of slow precipitation of the low molecular weight polymer chains.

Drug loading is an important determinant of morphology of microspheres. Rosilio et al. (1991) showed that for poly (lactic-co-glycolic acid) microspheres, when the theoretical progesterone loading was increased from 10 to 50%, the microsphere surface changed from a smooth, uniform appearance to an irregular surface containing well-defined progesterone crystals and numerous pores. A similar trend was also reported for poly (D,L-lactic acid) (20k g/mol) (Suzuki and Price, 1985) and PLLA (10k g/mol) microspheres (Kishida et al. 1990). However, in this study, all the microspheres with different drug loadings (0 to 25%) showed no paclitaxel crystals on the microsphere surfaces (Figure 9). This may have been due to the very hydrophobic nature of paclitaxel and its partitioning preferentially into the hydrophobic polymer phase.

#### **5.1.4. Paclitaxel content in PLLA microspheres**

Polymer MW has been reported to affect the drug content in microspheres. Liggins (1998) demonstrated that paclitaxel loading was increased with decreasing PLLA MW. In this study the paclitaxel-loaded PLLA (2k g/mol) microspheres (5-25%) showed higher drug content values than total theoretical drug content (Table 8). One possible explanation is that the water-soluble oligomer fraction in low molecular weight PLLA leached out and partitioned into the aqueous medium during the process of microsphere manufacture (Mumper and Jay, 1992). This is supported by the finding that at least 7% of the PLLA polymer was water-soluble. Furthermore, drug entrapment in the microspheres is affected by solubility of the drug in the organic solvent and aqueous phase (Conti et al., 1992). As a hydrophobic drug, paclitaxel would remain in the organic solvent rather than partition into aqueous phase during microsphere fabrication. Therefore, less PLLA than

paclitaxel was likely incorporated into the formed microspheres, producing drug content values apparently higher than theoretical drug content.

#### **5.1.5. X-ray powder diffraction patterns of PLLA microspheres**

The X-ray powder diffraction pattern of PLLA in control microspheres showed that the intensity of its characteristic peak decreased significantly compared to PLLA alone (Figure 11). This implies that the polymer chains rearranged during the microsphere manufacture process, and became more amorphous in the microspheres. The change in crystallinity of poly (DL-lactic acid) after preparation of microspheres was reported by Jalil and Nixon (1990<sup>o</sup>). Comparison of the characteristic peak of PLLA for PLLA microspheres with paclitaxel loading from 0 to 25% w/w showed that the peak intensity decreased with increasing paclitaxel loading (Figure 11). Hence, at least qualitatively it appeared that the PLLA matrix was less crystalline as paclitaxel loading increased. This could be due to the interference of paclitaxel with the alignment of PLLA polymer chains. No peaks due to crystalline paclitaxel were detected in PLLA microspheres up to 25% drug loading. This finding suggests that paclitaxel may be completely miscible in the PLLA microsphere matrix or that the paclitaxel was dispersed in an amorphous form in the matrix.

#### **5.1.6. Thermal properties of PLLA and PLLA microspheres**

Thermal properties of PLLA were studied using a heat-cool-reheat-recool two-cycle scan (Figure 13). The polymer subjected to the first cycle (heating) showed a broad melting peak with a shoulder at a lower temperature of the melting peak. The shoulder in the melting peak may be due to the melting of a fraction of crystallites which are less perfect and/or possess a smaller size range than the crystallites causing the high

temperature melting peak (Nakafuku, 1996). The crystallinity of PLLA in a second cycle was only 6% compared to 23% in the first cycle. This finding suggests that during cooling in the first cycle where PLLA solidified from the melted state, PLLA could not crystallize to the same extent as did the original materials.

Thermal analysis of 50-90  $\mu\text{m}$  PLLA microspheres showed that for 25% paclitaxel-loaded microspheres, PLLA showed a 7  $^{\circ}\text{C}$  increase in  $T_g$  and a 7  $^{\circ}\text{C}$  depression in  $T_m$  compared to control microspheres (Table 9). The  $T_m$  depression provides evidence that the polymer and paclitaxel were miscible and that paclitaxel was molecularly dispersed (dissolved) in the PLLA matrix over the loading range studied. The phenomenon of melting point depression in polymers by the addition of a second component has been documented by different authors (Nakafuku, 1995; Huh and Bae, 1999). Liggins (1998) showed a linear relationship between the melting point depression of PLLA and the percentage of paclitaxel incorporated over a range from 0 to 60% in the PLLA microspheres.

The  $T_g$  of paclitaxel-loaded microspheres increased compared to that of control microspheres. The increase in  $T_g$  of PLLA in microspheres containing paclitaxel suggests that the start of the segmental motion of PLLA in the microsphere matrix (at the  $T_g$ ) is delayed by possible hydrogen bonding between PLLA and paclitaxel. A similar increase in  $T_g$  of high MW PLLA (Miyajima et al., 1997), poly (D,L-lactic acid) (Yamakawa et al., 1992) and poly (lactic-co-glycolic acid) (Okada et al., 1994) was found to be due to electrostatic interactions between the basic drug incorporated and the carboxylic acids at the polymer end groups.

## **5.2. PLLA microspheres in chitosan films**

The distribution of control and paclitaxel-loaded PLLA microspheres in films was demonstrated to be uniform (Figure 16 and 17). There were no aggregates of microspheres found in film matrices. Thus, the hydrophobic paclitaxel encapsulated in microspheres was uniformly dispersed in the hydrophilic films. The cross-sectional view of microsphere-loaded films showed that all microsphere surfaces were entrapped within the film matrices; therefore, potentially, a complete control effect of film matrices on paclitaxel release could be achieved.

## **5.3. In vitro degradation of PLLA microspheres and chitosan and HA films**

### **5.3.1. In vitro degradation of PLLA microspheres**

The degradation of PLLA is mainly via simple hydrolysis. The hydrolysis of PLLA begins with a water uptake phase followed by random hydrolytic scission of the ester bonds in the polymer chains (Sodergard et al., 1996). The chemical structure, molar mass and its distribution, morphology, and geometry of the polymer matrix can strongly influence the hydrolytic degradation of PLLA (Delgado et al., 1996; Hiljanen-Vainio, et al., 1996; Sodergard et al., 1996). As MW and degree of crystallinity decrease, polymer degradation occurs more rapidly. The lower MW of a polymer results in greater hydrophilicity, and thus easier and more rapid hydration. In the amorphous regions of polymers, polymer chains are loosely packed, which causes a more rapid water penetration (Sodergard et al., 1996). Furthermore, depending on the geometry of the material, accelerated hydrolysis (autocatalysis) may occur at the core of the matrix due to a higher concentration of degradation products containing carboxylic acid groups,

compared to the matrix surface where the degradation products continuously dissolve in the surrounding buffer solution (Imai et al., 1999; Tsuje, 2000; Lu et al., 2000).

#### **5.3.1.1. Molecular weight**

Since no PLLA standards are available, polystyrene in the same range of MW as the samples is normally used for establishing the universal calibration curve to calculate the MW of samples. The viscosity of low MW polystyrene was too low to demonstrate any differences in flowing time through the Cannon-Fenske viscometer, and thus no viscosity gradient could be detected. In this case, no universal calibration curve could be made; thus the MW of PLLA in degraded microspheres could not be calculated. However, GPC separates molecules based on their sizes. The larger the molecules, the shorter the time needed to pass through the column. Therefore, the retention times of molecules on GPC correspond to their MWs. The retention time of PLLA became longer with incubation in PBS-A (Table 11). The longer retention time of PLLA revealed that the polymer chains in microspheres were becoming shorter due to hydrolytic degradation.

The GPC chromatograms of PLLA (MW 2k g/mol) in degraded microspheres (Figure 20) were monomodal with only one peak rather than multimodal as shown by high MW PLLA (Makino et al., 1985; Li et al., 1990; Pinster et al., 1993). In the multimodal chromatograms of high MW PLLA, there is one main peak corresponding to the bulk polymer and other peak(s) for low MW compounds produced from the hydrolysis. The molecular weight at which degradation products became soluble in water is at a critical value of about 1100 (Park, 1995). Therefore the material left in the microspheres after degradation should have a MW above 1100. Since the MW of PLLA

in this study prior to degradation was only 2k, it was not possible to differentiate other peak(s) due to such small differences in MW.

The stability of degraded PLLA samples upon dry storage in a desiccator was illustrated by running two samples with the same incubation times but different storage periods in the desiccator. The same retention time on GPC was found for both samples, suggesting that they had the same MW. This finding is supported by Jamshidi et al. (1988), who demonstrated that the MW decrease for a carefully dried sample was similar to that for a conventionally dried one, indicating that the possibility of hydrolysis of main-chain ester bonds due to trace amounts of water was insignificant.

#### **5.3.1.2. Thermal properties**

An increased T<sub>g</sub> of PLLA with incubation of microspheres in PBS-A was observed for both control and 25% paclitaxel-loaded microspheres (Table 12 and Figure 21). A similar change of T<sub>g</sub> upon degradation has been reported by other authors (Pistner et al., 1993; Leach and Mathiowitz, 1998). The T<sub>g</sub> of a polymer is a measure of the flexibility of the polymer chain and the ease with which the transition state for hydrolysis of the ester bond may be achieved (Pitt and Gu, 1987). The increased T<sub>g</sub> could be explained by considering that the shorter chains formed upon degradation could realign themselves and interact with each other more strongly, therefore more energy being needed to move segmental chains, resulting in a higher T<sub>g</sub>.

It has been established that polymer degradation results in an initial increase, followed by a decrease in crystallinity (Chu, 1981; Hiljanen-Vainio et al., 1996; Leach and Mathiowitz, 1998). The hydrolysis of PLLA starts in the amorphous part of the polymer because water can access those domains more readily due to their loosely

packed structure (Pistner et al., 1993). The initial increase in crystallinity is due to the preferential loss of amorphous regions, leaving behind only the more crystalline regions. As hydrolysis proceeds, the crystallinity would decrease with the degradation of the crystalline regions. In this study, 25% paclitaxel-loaded microspheres showed 10% crystallinity increase over 4 weeks incubation in PBS-A, pH 7.4 (Table 12b). However, control microspheres showed no significant change in crystallinity as degradation proceeded (Table 12a).

#### **5.3.1.3. Surface morphology**

The erosion of both control and paclitaxel-loaded PLLA microspheres was observed very soon after degradation had begun (Figure 23 and 24). It is clearly seen that pieces of the matrix peeled off from the initially smooth surface. There are two types of erosion mechanisms, surface (heterogeneous) erosion and bulk (homogeneous) erosion. The erosion occurring only at the polymer surface only is referred to as surface erosion (Holland et al., 1986). Depending on the physical properties of the specific polymer, such as molecular weight, polymer crystallinity, hydrophobicity, and glass transition temperature, a combination of both mechanisms usually occurs (Holland et al., 1986). The hydrophilicity of PLLA due to its low MW (2k g/mol) allows for rapid water penetration into the microsphere matrix, and it is more likely that bulk erosion mechanism predominates for the degradation of PLLA microspheres. It has been reported that poly (D,L-lactic acid) microspheres of diameter less than 10  $\mu\text{m}$  (Park, 1994, 1995) as well as poly (lactic-co-glycolic acid) microspheres of diameter ranging from 50 to 70  $\mu\text{m}$  (Chen et al., 1997) demonstrated heterogeneous bulk degradation with a faster degradation rate in the core of the matrix due to autocatalysis.

25% paclitaxel-loaded microspheres showed similar degradation patterns to control microspheres (Figure 24). The loss of structural integrity of the matrix occurred earlier in 25% drug-loaded microspheres compared to control microspheres. The faster degradation of 25% paclitaxel-loaded microspheres might be due to the lower crystallinity of PLLA in drug-loaded microspheres.

#### **5.3.1.4. Mass loss**

The rate of mass loss is important in terms of the resorption and removal of the polymers from the body (Reed and Gilding, 1980). During degradation, water-soluble oligomers from the biodegradation process diffused out of the matrix and into the medium, resulting in a mass loss of the matrix (Tsuji and Ikada, 1997). For high MW PLLA, no detectable mass loss of samples occurred until the molar mass had decreased to  $4 \times 10^4$  g/mol (Li and Vert, 1990). However, since the MW of the starting material is very low, 2k g/mol in this study, the mass loss of PLLA started very early as seen in Figure 25, which is in agreement with the observation of the surface morphology changes. There was a rapid mass loss in the first week of incubation compared to the following 2 weeks. Since the amorphous components of the polymer are preferentially degraded by simple hydrolysis (Pistner et al. 1993), the rapid mass loss can be explained by the more amorphous state of the sample prior to degradation allowing the water to permeate and thereby hydrolyze the amorphous polymer chains. Moreover, the water-soluble fraction of the polymer could dissolve into the medium during the early incubation period. After 2 weeks of slow degradation, there was a more rapid mass loss in week 4. The most likely explanation for the rapid mass loss is that the hydrolysis and erosion of the crystalline regions had started (Sodergard et al., 1996). However, it is also possible that at these later

time points, there may have been significant errors in the measurement of mass loss. For example, the breakdown of microspheres produced small particles, which were probably not centrifuged effectively and which would be removed with the medium, as during the degradation study the medium was replaced on alternate days.

### **5.3.2. In vitro degradation of chitosan films**

In this study the surface morphology change of chitosan films from smooth to dimpled and then porous (Figure 26) and over 30% mass loss of chitosan films in 6 weeks (Figure 30) indicated the degradation of chitosan films during their incubation in PBS-A, pH 7.4. This might be due to dissolution of a low molecular weight fraction of chitosan. As a polymer, chitosan molecules would have a molecular weight distribution. The lower molecular weight fraction may be more readily dissolved in the buffer solution compared to the higher molecular weight fraction. In addition, during the fabrication of chitosan films, chitosan was first dissolved in 1% v/v acetic acid and therefore would become protonated on the amine groups. The protonated chitosan could partially dissolve when brought into contact with PBS-A, pH 7.4. This may also be the cause of the mass loss of chitosan films. Chitosan is known to be biodegradable by the action of enzymes, such as chitosanase and lysozyme. It is expected that in vivo the mass loss of chitosan films would be much higher since enzymes would be involved in the degradation process.

### **5.3.3. In vitro degradation of crosslinked HA films**

As HA is soluble in water, some pharmaceutical applications need crosslinking of HA molecules to make them water insoluble. In our formulation, HA was crosslinked with carbodiimide through the intermolecular formation of ester bonds between the hydroxyl and carboxyl groups belonging to different polysaccharide molecules (Tomihata

and Ikada, 1997<sup>o</sup>). However, the ester bonds are very unstable and readily undergo hydrolysis at pH 7. The resultant non-crosslinked HA would dissolve and further degrade by simple hydrolysis (Tokita et al., 1997). Crosslinked HA was degraded and solubilized rapidly (Figure 31) with 83% mass loss after incubation in PBS-A, pH 7.4 for 20 hours.

As a polyelectrolyte, the degradation of HA is influenced by the salt concentration (Miyazaki et al., 1998). With increasing salt concentration, the electrostatic repulsion of charged side groups along the chains will be suppressed and the extension of molecules will be not significant. Generally, polyelectrolytes have the tendency that the more contacts that form, the less the molecules are attacked, that is, the chances of scission decrease with increasing salt concentration (Miyazaki et al., 1998). In this study, 0.15 M PBS-A was used as the degradation medium and it is possible that the presence of phosphate and sodium chloride slowed down the degradation of HA.

#### **5.3.4. In vitro degradation of PLLA microspheres in film matrices**

The control PLLA microspheres in both chitosan films and HA films were studied under the same conditions as for microspheres alone. The initially smooth surface of microspheres in both chitosan and HA films became rough after 2-4 hrs incubation in PBS-A (Figure 27, 28 and 29), suggesting the degradation of PLLA microspheres in the film matrices. For microspheres in chitosan films, the degradation appeared to begin almost immediately, as for microspheres alone. At later time points, the control microspheres in chitosan films also degraded similarly to microspheres alone. This indicates that the film matrices (hydrogel systems) absorbed extensive amounts of water when immersed in the incubation medium and there were sufficient water molecules available to penetrate and degrade the PLLA microsphere matrix.

#### **5.4. In vitro release study of paclitaxel from microspheres and microsphere-loaded films**

In our formulation, paclitaxel was encapsulated in PLLA microspheres and then the microspheres were dispersed in chitosan and HA films (hydrogels). To date there is no reported work on the drug release from this type of formulation. It is proposed that there were two main stages involved in the drug release; 1) paclitaxel was released from microspheres to hydrogels, and 2) paclitaxel diffused through the hydrogel to the external medium.

In all the in vitro release studies, albumin (0.4 g/L) was incorporated in the release media in order to enhance the ability to maintain sink conditions. Normal albumin concentrations in plasma and tissues are about 10-fold higher (Gibaldi, 1984) than the concentration we used in the release medium. However, we did not intend to simulate physiological albumin concentrations, but only to enhance paclitaxel solubility in the release medium. The effect of albumin on paclitaxel solubility was demonstrated by Winternitz (1999). A solubility of paclitaxel of  $1.4 \pm 0.3 \mu\text{g/ml}$  in PBS-A was obtained compared to  $0.2 \pm 0.1 \mu\text{g/ml}$  in PBS at  $37^\circ\text{C}$  in 25 hours. If the concentration of solute in the release medium is less than 15% of its solubility, sink conditions are considered to be in effect (Carstensen, 1977). The sampling interval was chosen so that sink conditions could be maintained. However, in the initial rapid release phase sink conditions were exceeded for all formulations despite sampling two or three times a day. It is likely that the amount of paclitaxel released under these conditions was underestimated, but the cumulative release should not be altered.

#### **5.4.1. In vitro release of paclitaxel from PLLA microspheres (to external medium)**

The release profiles of paclitaxel from microspheres were shown to be biphasic (Figure 33). The initial rapid phase lasted between 2 and 4 days, with about 30% of drug released. Generally, this rapid phase is believed due to the diffusional release of drug from the superficial surface region of the microspheres (Sanders et al., 1984). In this study, surface erosion of PLLA microspheres had been detected after 2 hours of immersion due to the hydrophilicity of low MW PLLA. The degradation and erosion of the amorphous component of the PLLA matrix may also contribute to the rapid release of paclitaxel. Following the initial rapid release phase, a phase of slower release occurred. The slower release rates may be due to the increased crystallinity of the matrix, with a slower water uptake, decreased paclitaxel diffusivity and decreased degradation rate.

Both the rate and extent of paclitaxel release from microspheres were found to be increased as the drug loading increased (Figure 33). With the increase in paclitaxel content in PLLA microspheres, the amount of PLLA as a diffusion barrier decreased. Therefore, there existed an increased driving force (drug concentration gradient) and a decreased diffusion barrier in microspheres with higher loadings, which resulted in increased paclitaxel release rate and extent.

#### **5.4.2. In vitro release of paclitaxel from film matrices loaded with microspheres**

##### **5.4.2.1. In vitro release of paclitaxel from chitosan films loaded with microspheres of different size ranges**

Release profiles of paclitaxel from chitosan films with microspheres of different size ranges (< 10, 10-50, and 50-90  $\mu\text{m}$ ) were studied and are shown in Figure 34. Generally, drugs are released faster from smaller size range microspheres (Wakiyama et

al., 1981; Jameela and Jayakrishnan, 1995), as smaller microspheres have a larger surface area of contact with the incubation medium (Thanoo et al., 1992). As the first step, paclitaxel would be released from microspheres to the interface of microsphere and film. In the second stage, drug molecules at the interface of the microsphere and the film (hydrogel) have to diffuse through the hydrogel to the external medium. When drug molecules cross a hydrogel, they either travel through pores in the hydrogel or partition into, diffuse through, and partition out of the hydrogel. Paclitaxel was released faster from chitosan films containing larger size range microspheres. It is reasonable that larger microspheres would be closer to the surface of chitosan films; in other words, paclitaxel released from larger microspheres would need to undergo a shorter diffusional path length to reach the external medium, leading to a faster release rate.

#### **5.4.2.2. In vitro release of paclitaxel from chitosan and HA films loaded with 50-90 $\mu\text{m}$ microspheres**

Paclitaxel release studies from 50-90  $\mu\text{m}$  microsphere-loaded chitosan films and HA films were conducted under the same conditions. They both exhibited a biphasic release (Figure 35 and 36). In our formulation, the release of paclitaxel from films involved the release of paclitaxel from PLLA microspheres and paclitaxel transport through the films. The initial release rates of paclitaxel from chitosan films ( $70 \pm 7.0$ ,  $66 \pm 6$  and  $60 \pm 3.3$   $\mu\text{g/day}$  for 1, 2 and 5% paclitaxel loading) were higher than from HA films ( $37 \pm 4.4$ ,  $42 \pm 3.5$  and  $39 \pm 7.5$   $\mu\text{g/day}$  for 1, 2 and 5% paclitaxel loading). The faster paclitaxel release from chitosan films than from crosslinked HA films could be related to the lower MW of chitosan compared to HA and the lack of crosslinking of the

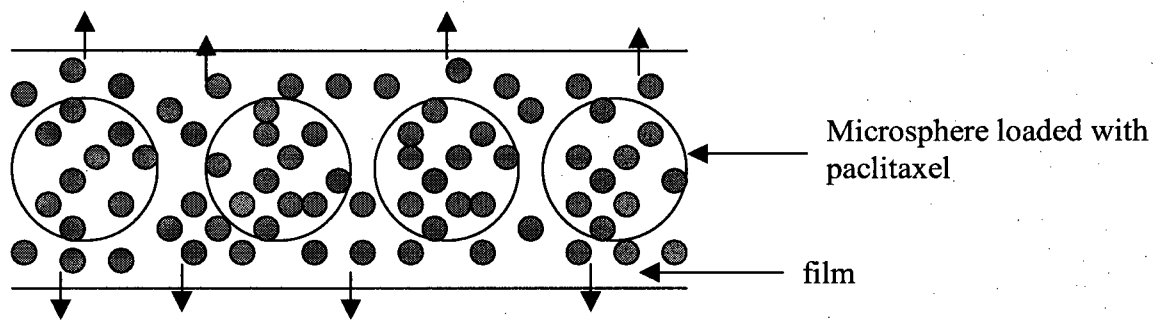
chitosan films, leading to greater paclitaxel diffusivity through the chitosan hydrogel. The MW of chitosan was 150k g/mol, while the MW of HA was 800 – 1600k g/mol.

A comparison of paclitaxel release profiles from microspheres and from chitosan and HA films containing microspheres is shown in Figure 37. During the fabrication of films, microspheres were mixed vigorously with chitosan or HA dispersions and it is likely that significant concentrations of paclitaxel were present in the dry chitosan and HA film matrices leading to initial rapid release of paclitaxel from microsphere loaded films (see Figure 38). It is perhaps not valid to draw any conclusions about relative rates of paclitaxel release from microspheres versus microspheres in films, since the total drug content in the 3 delivery systems is not the same. However, Figure 37 demonstrates that dispersing paclitaxel loaded microspheres in chitosan and HA films, leads to a small controlling effect of the hydrogel film on paclitaxel release. The controlling effect of the film on paclitaxel release is only evident in the slower second phase of drug release from microsphere-loaded films (see Figure 38).

For either chitosan or HA films, the release rate and extent increased as the paclitaxel loading in the films increased (Figure 35 and 36). This could be explained by a higher loading leading to more paclitaxel being available at the interface of microspheres and hydrogel, and consequently a faster transport of drug through the film matrix (Wood et al., 1982).

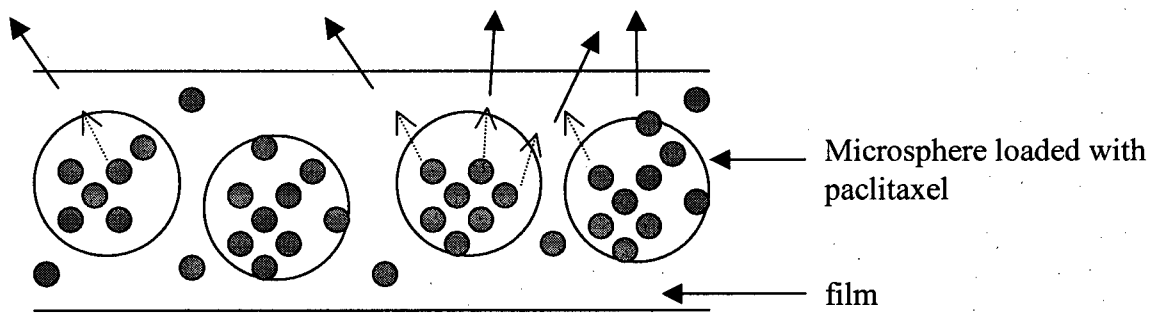
**Figure 38.** Schematic representation of paclitaxel release from films containing paclitaxel-loaded microspheres

**A. Initial rapid phase of paclitaxel release from microsphere loaded films**



↑ Rapid diffusional release of molecularly dispersed paclitaxel in film

**B. Second slower phase of paclitaxel release from microsphere loaded films**



↑ Step one: paclitaxel release from microsphere to film

↑ Step two: diffusional release of paclitaxel through film matrix

In terms of developing any film or membrane formulation to prevent post-surgical adhesions, it is believed that the film should act as a barrier over a few days. The degradation study of HA films showed that 83% mass loss occurred in 20 hours incubation in PBS-A and therefore the lifetime of the film in vivo would likely be only 1-3 days at most. It is possible that microspheres released on loss of the HA barrier films would adhere to tissue and release drug over days to weeks. The chitosan film released paclitaxel at a faster rate but the film would likely degrade with a lifetime much longer than crosslinked HA in vivo. We are unable, at this stage, to predict which would be the optimal film formulation for preventing post-surgical adhesions. Certainly, an elegant drug loaded film formulation could be achieved by dispersing paclitaxel-loaded microspheres into either chitosan or crosslinked HA matrices. This avoided the problem of loading a hydrophobic drug directly into a hydrophilic hydrogel with the resulting precipitation and aggregation of the drug particles in the film.

Future studies would involve the preclinical evaluation of these 2 film formulations in an animal model. A suitable model of post-surgical adhesion is the cecal side wall abrasion model in rats. Following controlled abrasion of the ventral and dorsal surfaces of the cecum, the films are placed over the surfaces and evaluated, typically 7 days following the surgical procedure. Adhesions are graded as a 0-4 rating scale with 0 measuring no adhesions and a score of 4 being dense adhesions with a non-dissectable plane. Paclitaxel loaded versus non-drug loaded film formulations would be evaluated for efficacy and biocompatibility / toxicity.

## 6. SUMMARY AND CONCLUSIONS

1. PLLA (2k g/mol) microspheres were prepared using the solvent evaporation method in size ranges of < 10, 10-50 and 50-90  $\mu\text{m}$  and paclitaxel loadings between 0 and 25% w/w. Both chitosan and crosslinked HA films either without or with microspheres were fabricated using the solvent casting method. The microspheres were shown to be uniformly dispersed in the film matrices and produced elegant drug loaded film formulations.

2. The degradation and erosion of PLLA microspheres and microsphere-loaded films started after 2 hours incubation in PBS-A and progressed with time. Over 60% mass loss occurred for PLLA microspheres in 5 weeks, 30% for microsphere-loaded chitosan films in 6 weeks, and 83% for microsphere-loaded HA films.

3. DSC results showed that there was a progressive decrease in  $T_m$  for PLLA microspheres as paclitaxel loading increased, indicating the miscibility of paclitaxel with PLLA.

4. In general, release profiles of paclitaxel from microspheres and from microsphere-loaded films were biphasic. Paclitaxel release from films occurred via diffusional release of paclitaxel from the microspheres followed by transport through the hydrogel film.

## 7. REFERENCES

Adams, J.D., Flora, K.P., Goldspiel, B.R., Taxol: a history of pharmaceutical development and current pharmaceutical concerns. *Journal. National Cancer Institute*, 15: 141-147, 1993.

Alastair, J.J. and Wood, M.D., Drug therapy, *The New England Journal of Medicine*, 332, 1004-1014, 1995.

Ambrosio, L., Borzacchiello, A., Netti, P.A., and Nicolais, L., Properties of new materials rheological study on hyaluronic acid and its derivative solutions, *Pure Applied Chemistry*, A36 (7&8), 991-1000, 1999.

Arnold, P.B., Green, C.W., Foresman, P.A., and Rodeheaver, G.T., Evaluation of resorbable barriers for preventing surgical adhesions, *Fertility and Sterility*, 73 (1), 157-161, 2000.

Arshady, R., Microspheres for biomedical applications: preparation of reactive and labeled microspheres, *Biomaterials*, 14 (1), 5-15, 1993.

Arshady, R., Preparation of biodegradable microspheres and microcapsules: 2. Polylactides and related polyesters, *Journal of Controlled Release*, 17, 1-22, 1991.

Aspden, T.J., Mason, J.D.T., Jones, N.S., Lowe, J., Skaugrud, Y., and Illum, L., Chitosan as a nasal delivery system: The effect of chitosan solutions in vitro and in vivo mucociliary transport rates in human turbinates and volunteers, *Journal of Pharmaceutical Sciences*, 86 (4), 509-513, 1997.

Benedetti, L.M., Topp, E.M., and Stella, V.J., Microspheres of hyaluronic acid esters – Fabrication methods and in vitro hydrocortisone release, *Journal of Controlled Release*, 13, 33-41, 1990.

Bergsma, J.E., Rozema, F.R., Bos, R.R.M., Biocompatibility and degradation mechanisms of predegraded and non-degraded poly (lactide) implants: an animal study, *Journal of Materials Science: Materials in Medicine*, 715-728, 1995.

Bergsma, J.E., Bos, R.R.M., Rozema, F.R., De Jong, W., and Boering, G., Biocompatibility of intraosseously implanted predegraded poly (lactide) implants: an animal study, *Journal of Materials Science: Materials in Medicine*, 7, 1-7, 1996.

Berriaud, N., Milas, M., and Rinaudo, M., Rheological study on mixtures of different molecular weight-hyaluronates, *International Journal of Biological Macromolecules*, 16 (3), 137-142, 1994.

Bhaskara Rao, S. and Sharma, C.P., Use of chitosan as a biomaterial: Studies on its safety and haemostatic potential, *Journal of Biomedical Materials Research*, 34, 21-28, 1997.

Boyers, S.P., Diamond, M.P., and DeCherney, A.H., Reduction of postoperative pelvic adhesions in the rabbit with Gore-Tex surgical membrane, *Fertility and Sterility*, 49 (6), 1066-1070, 1988.

Bulpitt, P. and Aeschlimann, D., New strategy for chemical modification of hyaluronic acid: preparation of functionalized derivatives and their use in the formation of novel biocompatible hydrogels, *Journal of Biomedical Materials Research*, 47, 152-169, 1999.

Carstensen, J.T., Dissolution of solids, 1977, In "Pharmaceutics of solids and solid dosage forms", John Wiley & Sons, Inc., New York, London, Sydney, Toronto, p 63-64.

Chen, I., Apte, R.N., and Cohen, S., Characterization of PLGA microspheres for the controlled delivery of IL- $\alpha$  for tumor immunotherapy, *Journal of Controlled Release*, 43, 261-272, 1997.

Chien, Y.W., Controlled-release drug administration: logic, 1982, In "Novel Drug Delivery Systems", Marcel Dekker, Inc., New York and Basel, p 4.

Chu, C.C., An in-vitro study of the effect of buffer on the degradation of poly (glycolic acid) sutures, *Journal of Biomedical Materials Research*, 15, 19-27, 1981.

Conti, B., Pavanetto, F., and Genta, I., Use of polylactic acid for the preparation of microparticulate drug delivery systems, *Journal of Microencapsulation*, 9 (2), 153-166, 1992.

Conti, B., Genta, I., Modena, T., and Pavanetto, F., Investigation on process parameters involved in polylactide-co-glycolide microspheres preparation, *Drug Development and Industrial Pharmacy*, 21 (5), 615-622, 1995.

Cowie, J.M.G., Introduction, 1973, In "Polymers: Chemistry and Physics of Modern Materials", Billing & Son Ltd, Worcester, Great Britain, p 5.

Crotts, G. and Park, T.G., Preparation of porous and nonporous biodegradable polymeric hollow microspheres, *Journal of Controlled Release*, 35, 91-105, 1995.

Dawkins, J.V., Calibration of separation systems, 1984, In "Steric Exclusion Liquid Chromatography of Polymers", Marcel Dekker, Inc., New York, p 54.

Deanin, R.D., Intermolecular Order, 1972, In "Polymer Structure, Properties and Applications", The Maple Press Company, York, U.S.A., p 189.

De Laco, P.A., Stefanetti, M., Pressato, D., Pianan, S., Dona, M., Pavesio, A., and Bovicelli, L., A novel hyaluronan-based gel in laparoscopic adhesion prevention: preclinical evaluation in an animal model, *Fertility and Sterility*, 69 (2), 318-323, 1998.

Delgado, A., Evora, C., and Llabres, M., Degradation of DL-PLA-methadone microspheres during in vitro release, *International Journal of Pharmaceutics*, 140, 219-227, 1996.

Diamond, M.P. and Hershlag, A., Adhesion Formation/Reformation, 1989, In "Treatment of Post Surgical Adhesions", DiZerega, G.S., Malinak, L.R., Diamond, M.P., and Linsky, C.B., A John Wiley & Sons, Inc., New York, p 23-34.

DiZerega, G.S., The cause and prevention of postsurgical adhesion: A contemporary update, 1993, In "Gynecologic Surgery and Adhesion Prevention", Diamond, M.P., DiZerega, G.S., Linsky, C.B., and Reid, R.L., Wiley-Liss, Inc., New York, p 3.

Dordunoo, S.K., Burt, H.M., Solubility and stability of taxol: effects of buffers and cyclodextrins, *International Journal of Pharmaceutics*, 133, 191-200, 1996.

Dunn, R.C., Tissue-type plasminogen activator and adhesion prevention, 1993, In "Gynecologic Surgery and Adhesion Prevention", Diamond, M.P., DiZerega, G.S., Linsky, C.B., and Reid, R.L., Wiley-Liss, Inc., New York, p 213.

Felt, O., Buri, P., and Gurny, R., Chitosan: a unique polysaccharide for drug delivery, *Drug Development and Industrial Pharmacy*, 24 (11), 979-993, 1998.

Finley, R.S. and Rowinsky, E.K., Patient Care Issues: The Management of Paclitaxel-Related Toxicities, *The Annals of Pharmacotherapy*, 28, s27-s34, 1994.

Furukawa, T., Matsusue, Y., Yasunaga, T., Shikinami, Y., Okuno, M., and Nakamura, T., Biodegradation behavior of ultra-high-strength hydroxyapatite/poly (L-lactide) composite rods for internal fixation of bone fractures, *Biomaterials*, 21, 889-898, 2000.

Ghaderi, R., Stureson, C., and Carlfors, J., Effect of preparative parameters on the characteristics of poly (DL-lactide-co-glycolide) microspheres made by the double emulsion method, *International Journal of Pharmaceutics*, 141, 205-216, 1996.

Ghezzi, E., Benedetti, L.M., Rochira, M., Biviano, F., and Callegaro, L., Hyaluronic derivative microspheres as NGF delivery devices: preparation methods and in vitro release characterization, *International Journal of Pharmaceutics*, 87, 21-29, 1992.

Gibaldi, M., Drug disposition-distribution, 1984, In "Biopharmaceutics and Clinical Pharmacokinetics", Lea & Febiger, Washington, USA, p 173.

Giunchedi, P., Alpar, H.O., and Conte, U., PDLLA microspheres containing steroids: spray-drying, o/w and w/o/w emulsifications as preparation methods, *Journal of Microencapsulation*, 15 (2), 185-195, 1998.

Goa, K.L. and Benfield, P., Hyaluronic acid – a review of its pharmacology and use as a surgical aid in ophthalmology, and its therapeutic potential in joint disease and wound healing, *Drug*, 47 (3), 536-566, 1994.

Goldberg, E.P., Burns, J.W., and Yaacobi, Y., Prevention of postoperative adhesions by precoating tissues with dilute sodium hyaluronate solutions, 1993, In "Gynecologic Surgery and Adhesion Prevention", Diamond, M.P., DiZerega, G.S., Linsky, C.B., and Reid, R.L., Wiley-Liss, Inc., New York, p 191.

Gomel, V., Urman, B., and Gurgan, T., Pathophysiology of Adhesion Formation and Strategies for Prevention, *The Journal of Reproductive Medicine*, 41, 35-41, 1996.

Haney, A.F., Murphy, A.A., Hesla, J., Roek, J.A., Hurst, B.S., Rowe, G., Kettel, L.M., and Schlaff, W.D., Expanded polytetrafluoroethylene (Gore-Tex Surgical Membrane) is superior to oxidized regenerated cellulose (Interceed TC 7) in preventing adhesions, *Fertility and Sterility*, 63 (5), 1021-1026, 1995.

Haney, A.F., The peritoneal response to expanded polytetrafluoroethylene and oxidized regenerated cellulose surgical adhesion barriers, *Artificial Cells, Blood Substitutes, and Immobilization Biotechnology*, 24 (2), 121-141, 1996.

Harris, E.S., Morgan, R.F., and Rodeheaver, G.T., Analysis of the kinetics of peritoneal adhesion formation in the rat and evaluation of potential antiadhesive agents, *Surgery*, 117 (6), 663-668, 1995.

He, P., Davis, S.S., and Illum, L., In vitro evaluation of the mucoadhesive properties of chitosan microspheres, *International Journal of Pharmaceutics*, 166, 75-88, 1998.

Hiljanen-Vainio, M., Varpomaa, P., Seppala, J., and Tormala, P., Modification of poly (L-lactides) by blending: mechanical and hydrolytic behavior, *Macromolecular Chemistry and Physics*, 197, 1503-1523, 1996.

Hill-West, J.L., Chowdhury, S.M., and Hubbell, J.A., Efficacy of a resorbable hydrogel barrier, oxidized regenerated cellulose, and hyaluronic acid in the prevention of ovarian adhesions in a rabbit model, *Fertility and Sterility*, 62 (3), 630-634, 1994.

Hiljanen-Vainio, M., Varpomaa, P., Seppala, J., and Tormala, P., Modification of poly (L-lactides) by blending: mechanical and hydrolytic behavior, *Macromolecular Chemistry and Physics*, 197, 1503-1523, 1996.

Holland, S.J., Tighe, B.J., and Gould, P.L., Polymers for biodegradable medical devices. 1. The potential of polyesters as controlled macromolecular release systems, *Journal of Controlled Release*, 4, 155-180, 1986.

Holtz, G., Prevention and management of peritoneal adhesions, *Fertility and Sterility*, 41 (4), 497-507, 1984.

Hooper, K.A., Macon, N.D., and Kohn, J., Comparative histological evaluation of new tyrosine-derived polymers and poly (L-lactic acid) as a function of polymer degradation, *Journal of Biomedical Materials Research*, 41, 443-454, 1998.

Hopkins, M.P., Von Gruenigen, W.W., Holda, S., and Weber, B., The effect of intermittent-release intraperitoneal chemotherapy on wound healing, *American Journal of Obstetrics and Gynecology*, 819-825, 1997 April.

Huh, K.M. and Bae, Y.H., Synthesis and characterization of poly (ethylene glycol)/poly (L-lactic acid) alternating multiblock copolymers, *Polymer*, 40, 6147-6155, 1999.

Hunt, J.A., Joshi, H.N., Stella, V.J. and Topp, E.M., Diffusion and drug release in polymer films prepared from ester derivatives of hyaluronic acid, *Journal of Controlled Release*, 12, 159-169, 1990.

Illum, L., Chitosan and its use as a pharmaceutical excipient, *Pharmaceutical Research*, 15 (9), 1326-1331, 1998.

Illum, L., Farraj, N.F., Fisher, A.N., Gill, I., Miglietta, M., and Benedetti, L.M., Hyaluronic acid ester microspheres as a nasal delivery system for insulin, *Journal of Controlled Release*, 29, 133-141, 1994.

Imai, Y., Nagai, M., and Watanabe, M., Degradation of composite materials composed of tricalcium phosphate and a new type of block polyester containing a poly (L-lactic acid) segment, *Journal of Biomaterials Science. Polymer Edition*, 10 (4), 421-432, 1999.

Ishiguro, K., Yoshie, N., Sakurai, M., and Inoue, Y., A <sup>1</sup>H NMR study of a fragment of partially N-deacetylated chitin produced by lysozyme degradation, *Carbohydrate Research*, 237, 333-338, 1992.

Izumikawa, S., Yoshioka, S., Aso, Y., and Takeda, Y., Preparation of poly (l-lactide) microspheres of different crystalline morphology and effect of crystalline morphology on drug release rate, *Journal of Controlled Release*, 15, 133-140, 1991.

Iwata, T. and Doi, Y., Morphology and enzymatic degradation of poly (L-lactic acid) single crystals, *Macromolecules*, 31, 2461-2467, 1998.

Jackson, J.K., Shinner, K.C., Burgess, L., Sun, T., Hunter, B.L., and Burt, H.M., Paclitaxel is a potent inhibitor of post-surgical adhesion formation in rats. Unpublished data.

Jain, R., Shah, N.H., Malick, A.W., and Rhodes, C., Controlled drug delivery by biodegradable poly (ester) devices: different preparative approaches, *Drug Development and Industrial Pharmacy*, 24 (8), 703-727, 1998.

Jalil, R., Biodegradable poly (lactic acid) and poly (lactide-co-glycolide) polymers in sustained drug delivery, *Drug Development and Industrial Pharmacy*, 16 (16), 2353-2367, 1990.

Jalil, R. and Nixon, J.R., Microencapsulation using poly (DL-lactic acid) II: Effect of polymer molecular weight on the microcapsule properties, *Journal of Microencapsulation*, 7 (2), 245-254, 1990.

Jalil, R. and Nixon, J.R., Biodegradable poly (lactic acid) and poly (lactide-co-glycolide) microcapsules: problems associated with preparative techniques and release properties, *Journal of Microencapsulation*, 7 (3) 297-325, 1990<sup>a</sup>.

Jalil, R. and Nixon, J.R., Microencapsulation using poly (L-lactic acid) II: Preparative variables affecting microcapsule properties, *Journal of Microencapsulation*, 7 (1), 25-39, 1990<sup>b</sup>.

Jalil, R. and Nixon, J.R., Microencapsulation using poly (DL-lactic acid) I: Effect of preparative variables on the microcapsule characteristics and release kinetics, *Journal of Microencapsulation*, 7 (2), 229-244, 1990<sup>c</sup>.

Jalil, R. and Nixon, J.R., Microencapsulation using poly (L-lactic acid) IV: Release properties of microcapsules containing phenobarbitone, *Journal of Microencapsulation*, 7 (1), 53-66, 1990<sup>d</sup>.

Jalil, R. and Nixon, J., Microencapsulation with biodegradable materials, 1992, in "Microencapsulation of Drugs", Whateley, T.L., Harwood academic publisher, Switzerland.

Jameela, S.R. and Jayakrishann, A., Glutaraldehyde cross-linked chitosan microspheres as a long acting biodegradable drug delivery vehicle: studies on the in vitro release of mitoxantrone and in vivo degradation of microspheres in rat muscle, *Biomaterials*, 16 (10), 769-775, 1995.

Jamshidi, K., Hyon, S-H., and Ikada, Y., Thermal characterization of polylactides, *Polymer*, 29, 2229-2234, 1988.

Juni, K. and Nakano, M., Poly (lactic acid) microspheres as drug carrier systems, 1987, In "Polymers in Controlled Drug Delivery", Illum, L. and Davis, S., Wright, Bristol, p 49-59.

Karjomaa, S., Suortti, T., Lempiainen, R., Selin, J.F., and Itavaara, M., Microbial degradation of poly (L-lactic acid) oligomers, *Polymer Degradation and Stability*, 59, 333-336, 1998.

Kas, H.S., Chitosan: properties, preparations and application to microparticulate systems, *Journal of Microencapsulation*, 14 (6), 689-711, 1997.

Kawashima, Y., Lin, S.Y., Kasai, A., Handa, T., and Takenake, H., *Chemical and Pharmaceutical Bulletin*, 22, 2107, 1985.

Kennedy, R., Costain, D.J., McAlister, V.C., and Lee, T.D.G., Prevention of experimental postoperative peritoneal adhesions by N, O-carboxymethyl chitosan, *Surgery* 120 (5), 866-870, 1996.

Kingston, D.G.I., *The Chemistry of Paclitaxel, Pharmacology and Therapeutics*, 52, 1-34, 1991.

Kishida, A., Dressman, J.B., Yoshioka, S., Aso, Y., and Takeda, Y., Some determinants of morphology and release rate from poly (L-lactic acid) microspheres, *Journal of Controlled Release*, 13, 83-89, 1990.

Knapczk, J., Krowczynski, L., Krzek, J., Brzeski, M., Nurnberg, E., Schenk, D., and Struszczyk, H., Requirements of chitosan for pharmaceutical and biomedical application, 1989, In "Chitin and Chitosan: Sources, Chemistry, Biochemistry, Physical Properties and Applications", Skjak-Braek, G., Anthonsen, T., and Sandford, P., Elsevier Science Publishers, Ltd., London and New York, p 657-664.

Kowalski, J. and Morrissey, R., Sterilization of implants, 1996, In "Biomaterials Science: An Introduction to Materials in Medicine", Ratner, B.D., Hoffman, A.S., Schoen, F.J., Lemons, J.E., Academic Press, London, p 415-419.

Kristiansen, A., Varum K.M., and Grasdalen, H., The interactions between highly de-N-acetylated chitosans and lysozyme from chicken egg white studied by <sup>1</sup>H-NMR spectroscopy, *International Journal of Biochemistry*, 251, 335-342, 1998.

Kristl, J., Smid-Korbar, J., Strue, Schara, M., and Rupprecht, H., Hydrocolloids and gels of chitosan as drug carriers, *International Journal of Pharmaceutics*, 99, 13-19, 1993.

Kulkarni, R.K., Moore, E.G., Hegyeli, A.F., and Fred Leonard, Biodegradable poly (lactic acid) polymers, *Journal of Biomedical Materials Research*, 5, 169-181, 1971.

Kydonieus, A., Diffusion-controlled matrix systems, 1992, In "Treatise on controlled drug delivery", Marcel Dekker, Inc., New York, Baser, and Hong Kong, p 172.

Leach, K.J.P. and Mathiowitz, E., Degradation of double-walled polymer microspheres of PLLA and P (CPP: SA) 20: 80. I. In vitro degradation, *Biomaterials*, 19, 1973-1980, 1998.

Lee, Y.L., Khor, E., Koo, O.,  $\gamma$  irradiation of chitosan, *Journal of Biomedical Materials Research*, 43, 282-290, 1998.

Leelarasamee, N., Howard, S.A., Malanga, C.J., Luzzi, L.A., Hogan, T.F., and Kandzari, S.J., Kinetics of drug release from polylactic acid-hydrocortisone microcapsules, *Journal of Microencapsulation*, 3 (3), 171-179, 1986.

Leenslag, J.W., Penning, A.J., Bos, R.R.M., Rozema, E.R., and Boering, G., Resorbable materials of poly (L-lactide) VII. In vivo and in vitro degradation, *Biomaterials*, 8, 311-314, 1987.

Lewis, D.H., Controlled release of bioactive agents from lactide/glycolide polymers, 1990, In "Biodegradable Polymers as Drug Delivery Systems", Chasin, M. and Langer, R., Marcel Dekker, Inc., New York, Basel, and Hong Kong, p 1-41.

Li, S. and Vert, G.M., Structure-property relationships in the case of the degradation of massive poly ( $\alpha$ -hydroxy acids) in aqueous media. Part 3 influence of the morphology of poly (L-lactic acid), *Journal of Materials Science: Materials in Medicine*, 1, 198-206, 1990.

Liggins, R., Paclitaxel loaded poly (L-lactic acid) microspheres: characterization and intraperitoneal administration, Ph.D. thesis, 1998.

Linhardt, R.J., Biodegradable polymers for controlled release of drugs, 1989, In "Controlled Release of Drugs: Polymers and Aggregate Systems", Rosoff, M., VCH publishers, Inc., New York, p 57

Linsky, C.B., Diamond, M.P., Cunningham, T., Constantine, B., DeCherney, A.H., and DiZerega, G.S., Adhesion reduction in the rabbit uterine horn model using an absorbable barrier, TC-7, *The Journal of Reproductive Medicine*, 32 (1), 17-20, 1987.

Lu, L., Peter, S.J., Lyman, M.D., Lai, H-L, Leite, S.M., Tamada, J.A., Vacanti, J.P., Langer, R., and Mikos, A.G., In vitro degradation of porous poly (L-lactic acid) foams, *Biomaterials*, 21, 1595-1605, 2000.

MacEachern-Keith, G.J., Wagner Butterfield, L.J., and Incorvia Mattina, M.J., Paclitaxel stability in solution, *Analytical Chemistry*, 69, 72-77, 1997.

Makino, K., Arakawa, M., and Kondo, T., Preparation and in vitro degradation properties of polylactide microcapsules, *Chemical and Pharmaceutical Bulletin*, 33 (3), 1195-1120, 1985.

Matsusue, Y. and Yamamuro, T., In vitro and in vivo studies on bioabsorbable ultra-high-strength poly (L-lactide) rods, *Journal of Biomedical Materials Research*, 26, 1553-1567, 1992.

Meerum Terwogt, J.M., Nuijnt, B., Ten Bokkel Huinink, W.W., and Beijnen, J.H., Alternative formulations of paclitaxel, *Cancer Treatment Reviews*, 23, 87-95, 1997.

Milena Rehakova, Busan Bakos, Maros Soldan and Katarina Vizarova, Depolymerization reactions of hyaluronic acid in solution, *International Journal of Biological Macromolecules*, 16 (3), 121-124, 1994.

Miller, J.A., Ferguson, R.L., Powers, D.L., Burns, J.W., and Shalaby, S.W., Efficacy of hyaluronic acid/Nonsteroidal anti-inflammatory drug systems in preventing post-surgical tendon adhesions, *Journal of Biomedical Materials Research*, 38 (1), 25-33, 1997.

Miyajima, M., Koshika, A., Okada, Jun'ichi, Ikeda, M., and Nishimura, K., Effect of polymer crystallinity on papaverine release from poly (L-lactic acid) matrix, *Journal of Controlled Release*, 49, 207-215, 1997.

Miyazaki, T., Yomota, C., and Okada, S., Degradation of hyaluronic acid at the metal surface, *Colloid and Polymer Science*, 276, 388-394, 1998.

Moore, A.R. and Willoughby, D.A., Hyaluronan as a drug delivery system for diclofenac: a hypothesis for mode of action, *International Journal of Tissue Reactions XVII* (4), 153-156, 1995.

Mumper, R.J. and Jay, M., Poly (L-lactic acid) microspheres containing neutron-activatable holmium-165: A study of the physical characteristics of microspheres before and after irradiation in a nuclear reactor, *Pharmaceutical Research*, 9 (1), 149-154, 1992.

Muzzarelli, R.A.A., Chemically modified chitosans, 1985, In "Chitin in Nature and Technology", Muzzarelli, R., Jeuniaux, C., and Gooday, G.W., Plenum Press, New York and London, p 295-321.

Muzzarelli, R.A.A., Human enzymatic activities related to the therapeutic administration of chitin derivatives, *Cellular and Molecular Life Sciences*, 53, 131-140, 1997.

Nakafuku, C., Effects of molecular weight on the melting and crystallization of poly (L-lactic acid) in a mixture with poly (ethylene oxide), *Polymer Journal*, 28 (7), 568-575, 1996.

Nakatsuka, S. and Andradý, A., Permeability of vitamin B-12 in chitosan membranes. Effect of crosslinking and blending with poly (vinyl alcohol) on permeability, *Journal of Applied Polymer Science*, 44, 17-28, 1992.

Nishioka, Y., Kyotani, S., Okamura, M., Miyazaki, M., Okazaki, K., Ohnishi, S., Yamamoto, Y., and Ito, K., Release characteristics of cisplatin chitosan microspheres and effect of containing chitin, *Chemical and Pharmaceutical Bulletin*, 38, 2871-2873, 1990.

Nordtveit, R.J., Varum, K.M., and Smidsrod, O., Degradation of partially N-acetylated chitosans with hen egg white and human lysozyme, *Carbohydrate Polymers*, 29, 163-167, 1996.

O'Donnell, P.B. and McGinity, J.W., Preparation of microspheres by the solvent evaporation technique, *Advanced Drug Delivery Reviews*, 28, 25-42, 1997.

Okada, H., Doken, Y., Ogawa, Y., and Toguchi, H., Preparation of three-month depot injectable microspheres of leuprorelin acetate using biodegradable polymers, *Pharmacological Research*, 11, 1143-1147, 1994.

Onishi, H. and Machida, Y., Biodegradation and distribution of water-soluble chitosan in mice, *Biomaterials*, 20, 175-182, 1999.

Park, K., Shalaby, W.S.W., and Park, H., Biodegradation, 1993<sup>a</sup>, In "Biodegradable Hydrogels for Drug Delivery", Technomic publishing company, Inc., Lancaster, Pennsylvania, U.S.A., p 13-33.

Park, K., Shalaby, W.S.W., and Park, H., Chemically-Induced Degradation, 1993<sup>b</sup>, In "Biodegradable Hydrogels for Drug Delivery", Technomic publishing company, Inc., Lancaster, Pennsylvania, U.S.A., p 143.

Park, T.G., Degradation of poly (D, L-lactic acid) microspheres: effect of molecular weight, *Journal of Controlled Release*, 30, 161-173, 1994.

Park, T.G., Degradation of poly (lactic-co-glycolic acid) microspheres: effect of copolymer composition, *Biomaterials*, 16, 1123-1130, 1995.

Pavanetto, F., Genta, I., Giunchedi, P., and Conti, B., Evaluation of spray drying as a method for polylactide and polylactide-co-glycolide microsphere preparation, *Journal of Microencapsulation*, 10 (4), 487-497, 1993.

Piskin, E., Biodegradable polymers as biomaterials, *Journal of Biomaterial Science, Polymer Edition*, 6 (9), 775-795, 1994.

Pistner, H., Bendix, D.R., Muhling, J., Reuther, J.F., Poly (L-lactide): a long-term degradation study in vivo, Part III. Analytical characterization, *Biomaterials*, 14 (4), 291-298, 1993.

Prestwich, G.D., Marecak, D.M., Mreck, J.F., Vercruyse, K.P., and Ziebell, M.R., Controlled chemical modification of hyaluronic acid: synthesis, applications, and biodegradation of hydrazide derivatives, *Journal of Controlled Release*, 53, 93-103, 1998.

Prisell, P.T., Camber, O., Hiselius, J., and Norstedt, G., Evaluation of hyaluronan as a vehicle for peptide growth factors, *International Journal of Pharmaceutics*, 85, 51-56, 1992.

Pouyani, T. and Prestwich, G., Functionalized derivatives of hyaluronic acid oligosaccharides: drug carriers and novel biomaterials, *Bioconjugate Chemistry*, 5, 339-347, 1994.

Reed, A.M. and Gilding, D.K., Biodegradable polymers for use in surgery – poly (glycolic)/(lactic acid) homo and copolymers: 2. In vitro degradation, *Polymer*, 22, 494-498, 1981.

Rehakova, M., Bakos, D., Vizarova, K., Soldan, M., and Jurickova, M., Properties of collagen and hyaluronic acid composite materials and their modification by chemical crosslinking, *Journal of Biomedical Materials Research*, 30, 369-372, 1996.

Rosen, S.L., Polymer morphology, 1993, In "Fundamental Principles of Polymeric Materials", John Wiley & Sons, Inc. New York, Chichester, Brisbane, Toronto, Singapore, p 40.

Rosilio, V., Benoit, J.P., Deyme, M., Thies, C., and Madelmont, G., A physicochemical study of the morphology of progesterone-loaded microspheres fabricated from poly (D, L-lactide-co-glycolide), *Journal of Biomedical Materials Research*, 25, 667-682, 1991.

Rowinsky, E.K., Onetto, N., Canetta, R.M., and Arbuck, S.G., Paclitaxel: the First of the Taxanes, an Important New Class of Antitumor Agents, *Seminars in Oncology*, 19 (6), 646-662, 1992.

Rudin, A., Mechanical properties of polymer solids and liquids, 1998, In "The Elements of Polymer Science and Engineering", Academic Press, San Diego, p 382.

Runt, J.P., 1985, *Encyclopedia of Polymer Science and Engineering*, Wiley, New York, p 487.

Sanders, L.M., Kent, J.S., McRae, G.I., Vickery, B.H., Tice, T.R., and Lewis, D.H., Controlled release of a luteinizing hormone-releasing hormone analogue from poly (d, l-lactide-co-glycolide) microspheres, *Journal of Pharmaceutical Science*, 73, 1294-1297, 1984.

Sansdrap, P. and Moes, A.J., Influence of manufacturing parameters on the size characteristics and the release profiles of nifedipine from poly (DL-lactide-co-glycolide) microspheres, *International Journal of Pharmaceutics*, 98, 157-164, 1993.

Saravelos, H. and Li, T.C., Physical barriers in adhesion prevention, *The Journal of Reproductive Medicine*, 41 (1), 42-51, 1996.

Sawayanagi, Y., Nambu, N., and Nagai, T., Permeation of drugs through chitosan membranes, *Chemical and Pharmaceutical Bulletin*, 30 (9), 3297-3301, 1982.

Shah, V.P., Midha, K.K., Dighe, S., McGilveray, I.J., Skelly, J.P., Yacobi, A., Layloff, T., Viswanathan, T., Edgar Cook, C., McDowall, R.D., Pittman, K.A., and Spector, S., Analytical methods validation: bioavailability, bioequivalence and pharmacokinetic studies, *Pharmaceutical Research*, 9 (4), 588-593, 1992.

Shukla, A.J. and Price, J.C., Effect of drug loading and molecular weight of cellulose acetate propionate on the release characteristics of theophylline microspheres, *Pharmacological Research*, 8, 1396-1400, 1991.

Shushan, A., Mor-Yosef, S., Avgar, A., and Laufer, N., Hyaluronic acid for preventing experimental postoperative intraperitoneal adhesions, *Journal of Reproductive Medicine*, 39 (5), 398-402, 1994.

Simkovic, I., Hricovini, M., Soltes, L., Mendichi, R., and Cosentino, C., Preparation of water-soluble/insoluble derivatives of hyaluronic acid by cross-linking with epichlorohydrin in aqueous NaOH/NH<sub>4</sub>OH solution, *Carbohydrate Polymers*, 41, 9-14, 2000.

Sinko, P. and Kohn, J., Polymeric drug delivery systems, 1993, In "Polymeric Delivery Systems: Properties and Applications", El-Nokaly, M.A., Piatt, D.M., and Charpertier, B.A., American Chemical Society, Washington, DC, p 18-41.

Sodergard, A., Selin, J-F, and Nasman, J.H., Hydrolytic degradation of peroxide modified poly (L-lactide), *Polymer Degradation and Stability*, 51, 351-359, 1996.

Soriano, I., Delgado, A., Diaz, R.V., and Evora, C., Use of surfactants in polylactic acid protein microspheres, *Drug Development and Industrial Pharmacy*, 21 (5), 549-558, 1995.

Spencer, C.M. and Faulds, D., Paclitaxel A Review of its Pharmacodynamic and Pharmacokinetic Properties and Therapeutic Potential in the Treatment of Cancer, *Drug Evaluation*, 48 (5), 794-847, 1994.

Spentlehauser, G., Vert, M., Benoit, J.P., Chabot, F., and Veillard, M., Biodegradable cisplatin microspheres prepared by the solvent evaporation method: morphology and release characteristics, *Journal of Controlled Release*, 7, 217-229, 1988.

Stevens, M.P., Molecular Weight and Solutions, 1990, In "Polymer Chemistry an Introduction", Oxford University Press, New York, Oxford, p 40 and 61.

Suzuki, K. and Price, J.C., Microencapsulation and dissolution properties of a neuroleptic in a biodegradable polymer, poly (d, l-lactide), *Journal of Pharmaceutical Sciences*, 74 (1), 21-24, 1985.

Thacharodi, D. and Rao, K.P., Propranolol hydrochloride release behavior of crosslinked chitosan membranes, *Journal of Chemical Technology and Biotechnology*, 58, 177-181, 1993<sup>a</sup>.

Thacharodi, D. and Rao, K.P., Release of nifedipine through crosslinked chitosan membranes, *International Journal of Pharmaceutics*, 96, 33-39, 1993<sup>b</sup>.

Thanoo, B.C., Sunny, M.C., and Jayakrishnan, A., Cross-linked chitosan microspheres: Preparation and evaluation as a matrix for the controlled release of pharmaceuticals, *Journal of Pharmacy and Pharmacology*, 44, 283-286, 1992.

Tobolsky, A.V.E. and Mark, H.F.E, 1971, *Polymer science and materials*, John Wiley and Sons, Inc., Toronto.

Tokita, Y., Ohshima, K., and Okamoto, A., Degradation of hyaluronic acid during freeze drying, *Polymer Degradation and Stability*, 55, 159-164, 1997.

Tokiwa, Y., Konno, M., and Nishida, H., Isolation of silk degrading microorganisms and its poly (L-lactide) degradability, *Chemistry Letters*, 355-6, 1999.

Tomihata, K. and Ikada, Y., Preparation of cross-linked hyaluronic acid films of low water content, *Biomaterials*, 18 (3), 189-195, 1997<sup>a</sup>.

Tomihata, K. and Ikada, Y., Crosslinking of hyaluronic acid with water-soluble carbodiimide, *Journal of Biomedical Materials Research*, 37, 243-151, 1997<sup>b</sup>.

Tomihata, K. and Ikada, Y., In vitro and in vivo degradation of films of chitin and its deacetylated derivatives, *Biomaterials*, 18 (7), 567-575, 1997<sup>c</sup>.

Tsai, D.C., Howard, S.A., Hogan, T.F., Malanga, J., Kandzari, S.J., and Mas, K.H., Preparation and in vitro evaluation of polylactic acid-mitomycin microcapsules, *Journal of Microencapsulation*, 3 (3), 181-193, 1986.

Tsuji, H., In vitro hydrolysis of blends from enantiomeric poly (lactide)s Part 1. Well-stereo-complexed blend and non-blended films, *Polymer*, 41, 3621-3630, 2000.

Tsuji, H. and Ikada, Blends of aliphatic polyesters. II. Hydrolysis of solution-cast blends from poly (L-lactide) and poly ( $\epsilon$ -caprolactone) in phosphate-buffered solution, *Journal of Applied Polymer Science*, 67, 405-415, 1998.

Urman, B., Gomel, V., and Jetha, N., Effect of hyaluronic acid on postoperative intraperitoneal adhesion formation in the rat model, *Fertility and Sterility*, 56 (3), 563-567, 1991.

Van Krevelen<sup>a</sup>, D.W., Typology of polymers, 1997, In "Properties of Polymers, Their Correlation with Chemical Structure; Their Numerical Estimation and Prediction from Additive Group Contributions", Elsevier Science B.V., Netherlands, p16.

Van Krevelen<sup>b</sup>, D.W., Typology of polymers, 1997, In "Properties of Polymers, Their Correlation with Chemical Structure; Their Numerical Estimation and Prediction from Additive Group Contributions", Elsevier Science B.V., Netherlands, p19.

Varum, K.M., Holme, H.K., Izume, M., Stokke, B.T., and Smidsrod, O., Determination of enzymatic hydrolysis specificity of partially n-acetylated chitosans, *Biochimica et Biophysica Acta*, 129, 5-15, 1996.

Varum, K.M., Myhr, M.M., Hjerde, R.J.N., and Smidsrod, O., In vitro degradation rates of partially N-acetylated chitosans in human serum, *Carbohydrate Research*, 299, 99-101, 1997.

Vercruyssen, K.P., Marecak, D.M., Marecek, J.F., and Prestwich, G.D., Synthesis and in Vitro degradation of new polyvalent hydrazide cross-linked hydrogels of hyaluronic acid, *Bioconjugate Chemistry*, 8, 686-694, 1997.

Vert, M., Schwach, G., Engel, R., and Coudane, J., Something new in the field of PLA/GA bioresorbable polymers?, *Journal of Controlled Release*, 53, 85-92, 1998.

Visser, S.A., Hergenrother, R.W., and Cooper, S.L., *Polymers*, 1996, In "Biomaterials Sciences: An Introduction to Materials in Medicine", Ratner, B.D., Hoffman, A.S., Schoen, F.J., and Lemons, J.E., Academic Press, San Diego, p 51.

Wakiyama, N., Juni, K., and Nakano, M., Preparation and evaluation in vitro polylactic acid microspheres containing local anesthetics, *Chemical and Pharmaceutical Bulletin*, 29 (11), 3363-3368, 1981.

Wakiyama, N., Juni, K., and Nakano, M., Influence of physiochemical properties of poly (lactic acid) on the characteristics and in vitro release patterns of poly (lactic acid) microspheres containing local anaesthetics, *Chemical and Pharmaceutical Bulletin*, 30 (7), 2621-2628, 1982.

Winternitz, C.I., Poly ( $\epsilon$ -caprolactone) and methoxypolyethylene glycol blends as a surgical paste delivery system for paclitaxel, Ph.D thesis, 1999.

Wiseman, D., *Polymers for the Prevention of Surgical Adhesions*, 1994, In "Polymeric Site-specific Pharmacotherapy", Domb, A.J., John Wiley & sons Ltd., p 371-410.

Wiseman, D.M., Hazards and Prevention of Post-surgical Pericardial Adhesions, Treutner, K.H., and Schumpelick, V., *Peritoneal Adhesions*, Springer-Verlag Berlin Heidelberg, Germany, 1997, p 240-254.

Wood, J.M., Attwood, D., and Collett, J.H., The influence of gel formulation on the diffusion of salicylic acid in polyHEMA hydrogels, *Journal of Pharmacy and Pharmacology*, 34, 1-4, 1982.

Yamakawa, I., Ashizawa, K., Tsuda, T., Watanabe, S., Hayashi, M., and Awazu, S., Thermal characteristics of poly (DL-lactic acid) microspheres containing neurotesin analogue, *Chemical and Pharmaceutical Bulletin*, 40 (10), 2870-2872, 1992.

Yasuda, H. and Lamaze, C.E., Permselectivity of solutes in homogenous water-swollen polymer membranes, *Journal of Macromolecular Science. Part B. Physics*, B5, 111-134, 1971.

Young, R.J. and Lovell, P.A., Introduction, 1991, In "Introduction to Polymers", Cambridge University Press, Great Britain, p 267.

Yui, N., Okano, T., and Sakurai, Y., Inflammation responsive degradation of crosslinked hyaluronic acid gels, *Journal of Controlled Release*, 22, 105-116, 1992.

Zentner, G.M., Cardinal, J.R., and Kim, S.W., Progesterin permeation through polymer membranes II: Diffusion studies on hydrogel membranes, *Journal of Pharmaceutical Sciences*, 67, 10, 1352-1355, 1978.

Zentner, G.M., Cardinal, J.R., Feijen, J., and Song, S-Z, Progesterin permeation through polymer membranes IV: Mechanism of steroid permeation and functional group contributions to diffusion through hydrogel films, *Journal of Pharmaceutical Sciences*, 68 (8), 970-975, 1979.

Zhou, M. and Donovan, M.D., Intranasal mucociliary clearance of putative bioadhesive polymer gels. *International Journal of Pharmaceutics*, 135, 115-125, 1996.